

**Andrea Díaz Roa**

**Isolating and characterizing antimicrobial peptides derived from larvae of the  
blowfly *Sarconesiopsis magellanica* (diptera: Calliphoridae)**

Director: Prof. Felio Jesús Bello García

Co-Director: Prof. Pedro Ismael da Silva Junior

Co-Director: Prof. Manuel Alfonso Patarroyo

PhD Program in Biomedical and Biological Sciences

Universidad del Rosario (UR)

2019

**Andrea Díaz Roa**

**Isolating and characterizing antimicrobial peptides derived from larvae of the  
blowfly *Sarconesiopsis magellanica* (diptera: Calliphoridae)**

Director: Prof. Pedro Ismael da Silva Junior

Co-Director: Prof. Felio Jesús Bello García

Co-Director: Prof. Manuel Alfonso Patarroyo

Interunits Postgraduate Program in Biotechnology

University of São Paulo (USP)

Butantan Institute (IBu)

Institute of Technological Research (IPT)

2019

## **Acknowledgements**

Firstly, I would like to thank God for giving me the strength and accompanying angels to complete this journey and not give up on the way.

I would like to express my gratitude to my supervisors, Prof. Felio Jesus Bello and Prof. Pedro Ismael da Silva Junior, for all their ideas, teaching and encouragement during these five years. I would like to thank Prof. Manuel Alfonso Patarroyo who was my Co-supervisor, also for greatly contributing with ideas and input ... thank you so much for your time and constant help.

My sincere thanks to all those who directly or indirectly shared a little of themselves, making the conclusion of this work possible, ... without all your help this would have been an unbearable task.

Funding: This work was financed by the Colombian Science, Technology, and Innovation Department (COLCIENCIAS) through COLCIENCIAS-UAN agreement FP44842-384-2016 (Project code No. 125371250687). Funding was also received from the São Paulo Research Foundation (FAPESP) Grant 13/07467-1 to CeTICS-CEPID and from the Brazilian National Technological and Scientific Development Council (CNPq) Grant 472744/2012-7. AD-R received a Colciencias grant (call for research projects 617, Colombia).

## Abstract

Larval therapy (LT) is an alternative treatment which uses fly larvae to heal chronic wounds; its action is based on debridement, bacterial removal and stimulating granulation tissue. The most important mechanism for fighting infection with LT depends on larval excretions and secretions (ES). The larvae are protected by an antimicrobial peptide (1) spectrum. *Sarconesiopsis magellanica* is a promising necrophagous fly for use in medicine. This study was thus aimed at identifying and characterizing *S. magellanica* AMPs contained in ES, for the first time. ES were fractionated by RP-HPLC using C18 columns. The products were lyophilized, and their antimicrobial activity characterized. The sequences were determined by mass spectrometry. The mechanism of action was evaluated by fluorescence and electronic microscopy. Toxicity was tested on HeLA cells and human erythrocytes; the physicochemical properties of the identified peptides were evaluated. Two molecules in the ES were characterized: sarconesin (a new peptide having antibacterial activity against Gram-negative (*Escherichia coli* D31, *Pseudomonas aeruginosa* 27853) and Gram-positive (*Staphylococcus aureus* ATCC 29213, *Micrococcus luteus* A270) bacteria and sarconsesin II, having activity against Gram-negative (*E. coli* MG1655, *P. aeruginosa* ATCC 27853) and Gram-positive (*S. aureus* ATCC 29213, *M. luteus* A270) bacteria. The minimum inhibitory concentrations ranged from 1.2  $\mu$ M upwards; the AMPs did not have toxicity in any tested cells and their action on bacterial membrane and DNA was confirmed. Sarconesin had similarity with the CDC42 protein belonging to the Rho-family of GTPases which are important in organelle development and wound repair. Sarconesin II was seen to be a conserved domain of the ATP synthase protein belonging to the FliI superfamily. The data reported here indicates that the peptides could be alternative therapeutic candidates for use in infections against Gram-negative and Gram-positive microorganisms and as new resources to combat resistance against antimicrobial agents.

**Key words:** Antimicrobial peptide, larval therapy, *Sarconesiopsis magellanica*.

## Resumo

A terapia larval é um tratamento alternativo que utiliza larvas de moscas para cicatrizar feridas crônicas: sua ação é baseada no desbridamento, remoção bacteriana e estimulação do tecido de granulação. O mecanismo mais importante para combater as infecções por TL depende das excreções e secreções (ES). As larvas são protegidas por um espectro de peptídeos antimicrobianos (PAMs). *Sarconesiopsis magellanica* é uma mosca necrófaga promissora para uso em medicina. Assim, este estudo teve como objetivo identificar e caracterizar os AMPs de *S. magellanica* contidos nas ES pela primeira vez. ES foram fracionados por RP-HPLC utilizando colunas C18. Os produtos foram liofilizados e sua atividade antimicrobiana caracterizada. As sequências foram determinadas por espectrometria de massas. O mecanismo de ação foi avaliado por fluorescência e microscopia eletrônica. A toxicidade foi testada em linhagens de células e eritrócitos humanos e as propriedades físico-químicas dos peptídeos identificados foram avaliadas. Duas moléculas presentes no ES foram caracterizadas: 1) sarconesin, um novo peptídeo, com atividade antibacteriana contra bactérias Gram-negativas (*Escherichia coli* D31, *Pseudomonas aeruginosa* 27853) e Gram-positiva (*Staphylococcus aureus* ATCC 29213, *Micrococcus luteus* A270); Um segundo peptídeo 2) Sarconesin II, com atividade contra Gram-negativo (*E. coli* MG1655, *P. aeruginosa* ATCC 27853) e Gram-positivo (*S. aureus* ATCC 29213, *M. luteus* A270). Nas concentrações mínimas inibitórias obtidas a partir de 1,2 µM, os PAMs não apresentaram toxicidade em nenhuma das células testadas e sua ação na membrana bacteriana e no DNA foi confirmada. Sarconesin apresentou similaridade com a proteína CDC42 pertencente à família Rho das GTPases, importante no desenvolvimento de organelas e reparo de feridas. Sarconesin II foi registrado como um domínio conservado da proteína ATP sintase pertencente à superfamília FliI. Os dados aqui relatados indicam que os peptídeos podem ser candidatos terapêuticos alternativos para uso em infecções contra microrganismos Gram-negativos e Gram-positivos e como novos recursos para combater a resistência a antimicrobianos.

**Palavras-chave:** Peptídeos antimicrobianos, terapia larval, *Sarconesiopsis magellanica*.

## Resumen

La terapia larva es un tratamiento alternativo que utiliza larvas de moscas para cicatrizar las heridas crónicas: su acción se basa en el desbridamiento, la eliminación bacteriana y la estimulación del tejido de granulación. El mecanismo más importante para combatir las infecciones por TL depende de las excreciones y las secreciones (ES). Las larvas están protegidas por un espectro de péptidos antimicrobianos (PAMs). *Sarconesiopsis magellanica* es una mosca necrófaga prometedora para su uso en medicina. Así, este estudio tuvo como objetivo identificar y caracterizar los PAM de *S. magellanica* contenidos en las ES por primera vez. Las ES fueron fraccionadas por RP-HPLC utilizando columnas C18. Los productos fueron liofilizados y su actividad antimicrobiana caracterizada. Las secuencias fueron determinadas por espectrometría de masas. El mecanismo de acción fue evaluado por fluorescencia y microscopía electrónica. La toxicidad se probó en líneas celulares y eritrocitos humanos, y se evaluaron las propiedades fisicoquímicas de los péptidos identificados. Dos moléculas presentes en las ES fueron caracterizadas: Sarconesin, un nuevo péptido con actividad antibacteriana contra bacterias Gram-negativas (*Escherichia coli* D31, *Pseudomonas aeruginosa* 27853) y Gram-positivas (*Staphylococcus aureus* ATCC 29213, *Micrococcus luteus* A270); adicionalmente, un segundo péptido denominado Sarconesin II, con actividad contra Gram-negativos (*E. coli* MG1655, *P. aeruginosa* ATCC 27853) y Gram-positivos (*S. aureus* ATCC 29213, *M. luteus* A270). Las concentraciones mínimas inhibitorias obtenidas partían desde 1,2  $\mu\text{M}$ ; los PAM no presentaron toxicidad en ninguna de las células probadas y su acción en la membrana bacteriana y en el ADN fue confirmada. Sarconesin presentó similitud con la proteína CDC42 perteneciente a la familia Rho de las GTPasas, importante en el desarrollo de organelos y reparación de heridas. Sarconesin II fue registrado como un dominio conservado de la proteína ATP sintasa perteneciente a la superfamilia FliI. Los datos aquí mostrados indican que los péptidos pueden ser candidatos terapéuticos alternativos para su uso en infecciones contra microorganismos gram-negativos y gram-positivos, y como nuevos recursos para combatir la resistencia a los antimicrobianos.

**Palabras clave:** Péptidos antimicrobianos, terapia larval, *Sarconesiopsis magellanica*.

---

*Contents*

Acknowledgements .....	3
Abstract .....	4
Resumo .....	5
Resumen .....	6
<i>Contents</i> .....	7
<i>List of Figures</i> .....	13
<i>List of Tables</i> .....	20
<i>Abbreviations</i> .....	21
<i>Amino acid list</i> .....	23
1. Chapter 1 .....	24
1.1. Introduction .....	24
1.1.1. Larval therapy .....	24
1.1.2. Wounds and incidence .....	24
1.1.3. LT mechanism of action (MoA) .....	25
1.1.3.1. Debridement .....	26
1.1.3.2. Granulation tissue .....	26
1.1.3.3. Antibacterial activity .....	27
1.1.3.4. Biofilm eradication .....	29
1.1.4. Diptera .....	30
1.1.5. Insects' innate immune system .....	32
1.1.5.1. Cellular response .....	32
1.1.5.2. Humoral response .....	33
1.1.5.3. Signaling pathways regulating the immune response .....	34

---

1.1.6. Antimicrobial peptides .....	35
1.1.7. Antimicrobial peptides' mechanism of action.....	40
1.1.8. AMP classification .....	42
1.1.9. Discovering new antimicrobial peptides potentially combating resistance .....	43
1.2. Objective.....	46
1.3. Materials and Methods.....	46
1.3.1. Fly Source and <i>S. magellanica</i> ES collection.....	46
1.3.1.1. Capturing adult <i>S. magellanica</i> specimens.....	46
1.3.1.2. Extracting larval excretions and secretions .....	47
1.3.2. Chromatographic fractionation.....	49
1.3.3. Bioassays .....	50
1.3.3.1. Bacterial strains .....	50
1.3.3.2. Standardizing growth curves .....	50
1.3.3.3. Turbidimetry.....	50
1.3.4. Structural characterization.....	51
1.3.4.1. Mass spectrometry.....	51
1.3.4.2. Bioinformatics analysis .....	51
1.4. Results.....	52
1.4.1. Purifying <i>S. magellanica</i> excretions and secretions .....	52
1.4.1.1. Fraction 2.....	53
1.4.1.2. Fraction 36.....	56
1.4.1.3. Fraction 44.....	56
1.4.1.4. Fraction 45.....	57
1.4.1.5. Fraction 46.....	58

---

1.4.1.6. Fraction 57 .....	59
1.5. Discussion .....	61
1.6. Conclusion .....	62
2. Chapter 2.....	64
2.1. Objectives .....	64
2.2. Materials and Methods.....	64
2.2.1. Peptide purification .....	64
2.2.2. Peptide synthesis .....	65
2.2.3. Peptides' analytical RP-HPLC .....	65
2.2.4. Antimicrobial assays .....	65
2.2.5. Cytotoxicity .....	66
2.2.6. Hemolytic activity.....	67
2.2.7. Mass spectrometry .....	67
2.2.8. Bioinformatics .....	67
2.2.9. Circular dichroism .....	68
2.2.10. Mechanism of action (MoA) .....	68
2.2.10.1. Membrane integrity and esterase activity.....	68
2.2.10.2. DNA staining.....	69
2.2.10.3. Gel retardation assay .....	69
2.2.11. Statistical analysis .....	69
2.3. Results.....	69
2.3.1. Peptide purification.....	69
2.3.2. Antimicrobial assays.....	70
2.3.3. Toxicity.....	73

---

2.3.4. Mass spectrometry .....	73
2.3.5. Protein model .....	74
2.3.6. Circular dichroism .....	76
2.3.7. Mechanism of action .....	77
2.3.7.1. Membrane integrity and esterase activity .....	77
2.3.7.2. DNA staining .....	80
2.3.7.3. DNA gel retardation .....	80
2.3.8. Synthetic sarconesin .....	80
2.3.8.1. Purifying synthetic sarconesin .....	80
2.3.8.2. Mass spectrometry .....	81
2.3.8.3. Hemolytic activity .....	82
2.3.8.4. Antimicrobial assay and therapeutic index (TI) .....	83
2.4. Discussion .....	84
2.5. Conclusion .....	89
3. Chapter 3 .....	90
3.1. Objective .....	90
3.2. Materials and Methods .....	90
3.2.1. Bacterial strains .....	90
3.2.2. Antimicrobial assays .....	90
3.2.3. Acid and solid phase extraction .....	91
3.2.4. Peptide purification .....	91
3.2.5. Toxicity .....	91
3.2.6. Mass spectrometry and sarconesin II identification .....	92
3.2.7. Bioinformatics tools .....	92

---

3.2.8. Circular dichroism .....	93
3.2.9. Mechanism of action (MoA) .....	93
3.2.9.1. Membrane damage and esterase activity .....	93
3.2.9.2. DNA binding activity and fluorescence microscopy.....	93
3.2.9.3. Sarconesin II-treated <i>E. coli</i> cells total protein profiling .....	94
3.2.10. Determining cell morphology.....	94
3.2.10.1. Gram assay .....	94
3.2.10.2. Scanning electron microscopy (31).....	94
3.2.11. Statistical analysis .....	95
3.3. Results.....	95
3.3.1. Purifying <i>S. magellanica</i> ES sarconesin .....	95
3.3.2. Bacterial growth curve and toxicity .....	96
3.3.3. Mass spectrometry and sarconesin II characterization.....	97
3.3.4. Sarconesin II's secondary structure.....	101
3.3.5. Mechanism of action (MoA) .....	102
3.3.5.1. Membrane integrity .....	102
3.3.5.2. Sarconesin II effects on <i>E. coli</i> DNA and protein profile .....	103
3.3.5.3. Fluorescence microscopy assays .....	104
3.3.6. Determining Cell Morphology .....	105
3.3.6.1. Gram-stained <i>E. coli</i> cells.....	105
3.3.6.2. Examining bacterial membrane change by SEM .....	106
3.4. Discussion .....	107
3.5. Conclusion .....	113
4. Overall conclusions.....	114

5. References .....	115
6. Additional files .....	141
6.1. Publications .....	141
6.2. Awards.....	142
6.3. Oral presentations .....	145
6.4. Courses .....	149

---

List of Figures

Figure 1. Bacteria in wounds before (left) and after LT. Image taken from Jaklic <i>et al.</i> (23).....	25
Figure 2. Drosophila signaling pathways regulating systemic immune responses against bacterial, fungal and viral infection. Image taken from <a href="http://what-when-how.com/insect-molecular-biology-and-biochemistry/insect-immunology-part-2/">http://what-when-how.com/insect-molecular-biology-and-biochemistry/insect-immunology-part-2/</a> .....	35
Figure 3. AMP discovery timeline. Image taken from Yazici <i>et al.</i> (104) .....	35
Figure 4. AMPs identified in insects upon pathogen infection (bacterial or parasitic). Parasites are shown in red, AMPs in blue and insects in black; MPAC, mature prodomain of attacin C. The relationships discussed regarding insects and parasites is shown by phylogenetic trees. Figure taken from Boulanger <i>et al.</i> , (108).....	36
Figure 5. Events occurring on bacterial cytoplasmic membrane following initial AMP adsorption. The figure was taken from Nguyen (145). .....	41
Figure 6. AMPs (a–c) and their application timeline. Selected AMPs in use (orange, top) or in clinical trials (blue, bottom) are depicted. Figure taken from Mishra <i>et al.</i> (155).....	44
Figure 7. <i>Sarconesiopsis magellanica</i> . Original image by Andrea Díaz.....	47
Figure 8. Scheme representing the steps used for isolating, extracting and purifying AMPs and pertinent bioassays. Original scheme by Andrea Díaz. ....	49
Figure 9. <i>S. magellanica</i> ES chromatographic profile. This was obtained by RP-HPLC on a Jupiter C18 semi-preparative reverse phase column (Phenomenex). Chromatography involved using 0%-80% ACN/H <sub>2</sub> O/0.05% TFA gradients for 60 minutes at 2mL/min flowrate. Absorbance was monitored at 225 nm. The 67 fractions were collected manually and separately. Those having antimicrobial potential against <i>Micrococcus luteus</i> A270 are highlighted in blue (fraction 2). Those marked as having activity against <i>P. aeruginosa</i> are indicated in red, i.e. fractions 36, 44, 45, 46 and 57.....	53
Figure 10. Calibrating standard molecules by gel filtration chromatography using a Superdex Peptide HR 10/30 column at 0.5 mL/min flowrate and 280 nm absorbance. The FPLC weight patterns gave a lysozyme having a 14 KDa molecular weight and 12 min RT, a known peptide having 2.1 KDa with RT=28 min and the gilpone AMP having 0.637 KDa molecular weight and RT=40 min. ....	54

---

Figure 11. Fractionation chromatographic profile for molecules from fraction 2 by gel filtration chromatography using Superdex Peptide HR 10/30 column at 0.5 mL/min flowrate, 280 nm absorbance. Elution of the molecule at 34 min RT having 1.2 KDa molecular weight. ....55

Figure 12. *S. magellanica* fraction 2 chromatographic profile. This was obtained by FPLC. Chromatography involved using isocratic elution in H<sub>2</sub>O acidified with 0.05% TFA for 60 minutes at 1.0 mL/min flowrate. Absorbance was monitored at 225 nm. Three fractions were obtained, i.e. the peaks in the chromatogram (2.65, 3.03, 4.01 min RT); all were collected manually and separately and their antibacterial action against *M. luteus* was evaluated. The fraction eluted at 4.01 RT had antibacterial activity and the result was sent for MS analysis. ....55

Figure 13. FPLC chromatographic purification profile for *S. magellanica* fraction 2 obtained from RP-HPLC at 4.01 min RT. ....56

Figure 14. Chromatographic profile for *S. magellanica* fraction 36. This was obtained by RP-HPLC on a Jupiter C18 analytical reverse phase column (Phenomenex). Chromatography involved using 30%-45% ACN/H<sub>2</sub>O/0.05% TFA gradients for 60 minutes at 1.5mL/min flowrate. Absorbance was monitored at 225 nm. Two fractions were obtained, i.e. the peaks observed in the chromatogram (12 and 14.5 min RT); both were collected manually and separately and their antibacterial action was evaluated. The fraction eluted at 12 min RT had antibacterial activity and the result was sent for MS analysis.....56

Figure 15. Chromatographic profile for *S. magellanica* fraction 44. This was obtained by RP-HPLC on Jupiter C18 analytical reverse phase column (Phenomenex). Chromatography involved using 44%-54% ACN/H<sub>2</sub>O/0.05% TFA gradients for 60 minutes with 1.5mL/min flowrate. Absorbance was monitored at 225 nm. Thirteen fractions were obtained, i.e. the peaks in the chromatogram (3.65, 5.78, 9.32, 9.99, 10.18, 10.57, 11.64, 12.01, 12.41, 13.6, 14.09, 15.53, 49.40 min RT); all were collected manually and separately and their antibacterial action against *M. luteus* was evaluated. The fraction eluted at 3.65 min RT had antibacterial activity and the result was sent for MS analysis. ....57

Figure 16. Chromatographic profile for *S. magellanica* fraction 45. This was obtained by RP-HPLC on a Jupiter C18 analytical reverse phase column (Phenomenex). Chromatography involved using 44%-54% ACN/H<sub>2</sub>O/0.05% TFA gradients for 60 minutes with 1.5mL/min flowrate. Absorbance was monitored at 225 nm. All the fractions were collected manually and separately and their antibacterial action against *M. luteus* evaluated. The fraction eluted at 14.58 RT had antibacterial activity and the result was sent for MS analysis.....58

Figure 17. Chromatographic profile for *S. magellanica* fraction 46. This was obtained by RP-HPLC on a Jupiter C18 analytical reverse phase column (Phenomenex). Chromatography involved using 44%-54% ACN/H<sub>2</sub>O/0.05% TFA gradients for 60 minutes at 1.5 mL/min flowrate. Absorbance was monitored at 225 nm. Fifteen fractions were obtained, i.e. the peaks in the chromatogram (3.9, 11.6, 12.4, 12.7, 13.01, 13.3, 13.68, 14.1, 14.64, 15.43, 15.7, 16.3, 17.2, 18.2, 19.77 min RT), all were collected manually and separately and their antibacterial action against *M. luteus* evaluated. The fraction eluted at 3.9 min RT had antibacterial activity and the result was sent for MS analysis. 59

Figure 18. Chromatographic profile of *S. magellanica* fraction 57. This was obtained by RP-HPLC on Jupiter C18 analytical reverse phase column (Phenomenex). Chromatography involved using 60%-70% ACN/H<sub>2</sub>O/0.05% TFA gradients for 60 minutes with 1.5mL/min flowrate. Absorbance was monitored at 225 nm. Thirteen fractions were obtained, i.e. the peaks in the chromatogram (4.01, 4.4, 6.2, 10.69, 11.44, 11.98, 12.7, 13.06, 14.14, 14.68, 15.8, 16.9, 25 min RT); all were collected manually and separately and their antibacterial action against *M. luteus* evaluated. The fraction eluted in 4.4 min RT had antibacterial activity and the result was sent for MS analysis. ...60

Figure 19. *S. magellanica* ES antimicrobial fractions eluted with 80% ACN from a Sep-Pak cartridge obtained from the first RP-HPLC purification step. Chromatography involved using a semi-preparative Jupiter C18 column (10µm; 300A; 10mm x 250mm) with a 0-80% ACN/0.05% TFA in H<sub>2</sub>O/0.05% TFA linear gradient for 60 min at 2 mL/min flowrate. Absorbance was monitored at 225 nm. The fractions indicated by an asterisk had antimicrobial activity and were eluted at 8.1, 50.9, 51.7, 52.1 and 64.9 min RT; fraction 3 (labelled with an arrow) was chromatographed again in the same system with an analytic Jupiter C18 column (10um; 300A; 4.6mm x 250mm) and run in 44%-54% solution B for 60 min (inset). The eluted 3.2 fraction (i.e. sarconesin) had antibacterial activity and was purified. ....70

Figure 20. Growth curve and toxicity assays. (A) Growth curve for *M. luteus* A270 incubated with sarconesin. Bacterial growth was inhibited and the antibacterial effect was detected during the exponential phase. (B) Sarconesin cytotoxicity regarding the VERO cell line and (C) hemolytic activity regarding fresh human RBC, showing very low toxicity, even at maximum 600 µM concentration. ....73

Figure 21. The complete sarconesin aa sequence was obtained by MS/MS fragmentation; representative de novo sequencing of sarconesin. CID spectrum from mass/charge (m/z) of its double-charged ion gave [M+2H]<sup>2+</sup>, m/z 736.9266. The ions from y (red) and b (blue) series (marked at the top of the spectrum) represent the primary

structure: TPm(+16)LLVGTKLDR. The sequenced peptide's internal fragments whose ions were found in the spectrum are represented by standard aa letter code.....73

Figure 22. Sarconesin alignment and protein model. (A) Sarconesin multiple sequence alignment against selected proteins (<https://www.ncbi.nlm.nih.gov/>): CDC42 cell division control protein 42 homologue OS=*Bos taurus* (Q2KJ93), CDC42\_HUMAN Chain A, structure of the Rho family Gtp-binding protein Cdc42 in complex with the multifunctional regulator Rhogdi (gi|7245832|1DOA\_A), CDC42\_DROME Cdc42 homologue OS=*Drosophila melanogaster* GN=Cdc42 PE=1 SV=1 (P40793), Ras-related protein Rac1 [*Lucilia cuprina*] GenBank: KNC23156.1. Sarconesin has 100% sequence similarity with CDC proteins and 69% with Rac from *L. cuprina*. Translated sequences from *L. sericata*. Genome scaffold (JXPF01028806.1), transcriptomes ERR658157.2222021.1 and pupa SRR350018.17744834.1 genome scaffold (JRES01000256.1) and *L. cuprina* transcriptome SRR1853100.27006533.2. (B) Conserved domains found in JXPF01028806.1 *L. sericata* Blastp, showing sarconesin as a conserved residue from the CDC42 domain. (C) Representative model of human CDC42 (PDB ID: 1DOA\_A). Sarconesin is encrypted in a site between residues 111 and 123 (215), which folds as a  $\beta$ -sheet.....75

Figure 23. Sarconesin CD spectra in water and different TFE/water ratios. ....77

Figure 24. Representative image showing the change in mean fluorescence intensity of fluorescence probes PI and CFDA (esterase activity) in *E. coli*. Histogram represents changes in the mean  $\pm$  SD of PI and CFDA fluorescence, obtained from three independent experiments (\*\*p < 0.05 vs. control). ....78

Figure 25. Confocal microscopy analysis of bacteria incubated with sarconesin. PBS-, ciprofloxacin- and sarconesin-treated bacteria stained with DAPI (1-3). PBS- and sarconesin-treated bacteria stained with PI (4-5). ..79

Figure 26. Sarconesin interaction with bacterial gDNA by gel migration assay. M: DNA marker GeneRuler 1Kb; 1-8: sarconesin concentrations were 0, 3.1, 6.25, 12.5, 25, 50, 100 and 200  $\mu$ M.....80

Figure 27. Chromatogram of RP-HPLC purification step from *S. magellanica* sarconesin synthetic peptide. Chromatography involved using a semi-preparative Jupiter C18 column (10 $\mu$ m; 300A; 10mm x 250mm) with a 0-80% ACN/H<sub>2</sub>O/0.05% TFA linear gradient for 120 min at 2 mL/min flow rate. Absorbance was monitored at 225 nm. Synthetic sarconesin was collected at TR=101 (Figure 9A), zoom image (B). ....81

Figure 28. CID spectrum for sequenced synthetic sarconesin. The ions belonging to -y (red) series indicated at the top of the spectrum show the peptide's primary structure: TPFLLVGTQIDLR. Internal fragments of the sequenced peptide, whose ions were found in the spectrum, are represented by standard aa code letters...82

Figure 29. Synthetic sarconesin hemolytic activity after 1 hour treatment. The peptide's concentration-response curve for percentage hRBC lysis is shown. IC<sub>50</sub>=1100  $\mu$ M dose-dependent hemolytic effect of sarconesin on hRBC. The control for 100% hemolysis was a sample of erythrocytes treated with 0.1% Triton-X 100. Peptide concentration is given in  $\mu$ M. GraphPad Prism was used for analyzing IC<sub>50</sub> data. Parameters: non-linear regression; (mean  $\pm$  standard deviation, n= 3).....83

Figure 30. RP-HPLC profile of lyophilized larval ES crude extract at 225 nm eluted on a Jupiter C18 Column (10 mm  $\times$  250 mm, 10  $\mu$ m; 300  $\text{\AA}$ ), using a 0–80% B linear gradient for 80 min with solvent A (0.05% TFA/can) and solvent B (0.05% TFA/H<sub>2</sub>O) at 1.5 mL/min flowrate. Inset: sarconesin II fraction labelled with an asterisk was chromatographed in the same solvent system on a Jupiter C18 column (4.6 mm  $\times$  250 mm, 10  $\mu$ m; 300  $\text{\AA}$ ) using a 30%–45% B linear gradient for 60 min.....95

Figure 31. Sarconesin II's effect in toxicity assays. (a) Growth curve for *E. coli* DH5 $\alpha$  incubated with sarconesin II MIC. Bacterial growth was inhibited at 240 min. (b) HeLa cell CC measured by MTT tetrazolium assay. Cells were incubated with sarconesin II at 25, 50 and 100  $\mu$ M for 24 h. Untreated HeLa cells were used as negative control and HeLa cells treated with 30% DMSO were used as positive control. (c) Hemolytic activity against hRBC. Sarconesin II was tested at 25, 50 and 100  $\mu$ M concentrations. PBS was added without peptide for determining 0% hemolysis. The arrow indicates the concentration at which the fraction had antimicrobial activity. The average of each experiment done in triplicate is presented in individual columns as mean  $\pm$  SD. One-way ANOVA followed by post hoc Dunnett's multiple comparison test was used. \*\*\* $p$  < 0.001.....97

Figure 32. MS/MS fragmentation was used to obtain the complete sarconesin II aa sequence. The CID spectrum from mass/charge ( $m/z$ ) of its double-charged ion gave  $[M + 2H]^{2+}$ ,  $m/z$  720.3984. The ions from y (red) and b (blue) series (marked at the top of the spectrum) represent the primary structure: VALTGLTVAEYFR. ....98

Figure 33. Sarconesin II sequence and conserved domains. (a) Sarconesin II spectrum match indicated by a blue line below the mitochondrial KNC23160.1 ATP synthase subunit beta sequence [*Lucilia cuprina*]. Sarconesin II was found between residues 260 and 274, covering 3% of the whole protein sequence. Sequences in green represent tryptic peptides. (b) Sarconesin II sequence embedded in *Calliphoridae* multiple sequence alignment search (301) shows the putative conserved domain. Sarconesin II appears as an ATP synthase beta subunit protein conserved residue belonging to the Fli-1 superfamily. (c) Representative model of the mitochondrial ATP synthase subunit beta (PDB ID: 2w6j) built with Chimera (215). Sarconesin II is exposed on the surface (red). ....100

Figure 34. Sarconesin II secondary structure. (a) A Jasco-1500 CD spectrophotometer was used for measuring sarconesin II's CD spectrum. Sarconesin II CD spectra variation at 0%, 30%, 70% and 100% trifluoroethanol (TFE) concentrations (b). I-TASSER sarconesin II secondary structure gave an  $\alpha$ -helix, depicted in spiral ribbon format, using ordinary colors. (c) Computation of sarconesin II  $\alpha$ -helical wheel (320). No hydrophobic face reported. Note slightly opposite arrangement of hydrophobic (yellow) versus charged (red, blue) aa.....102

Figure 35. PI and esterase change mean fluorescence of bacteria treated with sarconesin II MIC concentration (B). PI incorporation showing membrane-damaged bacteria. Treated cells (B) showing increased PI and CFDA fluorescence when incubated with sarconesin II. Esterase activity determined by 5,6-carboxyfluorescein diacetate cleavage, expressed as a percentage of control PBS (A) activity. Data is expressed as mean  $\pm$  SD ( $n = 3$ ). \* $p < 0.001$ : significantly different from the control. ....103

Figure 36. Assays for evaluating sarconesin II effects on *E. coli* DNA and proteins. (a) Gel retardation assay for evaluating sarconesin II effect on DNA. M, GeneRuler 1kb DNA ladder; 1–3. Sarconesin II concentrations were 0, 25, 50  $\mu$ M, showing proportionally suppressed migration regarding the increased amount of peptide compared to bDNA. The fourth concentration at 100  $\mu$ M showed that migration was suppressed, suggesting sarconesin II interaction with DNA. (b) Changes in protein profile for *E. coli* treated with sarconesin II. Cells treated with or without sarconesin II were washed and sonicated in lysis buffer and the protein profile was analyzed in 12% SDS-PAGE; proteins were visualized by silver nitrate staining. M, molecular weight marker (kDa) (SeeBlue Invitrogen). The streptomycin control (2) revealed no protein profile. There was no difference regarding sarconesin II (3)-treated bacteria compared to the PBS control (1) protein profile, suggesting no peptide action on proteins.....104

Figure 37. Fluorescence microscopy of *E. coli* cells incubated for 4 h at 37°C and stained with PI (321) or DAPI (blue). Untreated control cells, PBS (A), cells treated with sarconesin II (B), cells treated with ampicillin for PI or ciprofloxacin for DAPI (C). PI assay revealed bacterial membrane alteration when treated with sarconesin II and DAPI-stained cells had partial fluorescence, showing DNA fragmentation by sarconesin II. ....105

Figure 38. Confocal microscopy image obtained from *E. coli* bacterial cultures incubated for 4 h with PBS (a) or sarconesin II (b). Cultures were obtained after 4 h incubation at 37°C. The arrow indicates filamentous cell morphology.....106

Figure 39. Sarconesin II MIC effect on *E. coli* bacterial membrane by SEM (30). Untreated *E. coli* (A) had a normal smooth surface, while treatment with sarconesin II (B) gave an elongated pattern, membrane disruption

and blebbing on the outer face (arrows). Some bacteria had variable length, rough cell surfaces or globular protrusions on their surfaces. These images revealed that sarconesin II could induce alterations in cell morphology.

.....106

---

*List of Tables*

Table 1. Species of flies used in maggot therapy. Image taken from Sherman 2000 (10) .....	31
Table 2. <i>S. magellanica</i> ES isolated fractions and ACN elution concentration (%) .....	53
Table 3. Sequences obtained by MS from fractions having antimicrobial activity after second fractionation by RP-HPLC with C18 analytic column. ....	61
Table 4. Minimum inhibitory concentration (MIC); MIC refers to the concentration needed for achieving 100% inhibition of growth. ....	71
Table 5. Physicochemical parameters calculated using ExPASy PepDraw and Pep-Calc.com (accessed April 30 <sup>th</sup> 2018).....	74
Table 6. Synthetic sarconesin antimicrobial activity against different strains. ....	84
Table 7. Sarconesin II's antibacterial activity spectrum. ....	96
Table 8. Sarconesin II's theoretical physicochemical properties. ....	98
Table 9. Known antimicrobial peptides having similarity with sarconesin II, as identified in the Antimicrobial Peptide Database (APD2) (Wang <i>et al.</i> , 2009). ....	101

*Abbreviations*

ACN: Acetonitrile

AMP: antimicrobial peptide

°C: degrees Celsius

µg: micrograms

µM: micromolar

µL: microliter

Å: Angström

Abs: absorbance

Blast: basic local alignment search tool

CID: collision induced dissociation

CFU: colony-forming unit

RP-HPLC: reverse phase - high performance liquid chromatography

Da: Dalton

DNA: deoxyribonucleic acid

ESI: electrospray ionization

FA: Formic acid

Fmoc: fluorenylmethyloxycarbonyl

g: gravity

h: hours

kDa: kilodalton

L: liter

LC: liquid chromatography

LETA: Laboratório Especial de Toxinologia Aplicada

min: minute

mL: milliliter

mM: millimolar

MTT: 3-(4,5-dimethylthiazol-2-yl)-2,5-diphenyltetrazolium bromide

OD: optical density

PB: poor broth

PBS: Phosphate-buffered saline

pH: potential of hydrogen

TFA: trifluoroacetic acid

RT: retention time

*Amino acid list*

Alanine	A
Arginine	R
Asparagine	N
Aspartic acid	D
Cysteine	C
Glutamic acid	E
Glutamine	Q
Glycine	G
Histidine	H
Isoleucine	I
Leucine	L
Lysine	K
Methionine	M
Phenylalanine	F
Proline	P
Serine	S
Threonine	T
Tryptophan	W
Tyrosine	Y
Valine	V

## 1. Chapter 1

# Isolating and characterizing antimicrobial peptides derived from larvae of the blowfly *Sarconesiopsis magellanica*

## 1.1. Introduction

### 1.1.1. Larval therapy

Larval therapy (LT) is a simple, safe and highly successful natural method for healing chronic wounds; its action has been scientifically proven as using four primordial mechanisms: cleaning necrotic tissue, disinfection (2-5), inhibiting and eradicating biofilms (6-8) and stimulating granulation tissue growth (4, 9-13).

LT is an old technology that was used and recognized in the 1930s (14-16), being popular in many European and North American countries where more than 300 hospitals used it; however, it was abandoned later on in 1940 as a result of growing interest in antibiotics and surgical advances (17). There was a resurgence of awareness in it in 1989 as a means of combating bacterial resistance to antibiotics and treating difficult-to-heal chronic wounds (4, 11). Around 15,000 patients are treated with this technology annually in Europe and it is also used in most countries around the world (18).

### 1.1.2. Wounds and incidence

A wound is the loss of tissue continuity (19). Wounds are classified according to their healing time as acute or chronic. Acute wounds arise as a result of burns, surgeries or trauma and heal in an orderly way (2). Unlike these, chronic wounds are due to a physio-pathological condition, such as vascular insufficiency or underlying disease; these chronic wounds include arterial, venous, pressure or diabetic ulcers (20). These wounds do not heal normally, remaining infected during the inflammatory stage and inhibiting cell proliferation, remodeling incomplete extracellular matrix, thus requiring a longer healing time which can be longer than 6 weeks (21). The incidence of these wounds in the adult population is

0.18% to 1.3%, of which 75-80% are vascular insufficiencies, 5% pressure ulcers and 15-25% diabetic foot ulcers (22).

Open lesions enable microorganism entry which can lead to infection, recognized by redness, swelling, pain and heat. A wound provides the necessary environment for the proliferation of microorganisms found in/on the skin and which are normally harmless but can become pathogenic in a wound (23). Figure 1 shows the bacteria frequently found in wounds, the most frequently occurring being *S. aureus* and *P. aeruginosa* (24) (Figure 1).

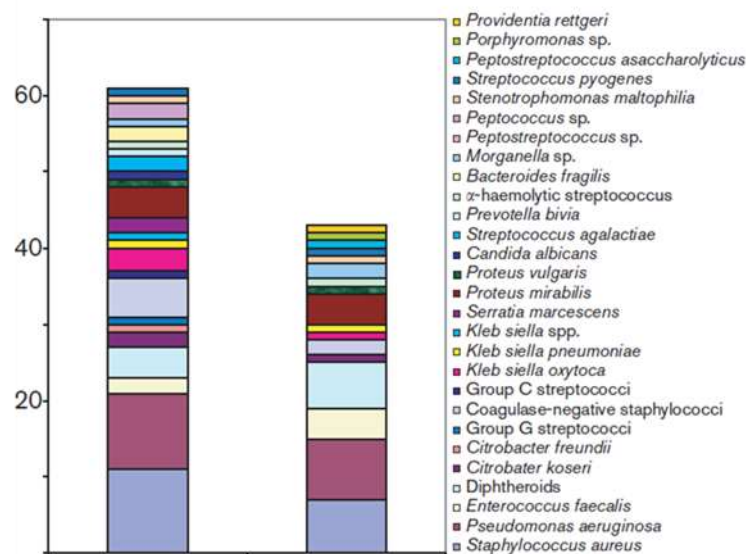


Figure 1. Bacteria in wounds before (left) and after LT. Image taken from Jaklic *et al.* (24).

### 1.1.3. LT mechanism of action (MoA)

Despite the beneficial effects of larval therapy since ancient times, its mechanisms of action (MoA) have only been better understood in relatively recent years. The larvae induce wound healing through the following MoA: removing necrotic tissue / debridement (25), stimulating granulation tissue (25, 26), inhibiting and eliminating biofilms (7, 8) and having an antibacterial effect (3, 4, 15, 21). Research into the mechanisms underlying the clinical effects of LT larval has led to identifying and isolating some molecules having proteolytic, antimicrobial activities and promoting chronic wound healing (27, 28).

#### 1.1.3.1. Debridement

It has been shown that when larvae meet their cephalic end when in contact with a wound, they can rapidly dissolve necrotic tissue as a result of collective proteolytic enzyme excretion and secretion (ES). These enzymes include collagenase and other enzymes having the same activity as trypsin, leucine aminopeptidase and carboxypeptidases A and B. The enzymes digest the extracellular matrix and increase the degree of tissue oxygenation so that necrotic tissue becomes eliminated. Larvae are indeed living chemical factories; they move on the surface of a lesion, secreting a mixture of proteolytic enzymes that dissolve the dead tissue so that this liquid is subsequently sucked up and ingested by them (29). Larval ES products include protease complexes (30). Some of these proteases have been identified as serine proteases and have been found in species such as *L. cuprina*, *Stomoxys calcitrans*, *Hypoderma lineatum*, *Chrysomya bezziana*, *Cochliomyia hominivorax* and *Haematobia irritans* (31, 32). Similarly, serine proteases have been found in wound fluids that are treated with LT, suggesting that they are released during debridement (33).

Once the necrotic tissue has been enzymatically liquefied, the larvae ingest and digest the resulting "soup". This action implies that any bacteria and possibly other microorganisms are subsequently lysed as they pass through the larvae's digestive tracts. Antibacterial activity seems to be mediated by several components, among which *Proteus mirabilis* is a commensal of larval intestine and which secretes two agents having antibacterial activity, identified as phenylacetic acid and phenylacetaldehyde having particular action in the intestine's low pH (11, 21).

#### 1.1.3.2. Granulation tissue

Initial theories regarding the effect of larvae on wounds highlighted larvae's physical action through their tracking movements in the lesion, stimulating the appearance of granulation tissue and promoting healing (34). This criterion was supported later on by the observation that larvae improved tissue oxygenation in chronic wounds (35). Furthermore, scientists have long suggested that the action of some substances excreted by *L. sericata*, such as allantoin (2,5-Dioxo-4-imadazolidinyl urea) or ammonium bicarbonate (36), could stimulate granulation tissue growth. In effect, Robinson in 1935, demonstrated stimulation of local granulation tissue growth by using these substances in wounds (36).

More recently, Prete (1997) found that food secretions and *L. sericata* hemolymph acting on human fibroblast tissues stimulated cell proliferation (26). This author observed that larval extracts caused significant fibroblast growth in the presence of the epidermal growth factor. Other researchers have pointed out that fibroblast proliferation is only one aspect of granulation tissue formation and that additional mechanisms may be involved. Thus, for example, Chambers *et al.*, (2003), indicated that when larvae are introduced into necrotic wounds they influence wound healing events with proteases in ES which are involved in remodeling components of the extracellular matrix (25). These authors suggested that proteinases cause fibrin lysis of the extracellular matrix, releasing proliferative factors (such as fragments of fibronectin) causing favorable effects in wound healing. Likewise, the metalloproteinases in ES are involved in collagen degradation to facilitate remodeling and keratinocyte migration (25). Previous researchers believed that a particular type of enzyme having trypsin-like activity could play an important role regarding the protease-activating receptor mediating cytokine proliferation in a wound (37).

Another action, no less important in LT-related lesion healing is the chemotaxis of several substances forming part of larval ES which enhance a patient's immune system through proinflammatory agents, involving cytokines and interferon gamma. These substances stimulate vasodilation and increase capillary permeability by enabling the extravasation of polymorphonuclear leukocytes and macrophages targeting a lesion site (4, 27, 38), acting against microbial agents, promoting granulation tissue and wound scarring.

#### 1.1.3.3. Antibacterial activity

Researchers began to study the underlying mechanisms regarding some of the beneficial effects of LT. The main focus of interest in the early 1930s was to examine the antimicrobial activity of the components of larval secretions and excretion products. In one of Simons' early studies (39), larval ES obtained from non-sterile *L. sericata* larvae were found to have considerable antimicrobial activity against some species of pyogenic bacteria which became removed following 5 or 10 minutes' exposure. Two decades later, Pavillard & Wright (40) used paper chromatography to show that larval washes combined with a suspension of their ES could be fractionated. The fraction was active against *S. aureus*. Relatively pure samples of the fraction of the antibiotic were obtained by using a cellulose column and

a modification of the chromatography technique. A series of injections of this preparation protected mice from the lethal effects of intraperitoneal inoculation with pneumococci. Final purification of this active compound was never done. Subsequent research by different laboratories showed that *L. sericata* larval ES contained a variety of alkaline compounds inhibiting bacterial growth and increasing pH, thus creating optimum conditions for the activity of the proteolytic enzymes secreted by the larvae liquefying necrotic tissue (41). It has been proposed that larvae release antimicrobial ingredients into wounds in response to infection. Some such ingredients are low molecular weight bacteriostatic compounds, such as p-hydroxybenzoic acid, p-hydroxyphenylacetic acid, dioxopiperazine proline (42) and an enigmatic compound having the empirical formula  $C_{10}H_{16}N_6O_9$ , known as seraticin (an antibiotic) (2). The other compounds may be antimicrobial peptides (AMPs) from the immune system which are released into wounds, thereby contributing to their healing (3, 10).

These insect peptides belong to the groups of dipterocins, cecropins and defensins (43, 44). Much research aimed at studying antibacterial activity against Gram-positive and Gram-negative germs has led to inconsistent findings. Some studies have revealed that larval ES are poorly effective against *S. aureus* and even less so against Gram-negative bacteria such as *Pseudomonas aeruginosa* and *Acinetobacter baumannii* (7); others have identified larval ES antibacterial molecules giving optimal results when evaluating their action against bacteria (17, 24, 42, 45, 46).

The reasons for such apparent discrepancy are not entirely clear; however, this may have been due to the different methods used for collecting larval ES, the types of assay used for detecting antimicrobial effects and the use of different larval ES concentrations (47).

For example, Bexfield *et al.*, (46) collected sterile larval ES and used different types of assay for evaluating antibacterial activity. The inhibition zone assay did not detect antibacterial activity, whereas the turbidimetric method demonstrated a significant reduction of bacterial growth regarding a significant amount of species, including *S. aureus* and *Escherichia coli*. However, such antibacterial effect was lacking against *S. aureus* and *P. aeruginosa* when these were evaluated using colony forming unit (CFU) assays and minimal inhibitory concentration (MIC). Mumcuoglu *et al.*, (4) demonstrated that the larvae ingested fluorescent bacteria and that these subsequently became reduced in the gastrointestinal tract, suggesting that the bacteria became destroyed in such microhabitat. By contrast, Daeschlein *et al.*,

(48) evaluated larval ability to ingest and excrete bacteria, finding that these microorganisms could be detected in viable form in larval intestine 48 hours after being exposed. However, it has recently been reported that bacterial control by genes controlling virulence led to increased consumption of these microorganisms by the larvae (49).

AMPs have been isolated from purified larvae in just *L. sericata* (45), *L. cuprina* (50) and *Calliphora vicina* (51), while lucifensins have been isolated from larvae, purified, characterized and evaluated. They have been shown to be mainly effective against Gram-positive bacteria, such as MRSA and its strains (52, 53). Among the most recent studies on AMPs isolated from flies from the Calliphoridae family different to those obtained from larval ES, it is worth mentioning a study by Yakovlev *et al.*, (2017) (54) who studied AMPs in culture medium from both fat bodies and hemocytes derived from *Calliphora vicina* larvae. They demonstrated that both cell types synthesized and released an AMP complex to the culture medium, containing defensins, cecropins, dipterocins and proline-rich peptides. Another study applied AMPs extracted from *C. vicina* larval hemolymph in environments extremely contaminated by germs forming biofilms (in *in situ* and *in vitro* conditions), highlighting strong destructive matrix activity and for the bacteria adhered to it; these bacteria (i.e. *Escherichia coli*, *Staphylococcus aureus* and *Acinetobacter baumannii*) were resistant to conventional antibiotics (55). This AMP complex containing a combination of defensins, cecropins, dipterocins and proline-rich peptides, and interacting synergistically with various classes of antibiotics, produced much stronger action targeting bacterial strains (*Staphylococcus aureus*, *Escherichia coli*, *Pseudomonas aeruginosa*, *Klebsiella pneumoniae* and *Acinetobacter baumannii*) and biofilm materials compared to the antibacterial effect on the same strains in a planktonic culture model (56).

#### 1.1.3.4. Biofilm eradication

Adherent bacteria in wounds can form micro-colonies producing a resistant and protective layer called biofilm. Biofilm-associated infections are notoriously difficult to treat; many topical treatments are not effective and antibiotics often fail to destroy bacteria in the biofilm (57). It has been established that bacterial biofilms play an important role in infection and the colonization of chronic wounds (58). For example, 60% of the samples taken from 77 individuals' chronic wounds in a relatively recent work

---

showed that they contained biofilms and, conversely, only 6% of acute wound samples had this structure (59).

It is widely accepted today that biofilms contribute towards wound chronicity (57, 60). Some research has shown that larval secretions break the established biofilm (59, 61), inferring an important role for AMPs in such action. Furthermore, it has been found that larval ES not only destroy biofilms but also prevent their formation on abiotic surfaces, such as polyethylene, surgical stainless steel and titanium (61, 62). It has been shown that larval ES degrade *S. aureus* biofilms (63). Likewise, such substances (when starting activity on biofilm) cause the release of bacteria associated with it and which are thus exposed to the action of the immune system and antibiotics if they are simultaneously attacked by both mechanisms and substances. It has been established that larval ES do not affect many antibiotics' antibacterial action in these conditions and, when used at high concentrations, improve the antibacterial action of molecules (antibiotics), i.e. daptomycin, gentamicin and flucloxacillin (62, 63).

It has been shown recently that a larval ES-derived recombinant chymotrypsin was responsible for degrading a protein-dependent mechanisms involved in bacterial biofilm formation; however, this protein's major effect was evidenced on *S. epidermidis* 5179-R1 nascent and established biofilms (37). The aforementioned chymotrypsin has been used efficiently for degrading molecules in chronic venous ulcers of the lower limbs and it has been shown that its action persisted in an environment having intrinsic gelatinase activity (64).

Researchers have also pointed out recently that externalized larvae collected from larvae pre-treated with bacteria prevented the formation of *P. aeruginosa* biofilms, having two dependent characteristics (65). Initial studies suggested that the expression of antibacterial molecules in larval ES can be induced, instead of being constitutive (42, 66). For example, antibacterial activity increased three- to six-fold when larvae removed from chronic wounds were compared to other sterile larvae (42). Kawabata *et al.*, (66) established that previously-infected larvae had higher antibacterial capability than sterile larvae. These researchers argued that the wounds' clinical situation could enable larvae in an infected environment to influence the production of their antibacterial activity. However, such hypothesis has not been clinically confirmed (67).

#### 1.1.4. Diptera

Flies, from the order Diptera, mainly belonging to the Calliphoridae family, have been used for LT, including *Calliphora vicina*, *Chrysomya rufifacies*, *C. megacephala*, *Lucilia caesar*, *L. cuprina*, *L. illustris*, *L. sericata*, *Phormia regina*, *Cochliomyia macellaria*, *Protophormia terraenovae* and *Sarconesiopsis magellanica*; the species *Wohlfahrtia nuba* from the Sarcophagidae family and *Musca domestica* from the Muscidae have also been used (Table 1) (11).

Table 1. Species of flies used in maggot therapy. Image taken from Sherman 2000 (11)

Family	Species	References
Calliphoridae	<i>Calliphora vicina</i>	Teich 1986 (130)
	<i>Chrysomya rufifacies</i>	
	<i>Lucilia caesar</i>	Baer 1931 (4), McLellan 1932 (78)
	<i>Lucilia cuprina</i>	Fine & Alexander 1934 (38)
	<i>Lucilia illustris</i>	Lectercq 1990 (70)
	<i>Lucilia sericata</i>	Baer 1931 (4)
	<i>Phormia regina</i>	Baer 1931 (4)
		Horn et al 1976 (64)
		Horn et al 1976 (64)
		Robinson 1933 (101)
	Reames 1988 (100)	
	Lectercq 1990 (70)	
Sarcophagidae	<i>Protophormia terraenovae</i>	
	<i>Wohlfahrtia nuba</i>	Grantham-Hill 1933 (44)
Muscidae	<i>Musca domestica</i>	

The taxonomic classification of the species *S. magellanica* from the subfamily Toxotarsine is as follows: Kingdom: Animalia. Phylum: Arthropod. Class: Insect. Order: Diptera. Suborder Brachycera. Family: Calliphoridae. Subfamily: Toxotarsine. Genus: *Sarconesiopsis*. Species: *Sarconesiopsis magellanica*. The synonyms used for this species are: *Sarconesia magellanica*, and *Sarconesiopsis chilensis*.

This species has been reported in Argentina (68), Bolivia, Chile, Colombia, Ecuador and Peru (69). It has been described by Figueroa-Roa *et al.*, (70) in Valdivia, Chile, from 1996-1997, as non-synanthropic species since it had a -6.3 synanthropic index (such index varies from +100 to -100, the first value representing the highest degree of association with man, while negative values show aversion to a human environment) indicating a poor relationship with man. Mariluis & Peris (71) described the species as living at heights greater than 900 masl; it is distributed in the Colombian departments of Boyacá and Cundinamarca (i.e. more than 2,000 masl) (72). *S. magellanica* has been reported as being the first colonizing species of decomposing pigs in Bogotá (a biomodel animal similar to humans) (73), specifically in an urban area of Bogotá (74, 75). Its antibacterial activity has been confirmed, giving better

---

results than those for *L. sericata* (76) and it has already been evaluated regarding LT, leading to good effects concerning diabetic wound healing (77) and in *Leishmania*-related lesions (77).

#### 1.1.5. Insects' innate immune system

Arthropods' immune system mechanisms are one of the factors which have led species to survive for so long in contaminated environments containing pathogenic microorganisms. The innate immune system's humoral and cellular responses become activated when a microorganism crosses arthropods' physical-chemical barrier (as in other living beings), i.e. the cuticle (78).

##### 1.1.5.1. Cellular response

Immune system cells (hemocytes) are also related to the phagocytosis, nodulation, microorganism encapsulation and the storage of molecules involved in humoral responses (78-80). The insects' hemocytes are the equivalent of vertebrates' blood cells (81). The hemocyte types most frequently encountered in insects are prohemocytes, spherulocytes, oocytes, granulocytes and plasmatocytes (82).

Phagocytosis involves plasmatocytes and oenocytoids and is a form of endocytosis in which particles foreign to the organism are recognized and sequestered into the cells in large vesicles (82). These vesicles are fused to lysosomes, in phagolysosomes, where exogenous material is digested. The remains of digested cells are expelled from a phagocytic cell through exocytosis, according to Götz & Boman, 1985, as reported by Brooks (83).

Hemocyte aggregation occurs in nodulation where one or more cell types can be recruited, in the sense of aggregating and retaining microorganisms or biotic and foreign abiotic materials (84, 85). The nodules contain pathogens more efficiently and synthesize the melanin around phagocytose, thereby accelerating elimination of infection (86).

Cellular encapsulation is an immune mechanism in which layers are formed, overlying foreign bodies and too large cells, or cells become trapped by nodules, such as invasive parasites' nematodes, eggs or larvae (87, 88). Furthermore, a pathogen can be killed within the capsule by the production of free radicals (such as nitrogen and oxygen reactants) from the hemocytes involved in encapsulation (85, 89). Encapsulation may also be associated with melanization due to profenoloxidase (PPO) system

---

(humoral response) activation, leading to the death of the microorganism by hypoxia (90); melanin is also responsible for cuticle sclerotization, wound healing and immune defense (91).

#### 1.1.5.2. Humoral response

The humoral immune system involves the specific synthesis of molecules, peptides or enzymes that may act toxically on an invasive microorganism, and includes AMPs, lysozymes, ROS and the PPO cascade (79, 92).

The PPO cascade occurs when a pro-enzyme (prophenoloxidase) is converted to phenoloxidase and catalyzes the oxidation of the phenolic compounds in hemolymph and the cuticle (93), thereby reducing the hemolymph when it becomes exposed to air and thus producing melanin (94). Laccase type enzymes are related to cuticle sclerotization and darkening while the other type has tyrosine activity, being able to hydroxylate tyrosines and oxidize diphenols in quinones (79, 95, 96). The oocytes are responsible for PPO synthesis in moths and mosquitoes' hemocytes (97, 98) while crystal cells synthesize them in *Drosophila* (99, 100).

Lysozymes catalyze the hydrolysis of the 1,4-glycosidic linkage between N-acetylmuramic acid and N-acetylglucosamine in peptidoglycans in the cell walls of many bacteria, causing cell lysis (101). Lysozymes play a digestive role, especially in insects ingesting a large amount of bacteria from their food source (101); they assume an immune function, preventing the systemic proliferation of microorganisms as well as acting in synergism with other immunological factors (102). Lysozymes' primary structures are known in the giant silk moth (*Hyalophora cecropia*), the tobacco horn worm (*Manduca sexta*) and the fruit fly (*Drosophila melanogaster*) (101).

ROS are free radicals produced by metabolic processes such as the ingestion and digestion of blood in hematophagous insects, and also by parasite infection (103, 104). Free radicals have an unpaired electron in the last layer, which defines their great oxidative potential. ROS interact with microorganisms' cell membranes through the peroxidation of lipids, proteins and DNA (105, 106), focusing antimicrobial agents helping in the fight against infection and also in controlling insects' intestinal microbiota (107). It has been observed that ROS are actively produced in low levels in the

digestive tract of *Drosophila*; however, oral infection with the bacteria greatly increases the production of these reagents (108).

### 1.1.5.3. Signaling pathways regulating the immune response

Three major *Drosophila* signaling pathways regulate systemic immune responses against bacterial, fungal and viral infection (Figure 2). The Toll pathway and the immune deficiency (IMD) pathway control inducible immune responses to bacteria and fungi. The Toll pathway is active in the fat body and, together with the IMD pathway, controls systemic AMP production. The IMD pathway is also active in barrier epithelial surfaces, including the gut, and functions in antimicrobial responses together with reactive oxygen species (ROS)-generating enzymes, such as dual oxidase (Duox) (109, 110). The Persephone (PSH) cascade senses virulence factors and is activated by live Gram-positive bacteria and fungi. The other two cascades are activated by pattern recognition receptors binding cell wall components from Gram-positive bacteria and fungi (111).

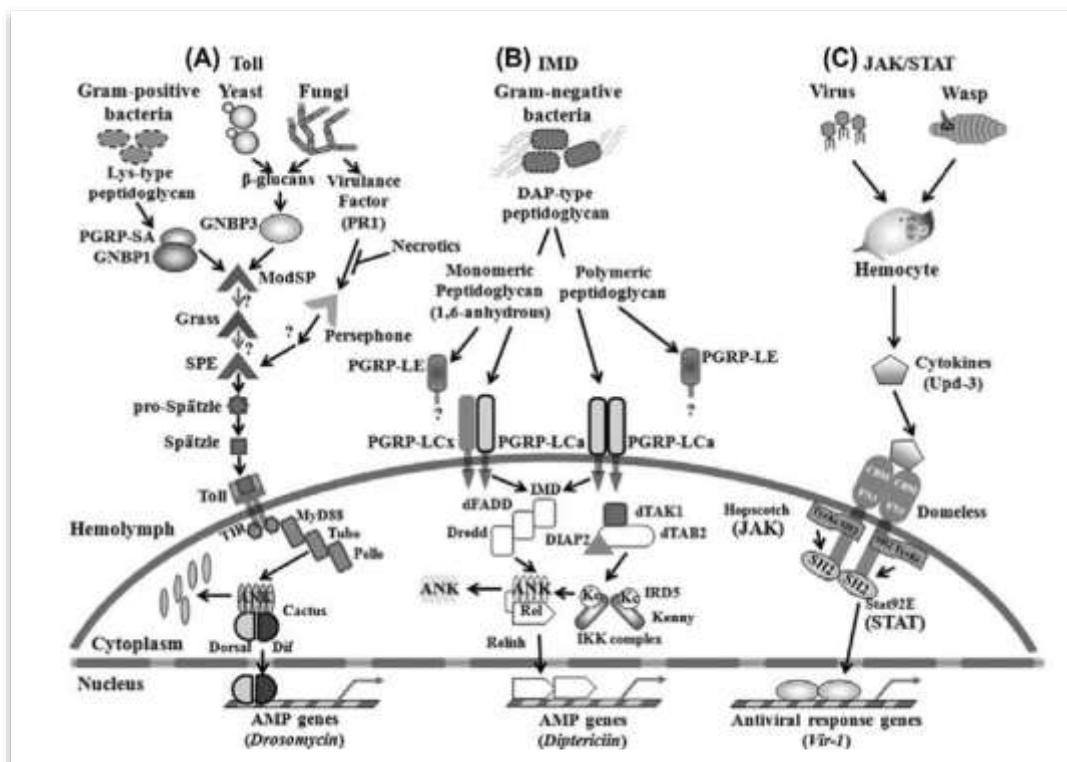


Figure 2. *Drosophila* signaling pathways regulating systemic immune responses against bacterial, fungal and viral infection. Image taken from <http://what-when-how.com/insect-molecular-biology-and-biochemistry/insect-immunology-part-2/>

### 1.1.6. Antimicrobial peptides

AMPs are present in most life forms, ranging from bacteria to plants, vertebrates and invertebrates (112). They form part of insects' complex innate immune system, conferring protection against microbial infections and are synthesized in fat bodies and hemocytes (44, 113, 114). They are released into the hemolymph after their proteolytic maturation to counteract pathogen action, although they can also have local synthesis in several epithelial tissues, such as the gut and epidermis in response to microbes' exposure in these sites (115-117).

Are small peptides having variable aa composition, usually ranging from 8 to 50 residues in length and their size could be 2 to 10 kDa. Many of these aa (around 40%) are hydrophobic and have amphipathic properties (118). They interact with pathogen surface through electrostatic or hydrophobic mechanisms to initiate killing bacteria using mechanisms such as lysis, disrupting microbial homeostasis, membrane permeabilization and rupture, inhibiting protein synthesis or inducing reactive oxygen species (ROS) synthesis causing cell death (119-121). Changes in AMPs' primary sequence directly influence their MoA, potency and selectivity against bacteria (122).

AMPs are positively-charged (123), amphipathic, structurally diverse and short (124). Figure 3 shows the discovery timeline for natural AMPs. Natural AMPs are one of the most important parts of the defense system in both prokaryotic and eukaryotic organisms; most have been reported to have a dual anti-inflammatory and antimicrobial effect, having a very diverse composition. Thousands of natural and synthetic AMPs have been discovered (125, 126).

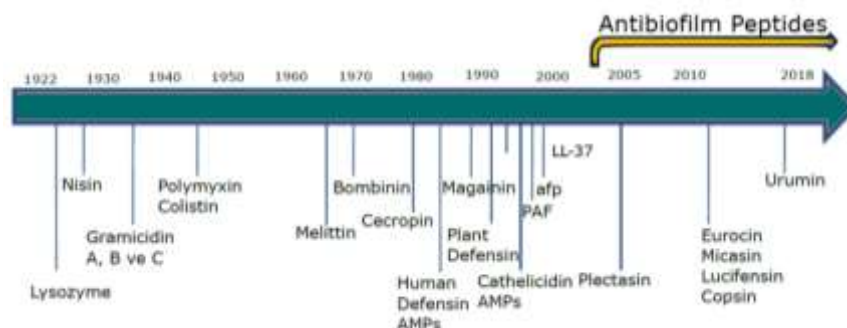


Figure 3. AMP discovery timeline. Image taken from Yazici *et al.* (125)

The first insect scavengers' defensins were isolated from an embryonic cell line from the fly *Sarcophaga peregrina* (127) and hemolymph of immunized larvae derived from another fly, *Phormia terranova* (128), including different insects (Figure 4) (129). Since then, more than 70 defensins have

been identified in various arthropods, such as spiders, ticks, scorpions and insect species from the orders Diptera, Lepidoptera, Coleoptera, Hymenoptera, Hemiptera and Odonata (43, 44).

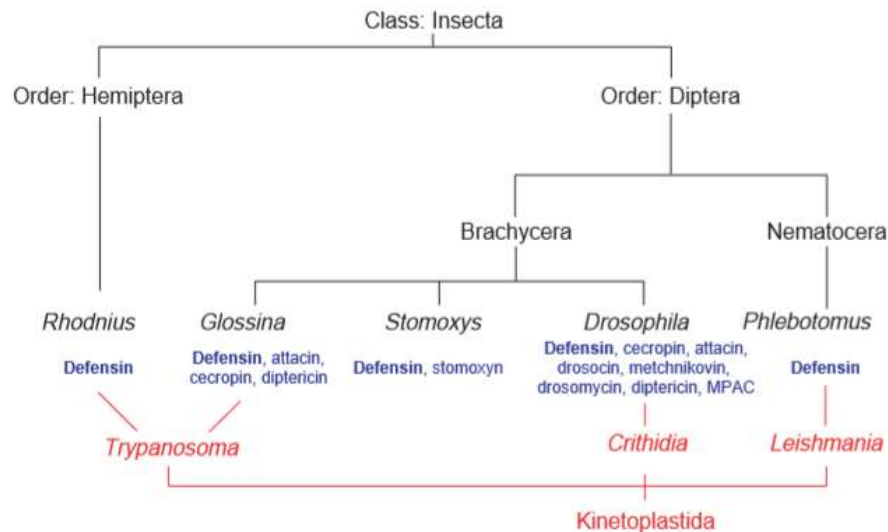


Figure 4. AMPs identified in insects upon pathogen infection (bacterial or parasitic). Parasites are shown in red, AMPs in blue and insects in black; MPAC, mature prodomain of attacin C. The relationships discussed regarding insects and parasites is shown by phylogenetic trees. Figure taken from Boulanger *et al.*, (129).

Isolated insect defensins are 33 to 46 amino acid (aa) long, with a few exceptions such as the N-terminally extended defensins from the fly *Stomoxys calcitrans* (130) and the C-terminally extended defensin found in bees and bumblebees (131). They have sequence similarity ranging from 58% to 95% (132). Defensins are classified according to their antibacterial activity or against filamentous fungi (44); antimicrobial defensins have activity against Gram-positive bacteria and antifungal defensins are mainly effective against filamentous fungi. Insect defensins have an N-terminal flexible loop, a central alpha-helix and a C-terminal anti-parallel beta sheet, as determined by 2D spectroscopy carried out on defensins isolated from *Sarcophaga peregrina* (133) and in recombinant A defensin from *Terranovae phormia* (134). Antimicrobial defensins have six cysteine residues participating in a characteristic conserved motif of three intramolecular disulphide bridges, connected in a Cys1-Cys4, Cys2-Cys5 and Cys3-Cys6 pattern. Drosomycin, an antifungal defensin from *Drosophila* contains an additional short beta chain terminal and four disulphide bridges (135). With the exception of royalisin, the defense of royal jelly bees (136) and bumblebee defensins (131), insect defensins' C-terminal aa are not amidated. Although insect defensins are believed to have originally been similar to mammalian defensins, their 3D structure and disulphide bridge pattern makes them different.

---

Cerovský *et al.*, have been working on identifying *L. sericata* AMPs since 2007, focusing on insect AMPs. They have contributed towards detecting defensins from larval ES (lucifensin), as well as different parts of the larval body, purifying them and determining their primary structure. These authors' experience highlights the fact that only by using modern separation techniques (such as high performance liquid chromatography (HPLC)) during part of the purification procedures could the desired peptides (45, 137) and MAMP (138) be discovered; others in larval ES had no clear homology for existing analogues and therefore justified the need for further research. A larval secretion fraction greater than 500 Da was recently shown to have activity against several pathogenic strains (*Staphylococcus* spp., *Bacillus* spp., *E. coli*, *Pseudomonas* spp., *Proteus* spp., *Enterococcus* spp., *Enterobacter* spp., etc.) and also against 12 out of 15 MRSA isolates (46). These active antibacterial agents' mass and empirical formula have been accurately determined as  $C_{10}H_{16}N_6O_9$  and one of the molecules has been patented and recorded as a new antibiotic named seraticin (2). This compound's molecular structure is currently being investigated, which will certainly allow chemical synthesis. The MoA, the minimal inhibitory concentration (MIC) and the determination of molecular targets are currently being studied. The presence of antibacterial molecules in *L. sericata* larval ES has thus been universally accepted as being totally successful against both Gram-positive and Gram-negative bacteria.

Lucifensin, an *L. sericata* larvae-derived AMP, has been well-characterized as being an antibacterial substance involved in LT (45) because it has been found to be a constituent of larval ES. This molecule was originally isolated from the larval intestine of the afore-mentioned fly, being then detected in the salivary glands, fat body and hemolymph. However, it has been shown that it is the larval immune system (activated in response to an infectious environment) which is responsible for inducing the production of this substance in the fatty body (139) for its rapid release into the hemolymph. The latter has been evidenced when septic injury to the larvae has occurred, producing high levels of lucifensin in the hemolymph, in turn, leading to an increase in antibacterial activity, a situation that was only detected in larvae in these conditions, compared to unstimulated ones, where this effect was absent (140).

Some antimicrobial molecules have been isolated from *L. sericata* and other species in recent years (17, 24, 42, 45-47). For example, a study on the structural characterization and antimicrobial activities of compounds externally released by *L. sericata* revealed a variety of antimicrobial products (141).

AMPs have been identified in necrophagous flies' salivary glands (139) and are important components of larval ES during this phase of their biological development. Larval external digestion means that digestive enzymes such as serine and metalloproteinases, antibacterial molecules and other biochemicals produced by them are constituents of ES (142, 143). As flies live in an environment contaminated by pathogens' oral ingestion, their innate defense system is activated, therefore inducing AMPs (144). These molecules' MoA acting synergistically with other larval ES components, and these living organisms' mechanical effect (due to their movement in hard-to-heal chronic wounds), thus facilitates LT success. Several works have led to identifying, characterizing and evaluating the antimicrobial activity of blowfly larvae-derived molecules, including AMPs (45, 50, 51, 54, 55, 144).

Studies on AMPs, specifically defensins from the lucifensin class, regarding two necrophagous flies, *L. sericata* (45) and *L. cuprina* (50) and their larvae, have shown that lucifensins produced by the aforementioned insects' immune system are mainly effective against Gram-positive bacteria such as *Staphylococcus aureus*; their methicillin-resistant multidrug strains known by the English acronym (MRSA) have been isolated, purified, characterized and evaluated.

These compounds have been categorized into two groups: polypeptides (6,466 to 9,025 Da) and small molecules (130 to 700 Da). Some of these molecules are AMPs known as lucifensins, defensins, cecropins, attacins, lebecins and other small proline-rich peptides, i.e. moricins, gloverins (145).

Insect AMPs were originally discovered by purifying active peptides/proteins from bacteria-induced hemolymph. This approach is limited, since only AMPs in relatively high concentrations in the hemolymph can be purified and identified. Orthologous AMP genes in insect species can also be identified by analyzing genome sequences. However, whole genome analysis (WGA) may not identify small AMPs, particularly small peptides generated from precursor proteins by proteolytic processing, such as proline-rich peptides, because precursor proteins in different insects may not have great similarity. Thus, a large amount of insect AMPs in hemolymph have not been purified or identified. Most insect AMPs, including insect defensins, cecropins, gloverins and basic attacins, are basic (i.e. cationic). Moricins also contain a long amphipathic  $\alpha$ -helix (145).

---

These insect AMPs are either positively-charged or have a positively-charged surface (even anionic AMPs contain amphipathic  $\alpha$ -helix) at physiological pH which can facilitate AMP binding to negatively-charged microbial surface via charge-charge interaction. Insect AMP binding to microbial surface is a prerequisite for antimicrobial activity. Cecropins, moricins, gloverins and attacins adopt unordered structures in aqueous solution, but convert to more helical structures in a hydrophobic environment, such as LPS. Insect AMPs can thus convert to more helical structures on binding to microbial surface, a key factor for antimicrobial activity (121, 146).

Insect AMPs have a broad spectrum of antibiotic activity against bacteria, fungi, some parasites and viruses. Even AMPs from the same class, but different insect species, may have activity against differing microorganisms. This may be because AMPs from different insect species may differ regarding their ability to bind to microorganisms. Whether an AMP is active against a microorganism depends on its ability to bind to a microorganism and conformational conversion to a more helical structure. Single insect AMPs may not have strong activity against microorganisms (147); however, AMPs overall activity in the hemolymph could be very strong and significant (148, 149). Insect AMPs have potential applications in agriculture, disease vector control and medicine; small peptides may represent more suitable candidates and must be chemically modified for creating more potent and stable peptides (121, 150).

Insects respond to bacterial attacks or lesions by rapidly producing AMPs which have a broad spectrum of activity against Gram-positive and Gram-negative bacteria and fungi; more recently, AMPs have been shown to have activity against some parasites and viruses (121). These peptides are conserved host immune system evolutionary components, forming part of the first line of defense against infections and have been identified in almost all life-forms. Insect isolates make up the most abundant group of the more than 2,500 AMPs listed in the antimicrobial peptide database (<http://aps.unmc.edu/AP/main.php>). AMPs are synthesized in the fat body (the equivalent of mammals' liver), epithelial cells and certain hemolymph cells (equivalent to mammalian blood) and spread throughout the body through such medium for counteracting infection. Most of these peptides belong to the category of cationic AMPs having less than 5 kDa molecular mass (151, 152). Iwanaga and Lee

(1998) identified different sized granules stored in granulocytes in limulid hemolymph. These AMPs were identified in the small granules, such as tachyplesin, tachycitin, tachystatin and a big defensin (93).

#### *1.1.7. Antimicrobial peptides' mechanism of action*

AMPs can be categorized into two subdivisions based on their mode of action, i.e. direct if directly interacting with the bacterial membrane by various methods or indirect relating to their interaction with intracellular components (153).

Most AMPs are capable of folding into highly amphipathic formations when interacting with the biological membrane or environment mimicking these structures, such as artificially-prepared liposomes or sodium dodecyl sulphate, having separate areas rich in hydrophobic aa residues and being positively-charged on the molecular surface (152, 154). The frequent occurrence of positively-charged aa residues (arginine and lysine) in their molecules enables them to interact with anionic phospholipids from bacterial membranes. This is followed by peptide integration into the lipid bilayer and the consequent rupture of the membrane structure in different ways, leading to cytoplasmic component filtration and cell death (154, 155). Some studies have revealed that cell death may proceed with relatively little membrane rupture, whether interfering with bacterial metabolism or through interactions with key putative intra-cellular targets (156). By contrast with conventional antibiotics, AMPs require only a short time to induce microorganism death (155).

Three models are typically associated with AMP-membrane interaction: barrel-stave, carpet or toroidal-pore (157, 158) (Figure 5). The first step in AMPs killing bacteria involves the attraction between a peptide and bacteria. This commonly takes the form of an electrostatic interaction due to opposite charges between the bacterial membrane and an AMP (159). Attachment only occurs after overcoming an array of external factors, such as capsular polysaccharides (in Gram-negative and Gram-positive bacteria), as well as teichoic and lipoteichoic acids (in Gram-positive bacteria). Once peptides interact with the cytoplasmic membrane (at low peptide/lipid ratios) they become adsorbed and embedded into and parallel with bacterial surface, spanning the bacteria in an inactive state, commonly known as the surface (S) state (160). When peptide/lipid ratios increase, peptide arrangement begins to become orientated perpendicularly and they become inserted into the bilayer forming pores, known as the I state (161).

Three membrane permeabilisation mechanisms have been proposed. The barrel-stave model involves the formation of small pores (around 1 nm in diameter) called the "barrel" pore which allows the indiscriminate leakage of ions from cells, an example being alamethicin (162, 163). The carpet model exerted by ovispirin involves AMPs' electrostatic attraction and aggregation when forming a "carpet" on the cell membrane, perpendicularly penetrating it and being attracted to the anionic head group complex with the phospholipids. This change entails their folding, culminating in the formation of "toroidal" pores facilitating ion leakage and macromolecule passage; the bilayer becomes breached and phospholipids are compartmentalized in micelles, opening up the bacterial wall in a detergent-like manner (164). The toroidal pore model (reported for magainins, protegrins and melittin) exerts its action through the formation of a pore lined with alternating lipid head groups and a peptide's hydrophilic regions. As peptide concentration rises, the phospholipids bend, exposing just the phospholipid head groups in the pore (162, 163, 165, 166).

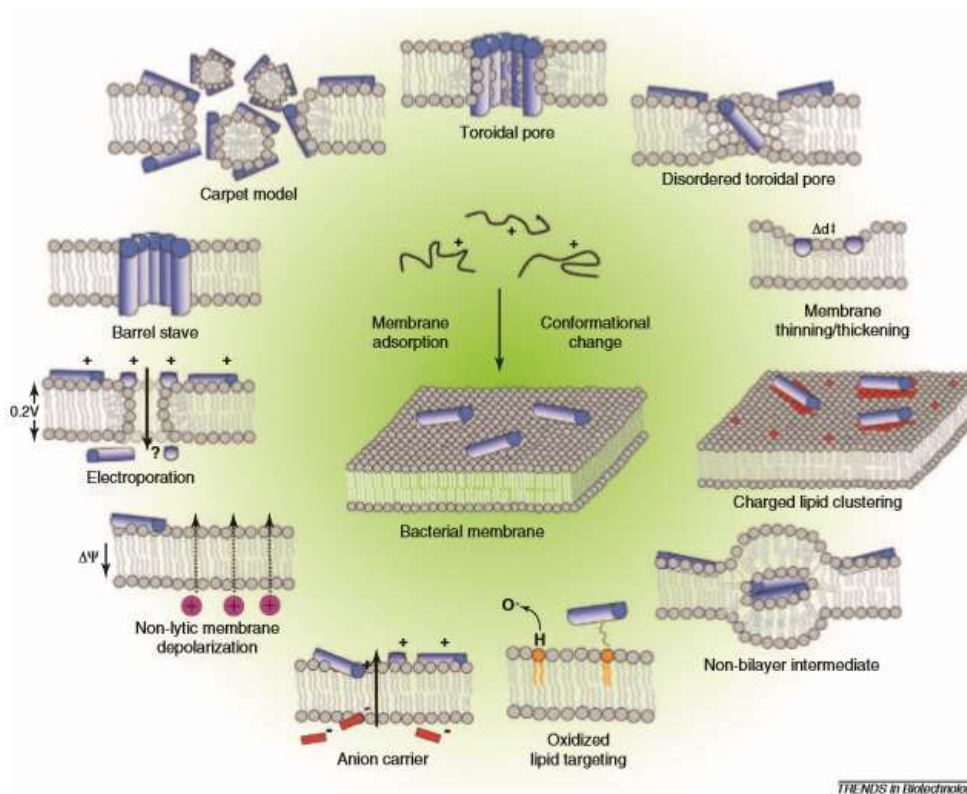


Figure 5. Events occurring on bacterial cytoplasmic membrane following initial AMP adsorption. The figure was taken from Nguyen (120).

The indirect mode of action is related to the damaging of critical intracellular targets following peptide internalization, as suggested for pyrrolicorin, PR-39 and indolicidin (158, 167). Some AMPs

can kill bacteria without permeabilizing or disrupting the membrane, causing DNA damage or inhibiting protein synthesis as two mechanisms for intracellular peptide action (168, 169). AMPs can have other target sites, including enzymatic activity and inhibiting cell wall synthesis (170, 171).

#### 1.1.8. AMP classification

Such molecules are usually cationic, having net charges ranging from +2 to +9, with an abundance of lysine and arginine residues (172). Few anionic antimicrobial peptides (AAMPs) have been recorded from some animal species and human tissues (173). Insect AMPs are usually small, cationic and have great diversity and repertoire among species (114). AMPs can be classified according to their structure or function; for instance, there are four structural groups, including  $\alpha$ -helical peptides (cecropin and moricin), cysteine-rich peptides (insect defensin and drosomycin), proline-rich peptides (apidaecin, drosocin and lebocin) and glycine-rich proteins (attacin and gloverin) (44, 174). Functional classification tends to be based on target pathogen range instead of any MoA (being very broad in some cases and specific in others) (114, 175, 176). Insect-derived AMPs (i.e. Diptera, blowflies from the *Calliphoridae* family) have a broad antibacterial, antifungal, antiparasitic and antiviral spectrum, even covering anticancer activities (114, 175-177).

AMPs can also be classified according to their physicochemical properties; however, only two MoA have been described to date: membranolytic and non-membranolytic (177), see 1.1.7 for examples of AMP direct and indirect MoA.

AMPs can be divided into three groups based on their structure:  $\alpha$ -helical peptides are linear molecules mainly existing as disordered structures in aqueous media which become amphipathic helices upon interaction with hydrophobic membranes, e.g. cecropins, magainins and melittins (178).  $\beta$ -sheet or  $\beta$ -hairpin, stabilized by disulphide bonds are cyclic peptides constrained in such formation by intramolecular disulphide bonds (e.g. defensins and protegrins) or by an N-terminal to C-terminal covalent bond (e.g. gramicidin S and tyrocidines). The third group consists of extended AMPs (e.g. indolicidin and PR-39) (120, 178, 179).

Other researchers have classified them into three categories: linear peptides forming an  $\alpha$ -helical structure and containing no cysteine residues (such as cecropins), cyclic peptides containing disulphide bridges (defensins, drosomycin and thanatin) and linear peptides having remarkable content of one or two aa residues (mostly proline (drosocin, lebocins, formaecins) and/or glycine residues (gloverins, pyrocoricins and dipterocins)) (132).

---

Although they have differing structural characteristics, most AMPs are cationic and can also be classified into five main groups depending on their primary and secondary structure. Important cationic peptide subfamilies include cecropins, defensin, thionins, amino acid-enriched class, histone-derived compounds, beta hairpin and other natural and structural proteins (180).

#### 1.1.9. Discovering new antimicrobial peptides potentially combating resistance

Pathogen microorganisms' resistance to the antibiotics currently being used is one of the serious health problems facing humanity. A recent 2018 WHO fact sheet (<https://www.who.int/news-room/fact-sheets/detail/antibiotic-resistance>) has stated that antibiotic resistance has increased worldwide, reaching dangerous levels. New resistance mechanisms are appearing and spreading throughout the planet day by day, endangering health services' ability to treat common infectious diseases. Superbugs, such as vancomycin-resistant enterococci, methicillin-resistant *Staphylococcus aureus* (MRSA), carbapenem-resistant *E. coli* and *Klebsiella pneumoniae*, as well as third-generation cephalosporin-resistant strains and drug-resistant tuberculosis are recorded every day in many patients in hospitals worldwide (181). This situation could lead to the deaths of hundreds of thousands of people who acquire infections around the world every year (i.e. caused by bacteria resistant to one or more current antibiotics), in addition to the loss of hundreds of billions of dollars regarding direct excess healthcare costs and annual productivity losses.

It has been reported that two million people per year acquire serious infections in the USA due to the action of bacteria which are resistant to current antibiotics, 23,000 of whom die. Excess health service costs could reach up to US\$20 billion and annual productivity losses could exceed US\$35 billion (114). The search for new strategies for fighting antibiotic resistance has become a universal priority, one of which could involve insect AMPs and this is why this chapter describes a new peptide derived from *Sarconesiopsis magellanica* larval ES.

Microorganism resistance to antibiotics is extremely serious and becomes more important every day (Figure 6). Unlike conventional antibiotics, such as penicillin where microbes readily circumvent it, it is surprisingly improbable that sensitive microbial strains will acquire resistance against AMPs (158). After Alexander Fleming's discovery of human lysozyme (the first antimicrobial protein) in 1922, multiple peptides have been discovered since, though few of them are currently being used (Figure 6) (182).

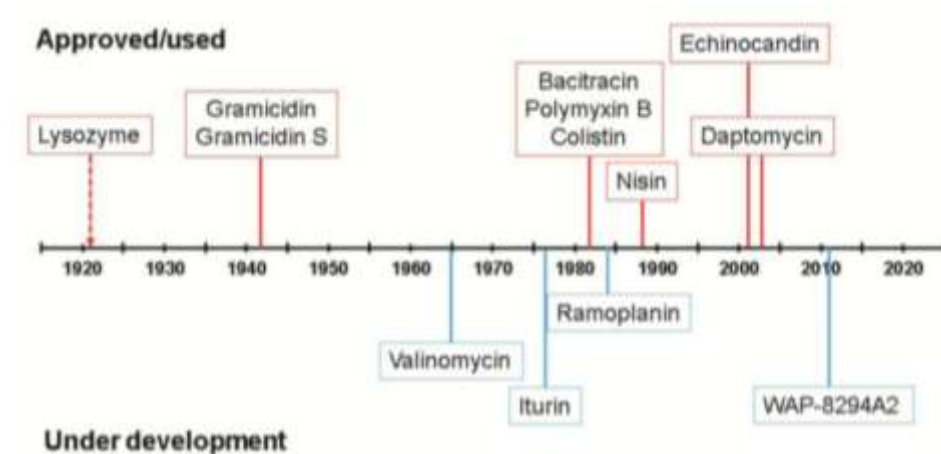


Figure 6. AMPs (a–c) and their application timeline. Selected AMPs in use (orange, top) or in clinical trials (blue, bottom) are depicted. Figure taken from Mishra *et al.* (182)

This situation is even more relevant regarding difficult-to-heal chronic wounds in patients suffering underlying disease, such as diabetes and cardiovascular insufficiency. These types of lesion, frequently involving polymicrobial colonization of different bacterial strains, forming a "biofilm", makes them more difficult to treat, control and/or eradicate. Recent studies have shown (183) that while conventional antibiotics generate resistance to bacteria, they do not promote chronic wound healing; however, they are still used for treating bacteria colonizing this type of wound. Hence the need to introduce new or reemerging strategies that can be effective against microorganisms in chronic, necrotic and infected wounds which do not respond to antibiotic therapy.

Identifying and characterizing antibacterial compounds involved in larval ES is the starting point for such search and typing natural molecules in insects, mainly Diptera from the family Calliphoridae, as it has been demonstrated (with some species) that this is an appropriate source for achieving such ends. It is singularly important that insect-derived antimicrobial peptides do not generate microbial resistance and can induce pathogen death in a relatively short period of time (155). *S. magellanica* represents a good resource for isolating, characterizing and evaluating peptides precisely because it is a native species which has been studied in relation to biological aspects, life-cycle, population and reproductive parameters (184), proteolytic profiles (from their larval ES) (185), establishing and characterizing an embryonic egg-derived cell line (186, 187) and LT using an animal model. Even more important though is that larval ES constituents have been shown to have potent antibacterial activity (188). Antibacterial activity has been established from fat bodies and hemolymph derived from this fly's

larvae and evaluated *in vitro* (189); the effect of these substances used topically in diabetic rabbits' chronic and infected wounds has also been evaluated (190). Research continuity thus involved isolating and typing this specie's sarconesins and evaluating their action against Gram-positive and Gram-negative bacteria.

## 1.2. Objective

### General objective

Isolating, characterizing and evaluating the antimicrobial activity of AMPs derived from the blowfly *S. magellanica*'s larval ES

### Specific objectives

1. Identifying *S. magellanica* AMPs from the ES of III instar maggots;
2. Determining the isolated peptides' primary structure and physicochemical properties;
3. Determining the previously characterized peptides' antibacterial activity against *Staphylococcus aureus*, *Pseudomonas aeruginosa*, *Escherichia coli* and *Micrococcus luteus*.
4. Analyzing the selected peptides' safety using cytotoxicity (CC) and hemolytic assays; and
5. Comparing the biological activity of the AMPs selected for synthesis with that of native AMPs.

## 1.3. Materials and Methods

### 1.3.1. Fly Source and *S. magellanica* ES collection

#### 1.3.1.1. Capturing adult *S. magellanica* specimens

Insect capture and colony maintenance followed a previously described procedure (76). Adult *S. magellanica* forms were captured in the mountainous part of Bogotá's Parque Nacional; the park is located at 2,600 masl (4°37'8.90N; 74°3'27.73W) (Figure 7); 6 lb. portions of pig liver were used as bait for attracting adult insects, which were carefully collected with entomological nets, stored in vials and transported to the insectary at the Universidad del Rosario's Medical and Forensic Entomology laboratory.



Figure 7. *Sarconesiopsis magellanica*. Original image by Andrea Díaz.

The insects were periodically collected in the morning throughout one continuous year. The material collected in the field was taxonomically identified using Mariluis & Peris' taxonomic keys (Mariluis and Peris, 1984). Adult insects from the selected species were placed in 45x45x45 cm Gerberg cages at 20–25°C, with 60%–70% relative humidity and a 12/12 h photoperiod. The adult forms were fed on a sugar solution (carbohydrate source) and pigs' liver as protein feed necessary for providing continuity for the biological cycle (191); after adults had laid eggs on the liver they were placed in a glass flask with a liver slice until maggots hatched. The maggots were kept in this flask throughout the 3 instars until they reached the pre-pupa stage; they were then put in a flask containing sand until the adults emerged to be released in the same cages to continue the cycle. Third instar maggots were used for extracting their ES.

#### 1.3.1.2. Extracting larval excretions and secretions

*S. magellanica*-derived ES were collected from third instar larvae, following a previously described procedure (7); about 200 larvae were used in each assay. Third-instar larvae were incubated with a bacterial suspension ( $OD_{595} = 0.5$ ) of each selected strain to activate the immune system and enhance the expression of products having antibacterial activity (57, 58). They were then placed in a 15 mL Falcon tube and disinfected by adding 0.5% formaldehyde for 5 min followed by replacing this solution with 0.5% hypochlorite with constant shaking for the same amount of time and washed with sterile PBS; 2 mL sterile PBS was then added to the larvae which were incubated at 25°C for 1 h. The larval ES mixture

was removed by syringe and placed in another tube to continue spinning at 13,000 g for 10 min at 4°C. The precipitate was discarded and the supernatant with the ES was sterilized by filtering through a 0.22 µm membrane and stored at -70°C.

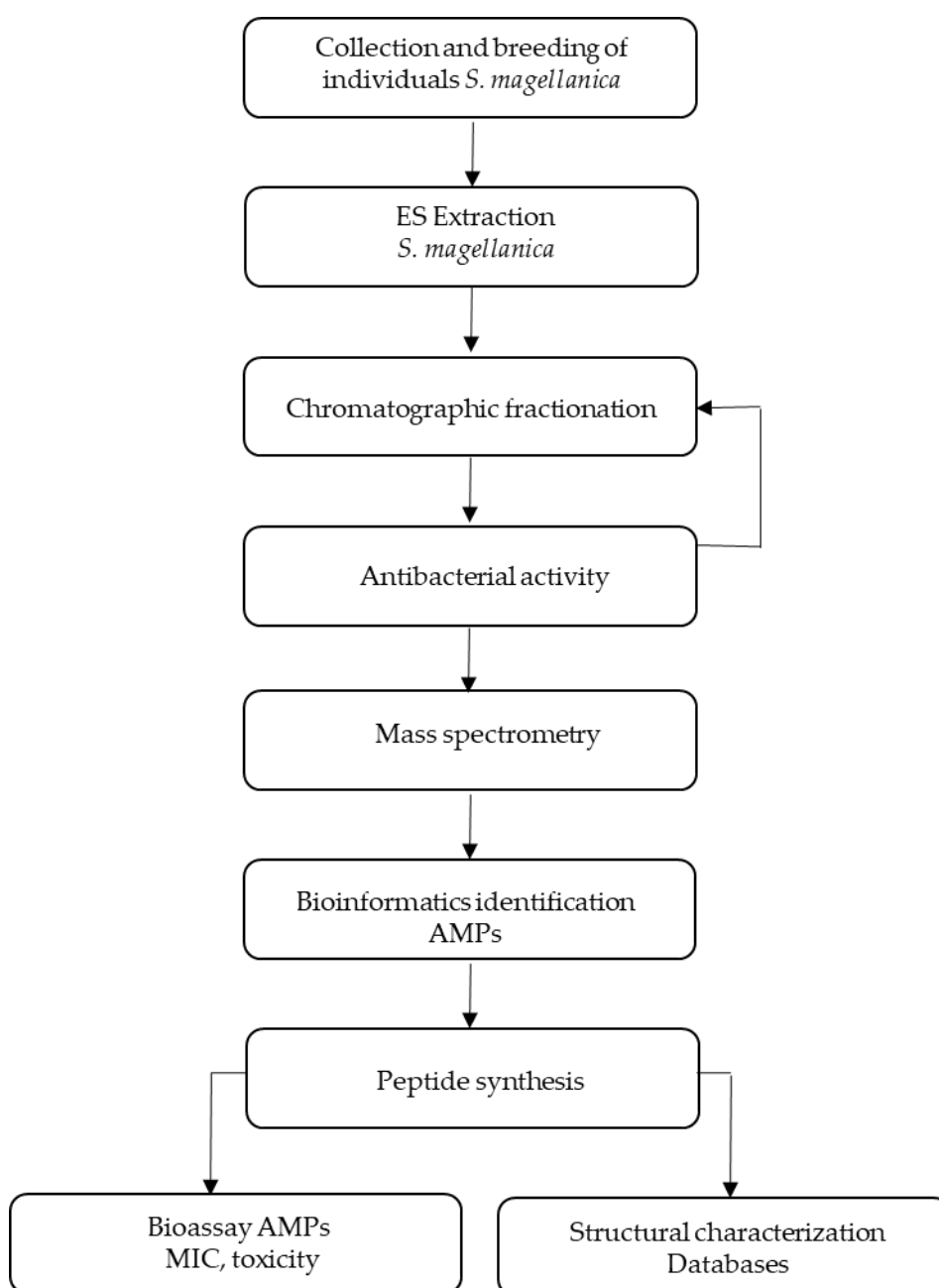


Figure 8. Scheme representing the steps used for isolating, extracting and purifying AMPs and pertinent bioassays. Original scheme by Andrea Díaz.

The antibacterial action of the larval ES sample-derived products was evaluated (Figure 8). The compounds were separated by reverse-phase high-performance liquid chromatography (RP-HPLC) for subsequent analysis by mass spectrometry (MS) and bioinformatics characterization, where antimicrobial peptides' aa sequences were obtained. Peptides having antibacterial action were produced by the Fmoc solid phase peptide synthesis procedure and their action against Gram-positive and Gram-negative bacteria evaluated by bioassays.

### 1.3.2. Chromatographic fractionation

#### RP-HPLC

The products obtained after extraction (ES) were separately homogenized in 1.5 mL of 2 M acetic acid. The supernatant obtained by spinning at  $13,800 \times g$  for 3 min at  $4^{\circ}\text{C}$  was loaded into a Sep-Pak C18 cartridge and equilibrated in acidified water (0.05% TFA). After washing with this solution, 2 elutions were made with 0% and 80% ACN / 0.05% TFA. The 80% Sep-Pak fraction was concentrated in a vacuum centrifuge, reconstituted with ultra-pure water (Milli-Q Millipore) and subjected to reverse phase C18 on a Jupiter C18 column ( $10 \mu\text{m}$ ,  $300 \text{ \AA}$ ,  $10 \text{ mm} \times 250 \text{ mm}$ ) (Phenomenex, Torrance, California, USA) balanced in water with 0.05% TFA. The RP-HPLC technique was used for obtaining the AMPs. Samples were purified using 0-80% ACN/ $\text{H}_2\text{O}$ / 0.05% TFA gradients for 60 min at a 2 mL / min flowrate using a Prominence LC-20A system (Shimadzu, Kyoto, Japan).

Ultraviolet absorbance was monitored at 225 nm and 280 nm. Elution peak fractions were manually collected and vacuum dried (Speed-Vac Savant), suspended in 500  $\mu\text{L}$  deionized water and used in antibacterial activity tests. Fractions maintaining antibacterial action were purified using a Jupiter C18 analytical reverse phase column ( $4.6 \mu\text{m}$ ,  $12 \text{ nm}$ ,  $4.6 \text{ mm} \times 250 \text{ mm}$ ). A specific gradient was used for each fraction; this was calculated according to the retention time (RT) observed for each fraction during the first chromatography stage. A 1 mL / minute flowrate was used for 30 minutes (192). MS analysis of the fractions was subsequently used for determining aa sequences for elucidating the peptides' primary structure (193, 194).

## FPLC

The hydrophilic fraction was passed by vacuum centrifugation (Savant Instrument Inc.); the samples were concentrated and reconstituted in Milli-Q ultrapure water in acidified water (0.05% TFA). The FPLC system was used with the samples, involving pre-packaged column Superdex Peptide HR 10/30 (300 x 10 mm I.D.) in 50 mM ammonium acetate at 0.5 mL / min flowrate. The peak fractions were collected manually, concentrated by vacuum centrifuge (Savant Instrument Inc.), reconstituted in 1 mL ultra-pure Milli-Q water and refrigerated at -80°C until use. When required, they were purified by analytical RP-HPLC column.

### 1.3.3. Bioassays

#### 1.3.3.1. Bacterial strains

Previously characterized ATCC strains and those from the species *Staphylococcus aureus*, *S. epidermidis*, *Micrococcus luteus* and *Pseudomonas aeruginosa*, frequently found in chronic wounds, were used (Jacklic *et al.*, 2008). These were kept in Muller-Hinton broth until use, after having activated them by incubation at 37°C for 18 hours. When the bacterial strains reached exponential phase they were quantified using an ELISA reader at 0.2 optical density (OD). According to previous reports, OD<sub>620</sub> = 0.2 absorbance units are equivalent to (au) =  $5 \times 10^7$  CFU / mL.

#### 1.3.3.2. Standardizing growth curves

Growth curves were constructed for the selected strains. Bacteria were sown by exhaustion in Mueller-Hinton agar culture medium and incubated overnight at 37°C for isolating colonies. Subsequently, 4 morphologically similar colonies were taken and inoculated in 5 mL LB culture medium at 37°C with constant shaking. OD absorbance was measured at 595 nm every hour for 14 h. This determined the time during which the bacteria reached exponential phase, thus establishing the incubation period required for preparing subsequent antibacterial tests.

#### 1.3.3.3. Turbidimetry

Serial 1: 2 dilutions of the selected *S. magellanica*-derived peptides were evaluated, starting with the protein concentration obtained after suspending peptides in water. ES dilutions at 20 µL volume were

---

placed in 96-well plates; 80  $\mu\text{L}$  of each bacterial strain were then added separately at  $5 \times 10^6$  CFU / mL concentration. The plates were incubated at  $37^\circ\text{C}$  for 18 h and ES MIC was determined (i.e. the lowest amount of protein concentration inhibiting bacterial growth). The tests were carried out in triplicate. Ciprofloxacin at 50  $\mu\text{g}$  / mL concentration over wells containing the bacteria was used as positive control and LB medium with the respective bacterial solutions as negative control.

#### 1.3.4. Structural characterization

##### 1.3.4.1. Mass spectrometry

The samples were concentrated in a vacuum centrifuge, reconstituted in 10  $\mu\text{L}$  of 0.1% formic acid (FA) solution and analyzed by liquid chromatography coupled to tandem mass spectrometry LC-MS / MS, using an LTQ-Orbitrap Velos mass spectrometer (Thermo Fisher Scientific Inc.) coupled to an Easy-nLCII liquid nano-chromatography system (Thermo Fisher Scientific Inc.). 5  $\mu\text{L}$  of each sample were automatically injected into a Jupiter C-18 pre-column (10  $\mu\text{m}$ , 100  $\mu\text{m}$  x 50 mm) (Phenomenex) coupled to an ACQUA C-18 analytical reverse phase column (5  $\mu\text{m}$ , 75  $\mu\text{m}$  x 100 mm) (Phenomenex). Samples were eluted on a 5% to 95% solvent B (0.1% FA in ACN) linear gradient for 15 minutes at 200 nL / minute flowrate. The electrospray ionization source was operated in positive mode, at 2.0 kV voltage and  $200^\circ\text{C}$ . The mass scan interval considered for the full scan (MS1) was 200-2,000 m / z (60,000 resolution in 400 m / z), operating in data-dependent acquisition mode, where the five most intense values per scan were selected for the collision-induced dissociation fragmentation event. The minimum signal required to trigger fragmentation events (MS2) for a given ion was set at 5000 cps and 30 seconds was used as dynamic exclusion time.

##### 1.3.4.2. Bioinformatics analysis

MSConvert software was used for collecting and processing spectra in "\*.RAW" format (195), then converted to "\*.mgf" (mascot generic format) format and used in database searches using the Mascot tool (196). Mascot-analyzed files were subjected to searches in databanks such as SwissProt, NCBI, using filters like "Lucilia" in some cases. Peptides having the highest similarity probability were selected.

PEAKS 7.5 software (Bioinformatics Solutions Inc., Waterloo, Ontario, Canada) was also used for analyzing MS results. The PEAKS DB function and *de novo* sequence were used for comparing the

samples' spectra with those for AMPs deposited in the National Center for Biotechnology Information-NCBI data banks and in the Universal Protein Resource-UNIPROT. Analysis involved a 10 ppm error tolerance for the precursor ion and 0.6 Da for the fragments. Methionine oxidation was used as variable modification. The basic local alignment search tool (BLASTp) was used for searching for fragments having similarity with data bank molecules (197).

## 1.4. Results

### 1.4.1. Purifying *S. magellanica* excretions and secretions

The ES were fractionated by RP-HPLC for isolating and characterizing the AMPs; 67 fractions were obtained and evaluated against *M. luteus* and *P. aeruginosa*, using the turbidimetric technique (Figure 9). Six fractions capable of preventing target microorganism growth were identified. Fraction 2 (RT 8.06) had activity against *M. luteus*. Fractions lacking activity against the previous strain were tested against *P. aeruginosa* and bacterial growth was inhibited in fractions 36 (RT 46), 44 (RT 50.87), 45 (RT 51.72), 46 (RT 52.15) and 57 (RT 64.9).

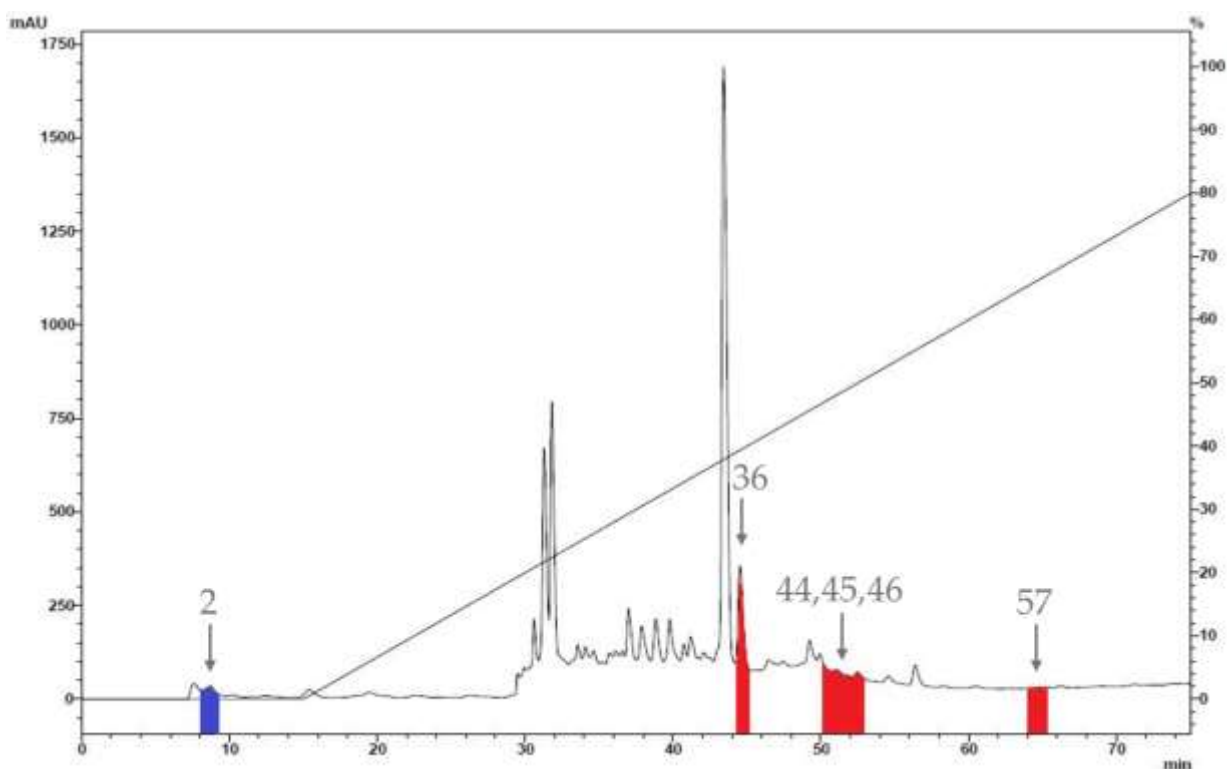


Figure 9. *S. magellanica* ES chromatographic profile. This was obtained by RP-HPLC on a Jupiter C18 semi-preparative reverse phase column (Phenomenex). Chromatography involved using 0%-80% ACN/H<sub>2</sub>O/0.05% TFA gradients for 60 minutes at 2mL/min flowrate. Absorbance was monitored at 225 nm. The 67 fractions were collected manually and separately. Those having antimicrobial potential against *Micrococcus luteus* A270 are highlighted in blue (fraction 2). Those marked as having activity against *P. aeruginosa* are indicated in red, i.e. fractions 36, 44, 45, 46 and 57.

Table 2 shows the fractions having antibacterial activity which were then forwarded for second step RP-HPLC fractionation.

Table 2. *S. magellanica* ES isolated fractions and ACN elution concentration (%)

Bacteria	<i>S. magellanica</i> (SM)	
	Fraction	[ % ]
<i>M. luteus</i>	2	0
	36	39
<i>P. aeruginosa</i>	44	51
	45	51.5
	46	52
	57	67

#### 1.4.1.1. Fraction 2

Additional purification steps involving size exclusion chromatography on a fast protein liquid chromatography (FPLC) apparatus were used for effectively fractionating as fraction 2 was obtained during RP-HPLC hydrophilic stage (Figures 10-13). The FPLC weight patterns gave a lysozyme having 14 KDa molecular weight and 12 min RT (RT), a known peptide having 2.1 KDa with RT=28 min and the gilpone AMP having 0.637 KDa molecular weight and RT=40 min.

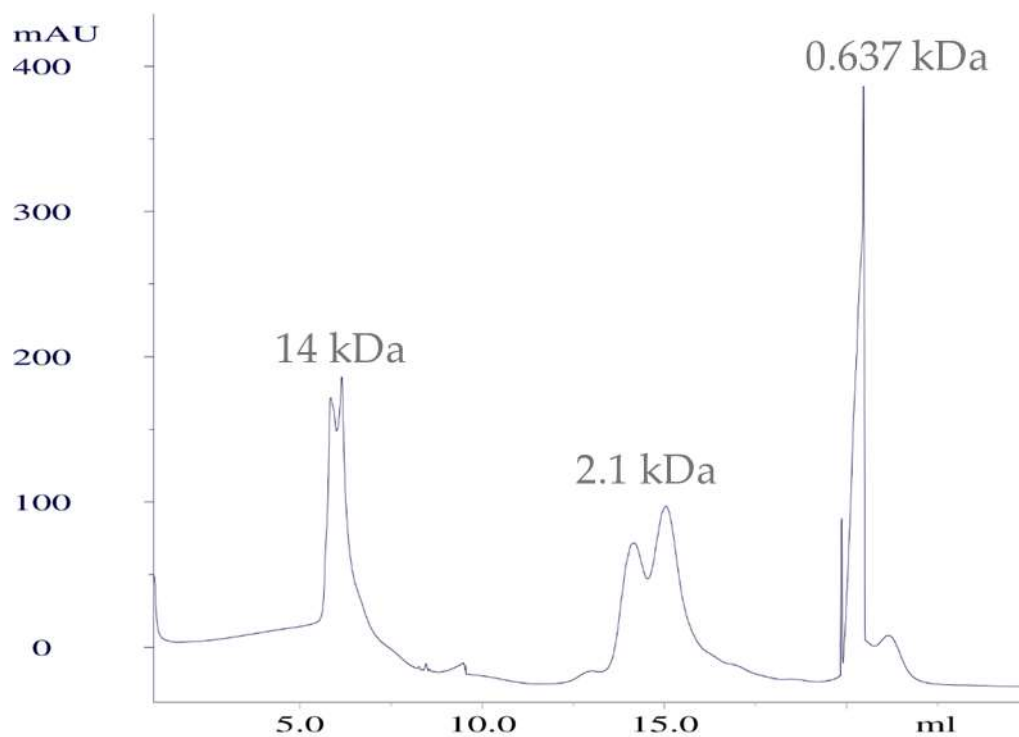


Figure 10. Calibrating standard molecules by gel filtration chromatography using a Superdex Peptide HR 10/30 column at 0.5 mL/min flowrate and 280 nm absorbance. The FPLC weight patterns gave a lysozyme having a 14 KDa molecular weight and 12 min RT, a known peptide having 2.1 KDa with RT=28 min and the gilpone AMP having 0.637 KDa molecular weight and RT=40 min.

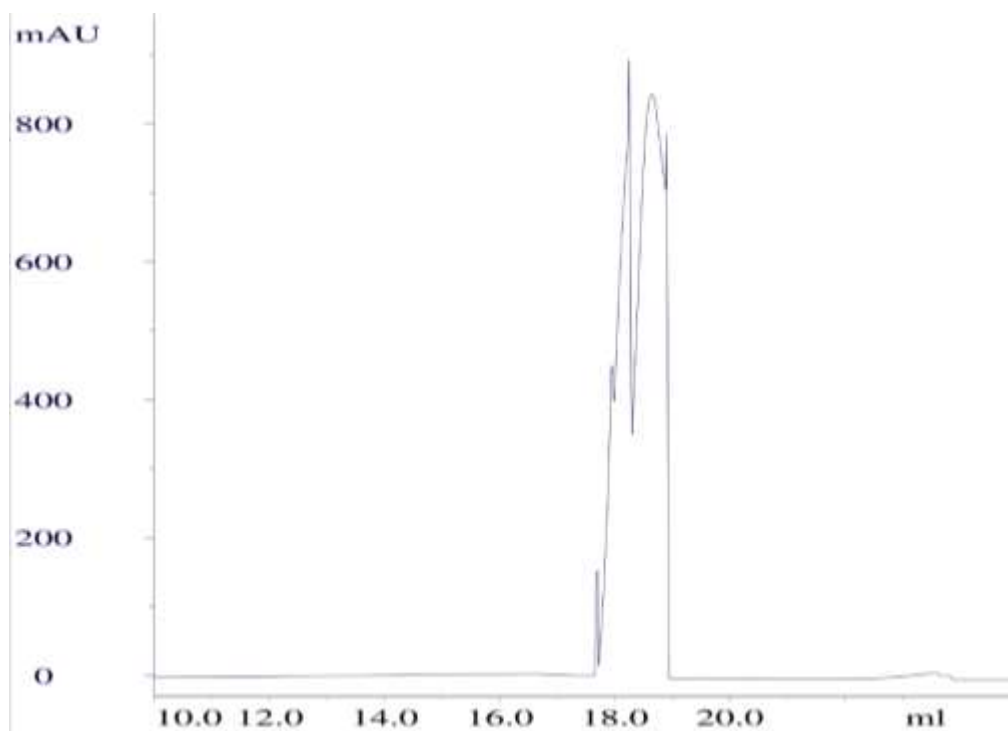


Figure 11. Fractionation chromatographic profile for molecules from fraction 2 by gel filtration chromatography using Superdex Peptide HR 10/30 column at 0.5 mL/min flowrate, 280 nm absorbance. Elution of the molecule at 34 min RT having 1.2 KDa molecular weight.

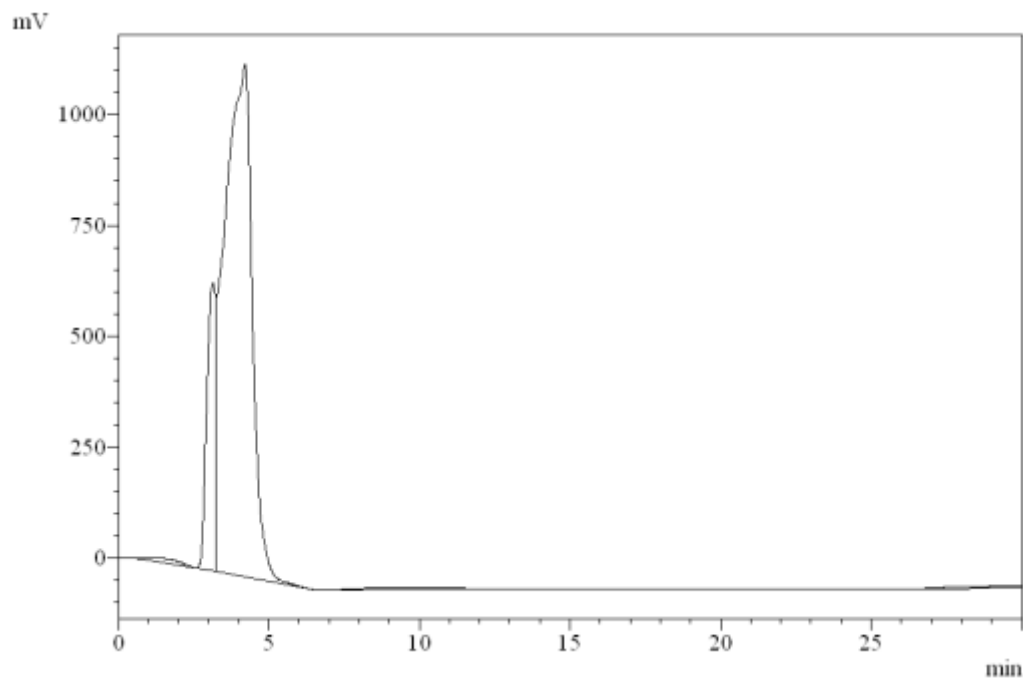


Figure 12. *S. magellanica* fraction 2 chromatographic profile. This was obtained by FPLC. Chromatography involved using isocratic elution in H<sub>2</sub>O acidified with 0.05% TFA for 60 minutes at 1.0 mL/min flowrate. Absorbance was monitored at 225 nm. Three fractions were obtained, i.e. the peaks in the chromatogram (2.65, 3.03, 4.01 min RT); all were collected manually and separately and their antibacterial action against *M. luteus* was evaluated. The fraction eluted at 4.01 RT had antibacterial activity and the result was sent for MS analysis.

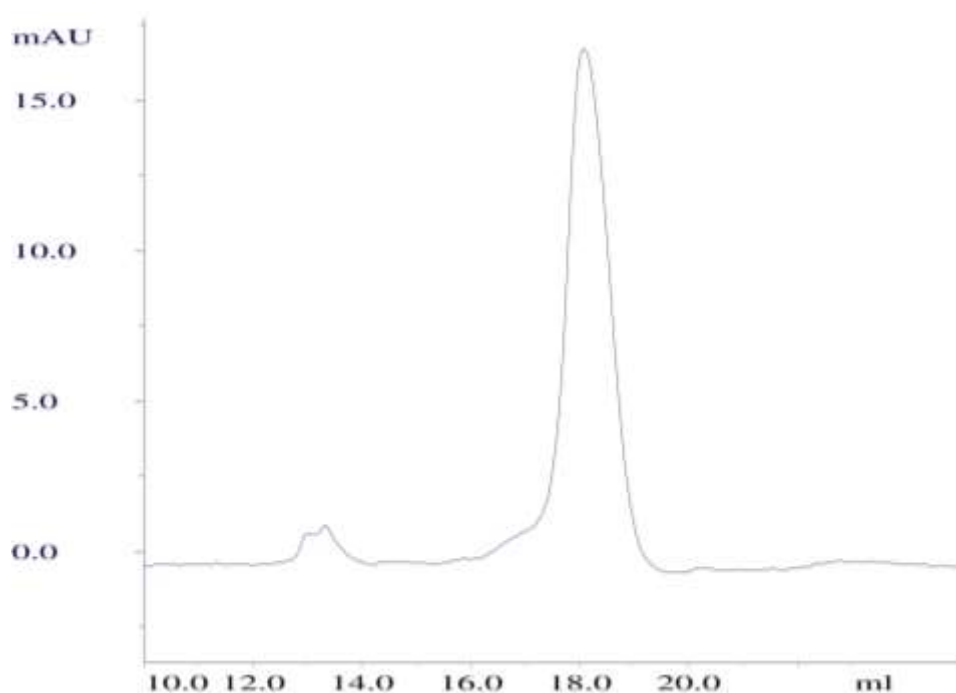


Figure 13. FPLC chromatographic purification profile for *S. magellanica* fraction 2 obtained from RP-HPLC at 4.01 min RT.

#### 1.4.1.2. Fraction 36

Fraction 36 second step chromatography involved using 30%-45% ACN/H<sub>2</sub>O/0.05% TFA gradients for 60 minutes with 1.5mL/min flowrate. Absorbance was monitored at 225 nm. Two fractions were obtained, i.e. the peaks in the chromatogram (12 and 14.5 min RT); both were collected manually and separately and their antibacterial action was evaluated. The fraction eluted at 12 min RT had antibacterial activity and the result was sent for MS analysis (Figure 14).

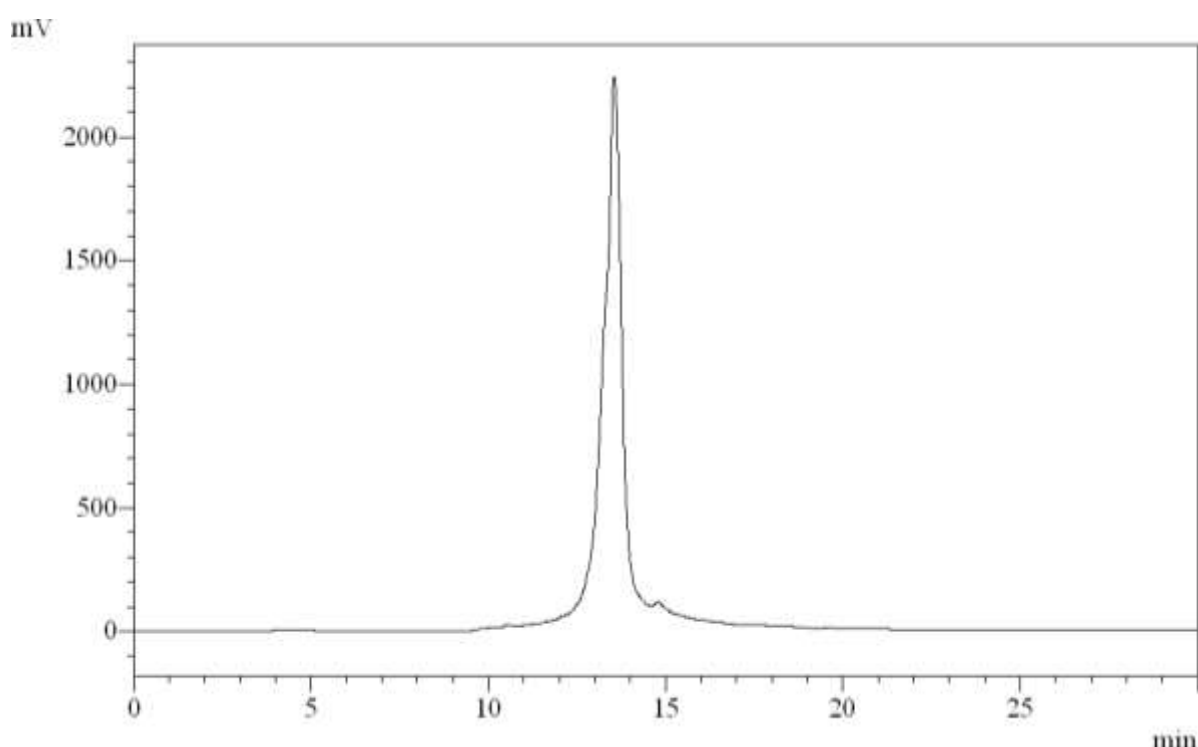


Figure 14. Chromatographic profile for *S. magellanica* fraction 36. This was obtained by RP-HPLC on a Jupiter C18 analytical reverse phase column (Phenomenex). Chromatography involved using 30%-45% ACN/H<sub>2</sub>O/0.05% TFA gradients for 60 minutes at 1.5mL/min flowrate. Absorbance was monitored at 225 nm. Two fractions were obtained, i.e. the peaks observed in the chromatogram (12 and 14.5 min RT); both were collected manually and separately and their antibacterial action was evaluated. The fraction eluted at 12 min RT had antibacterial activity and the result was sent for MS analysis.

#### 1.4.1.3. Fraction 44

The chromatographic profile for fraction 44 involved using 44%-54% ACN/H<sub>2</sub>O/0.05% TFA gradients for 60 minutes with 1.5mL/min flowrate (Figure 15). Absorbance was monitored at 225 nm. Thirteen fractions were obtained, i.e. the peaks in the chromatogram (3.65, 5.78, 9.32, 9.99, 10.18, 10.57,

11.64, 12.01, 12.41, 13.6, 14.09, 15.53, 49.40 min RT); all were collected manually and separately and their antibacterial action against *M. luteus* was evaluated. The fraction eluted at 3.65 min RT had antibacterial activity and the result was sent for MS analysis.

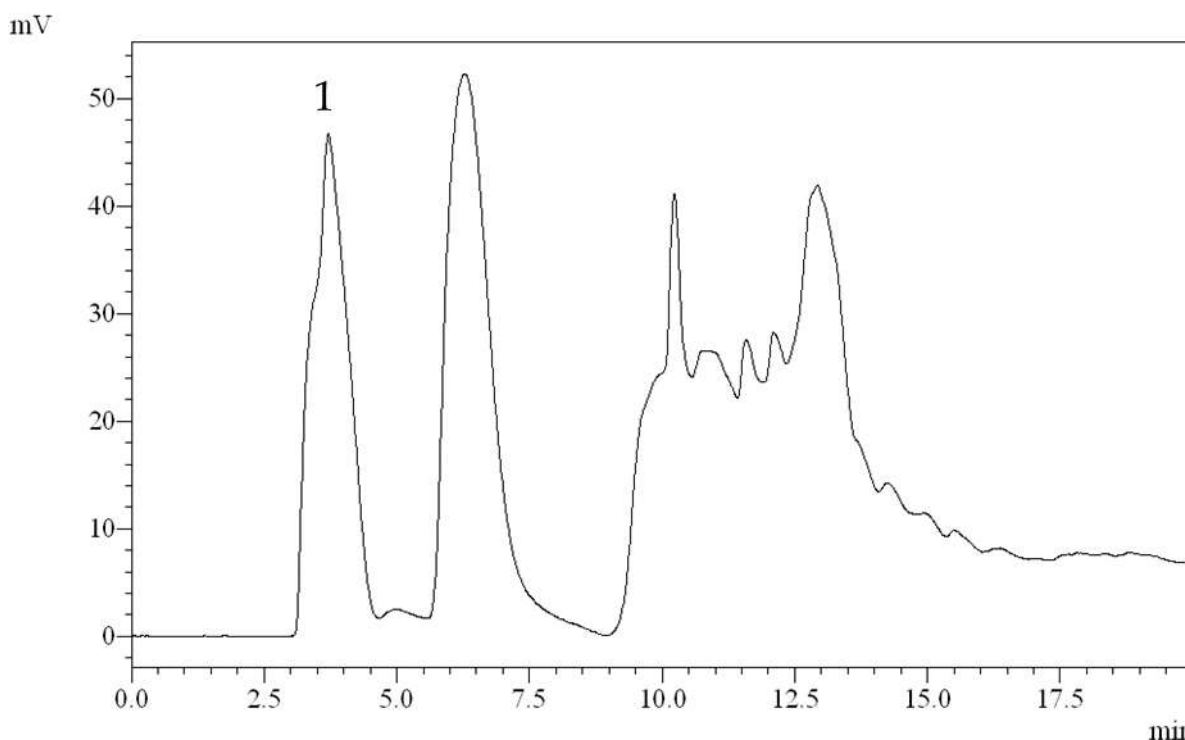


Figure 15. Chromatographic profile for *S. magellanica* fraction 44. This was obtained by RP-HPLC on Jupiter C18 analytical reverse phase column (Phenomenex). Chromatography involved using 44%-54% ACN/H<sub>2</sub>O/0.05% TFA gradients for 60 minutes with 1.5mL/min flowrate. Absorbance was monitored at 225 nm. Thirteen fractions were obtained, i.e. the peaks in the chromatogram (3.65, 5.78, 9.32, 9.99, 10.18, 10.57, 11.64, 12.01, 12.41, 13.6, 14.09, 15.53, 49.40 min RT); all were collected manually and separately and their antibacterial action against *M. luteus* was evaluated. The fraction eluted at 3.65 min RT had antibacterial activity and the result was sent for MS analysis.

#### 1.4.1.4. Fraction 45

Chromatographic profile for fraction 45 involved using 44%-54% ACN/H<sub>2</sub>O/0.05% TFA gradients for 60 minutes with 1.5mL/min flowrate (Figure 16). Absorbance was monitored at 225 nm. All the fractions were collected manually and separately and their antibacterial action against *M. luteus* evaluated. The fraction eluted at 14.58 min RT had antibacterial activity and the result was sent for MS analysis.

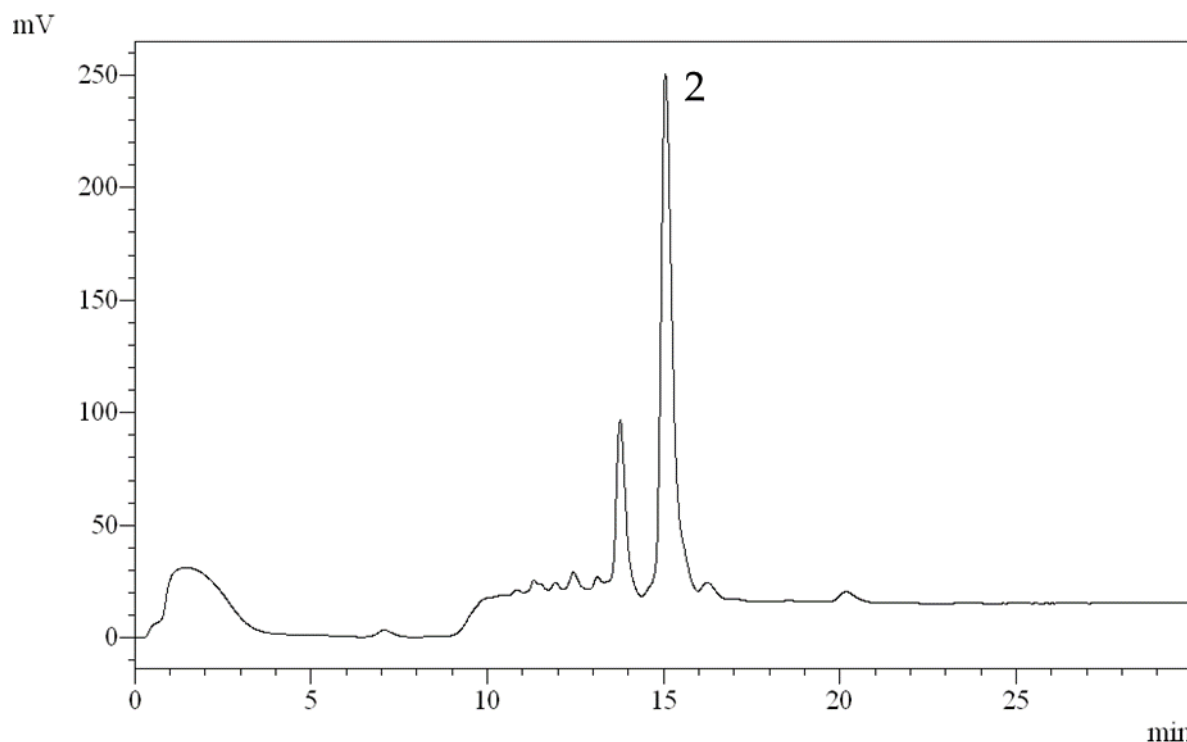


Figure 16. Chromatographic profile for *S. magellanica* fraction 45. This was obtained by RP-HPLC on a Jupiter C18 analytical reverse phase column (Phenomenex). Chromatography involved using 44%-54% ACN/H<sub>2</sub>O/0.05% TFA gradients for 60 minutes with 1.5mL/min flowrate. Absorbance was monitored at 225 nm. All the fractions were collected manually and separately and their antibacterial action against *M. luteus* evaluated. The fraction eluted at 14.58 RT had antibacterial activity and the result was sent for MS analysis.

#### 1.4.1.5. Fraction 46

Chromatographic profile for fraction 46 involved using 44%-54% ACN/H<sub>2</sub>O/0.05% TFA gradients for 60 minutes with 1.5mL/min flowrate (Figure 17). Absorbance was monitored at 225 nm. Fifteen fractions were obtained, i.e. the peaks in the chromatogram (3.9, 11.6, 12.4, 12.7, 13.01, 13.3, 13.68, 14.1, 14.64, 15.43, 15.7, 16.3, 17.2, 18.2, 19.77 min RT); all were collected manually and separately and their antibacterial action against *M. luteus* evaluated. The fraction eluted at 3.9 min RT had antibacterial activity and the result was sent for MS analysis.

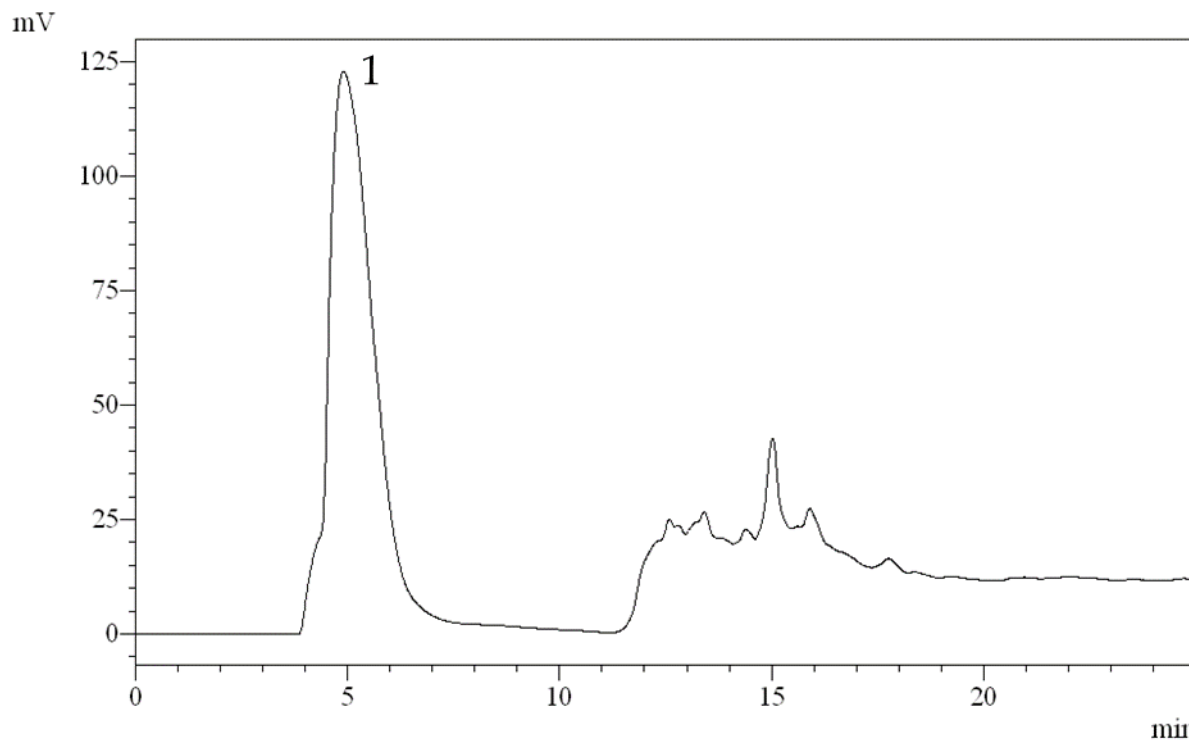


Figure 17. Chromatographic profile for *S. magellanica* fraction 46. This was obtained by RP-HPLC on a Jupiter C18 analytical reverse phase column (Phenomenex). Chromatography involved using 44%-54% ACN/H<sub>2</sub>O/0.05% TFA gradients for 60 minutes at 1.5 mL/min flowrate. Absorbance was monitored at 225 nm. Fifteen fractions were obtained, i.e. the peaks in the chromatogram (3.9, 11.6, 12.4, 12.7, 13.01, 13.3, 13.68, 14.1, 14.64, 15.43, 15.7, 16.3, 17.2, 18.2, 19.77 min RT), all were collected manually and separately and their antibacterial action against *M. luteus* evaluated. The fraction eluted at 3.9 min RT had antibacterial activity and the result was sent for MS analysis.

#### 1.4.1.6. Fraction 57

Chromatographic profile of fraction 46 involved using 60%-70% ACN/H<sub>2</sub>O/0.05% TFA gradients for 60 minutes with 1.5mL/min flowrate (Figure 18). Absorbance was monitored at 225 nm. Thirteen fractions were obtained, i.e. the peaks in the chromatogram (4.01, 4.4, 6.2, 10.69, 11.44, 11.98, 12.7, 13.06, 14.14, 14.68, 15.8, 16.9, 25 min RT); all were collected manually and separately and their antibacterial action against *M. luteus* evaluated. The fraction eluted in 4.4 min RT had antibacterial activity and the result was sent for MS analysis.

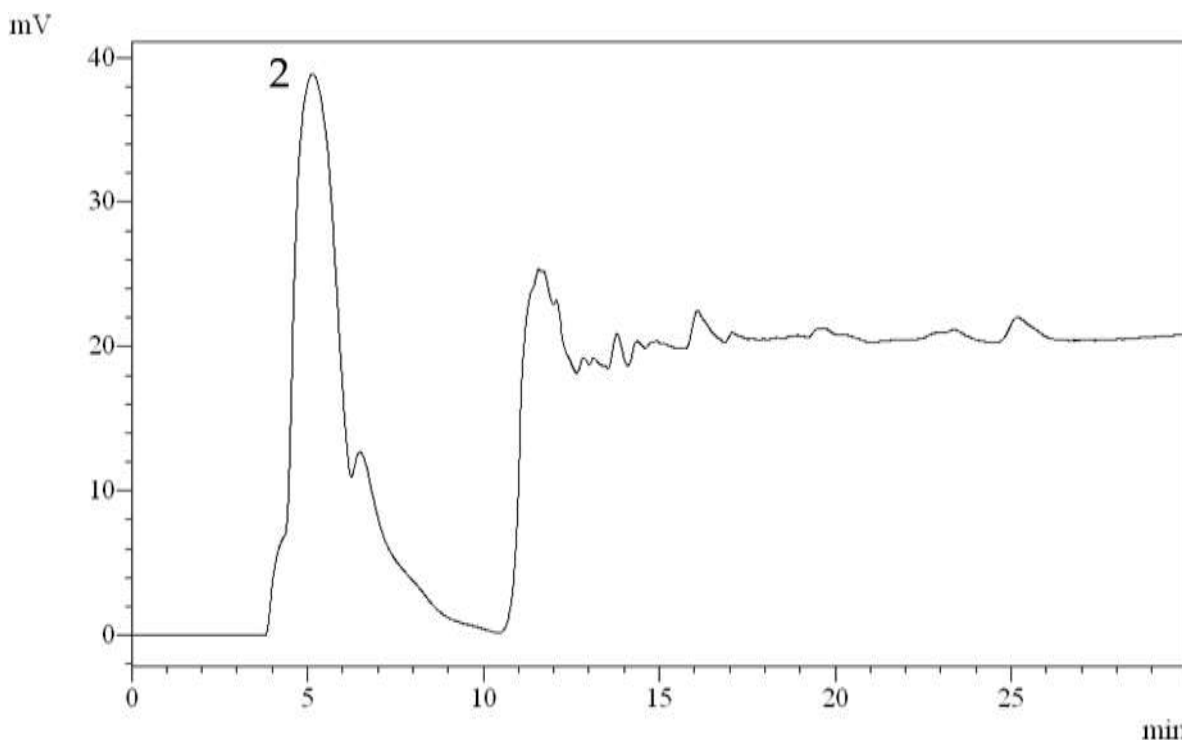


Figure 18. Chromatographic profile of *S. magellanica* fraction 57. This was obtained by RP-HPLC on Jupiter C18 analytical reverse phase column (Phenomenex). Chromatography involved using 60%-70% ACN/H<sub>2</sub>O/0.05% TFA gradients for 60 minutes with 1.5mL/min flowrate. Absorbance was monitored at 225 nm. Thirteen fractions were obtained, i.e. the peaks in the chromatogram (4.01, 4.4, 6.2, 10.69, 11.44, 11.98, 12.7, 13.06, 14.14, 14.68, 15.8, 16.9, 25 min RT); all were collected manually and separately and their antibacterial action against *M. luteus* evaluated. The fraction eluted in 4.4 min RT had antibacterial activity and the result was sent for MS analysis.

#### 1.4.2. Mass spectrometry, bioinformatics analysis by Mascot and Peaks tools

Mascot and Peaks bioinformatics tools were used for analyzing MS data regarding *S. magellanica* fractionated peptides for possible similarity (sequence) with previously reported peptide sequences (protein) (Table 3). No spectra could be obtained for fraction 2, nor were validated sequences confirmed for fractions 44, 46 and 57 as the material was not homogenous. Additional purification steps would have been required and the quantities were not enough for in-depth research with these fractions. Fractions 44 and 46 contained other sequences, including the same sequence obtained in fraction 45.

Table 3. Sequences obtained by MS from fractions having antimicrobial activity after second fractionation by RP-HPLC with C18 analytic column.

Fraction	Sequence
2	No spectrum
36	<b>VALTGLTVAEYFR</b>
44	TPM(+15.99)LLVGTKLDLR; VLSGNIILFDP
45	<b>TPM(+15.99)LLVGTQIDLR</b>
46	TPM(+15.99)LLVGTKLDLR; EGVGSAFLLR
57	AELSM(+15.99)LEGAVLDLR; LLEYLEEK; LTQSM(+15.99)ALLR

The AELSM(+15.99)LEGAVLDLR sequence obtained from fraction 57 was sought in the transcriptomes reported for *L. cuprina* (transcriptome SRX907163), *L. sericata* (transcriptome ERX614478, 3-4 day pupa transcriptome SRX087348) and also in a complete search for blast proteins in the NCBI database using diptera, Calliphoridae and Lucilia as search criteria. This fraction 57 was not found in any of them (accessed May 16<sup>th</sup> 2018). The fraction was not pure, having other sequences. The sequence could be identified in fractions 36 and 45 and they were chosen to continue studies reported in Chapters 3 and 2, respectively.

## 1.5. Discussion

This thesis gives the initial results for 4 fractions purified from the *S. magellanica* blowfly's third instar larval ES and the isolation and characterization of two AMPs (sarconesin and sarconesin II). The first part of this thesis has involved the initial purification of ES extracts and preliminary screening of these fractions' antimicrobial activity (Chapter 1).

Antibacterial activity detected in fractions 44, 45 and 46 was probably due to the same peptide; however, we could not confirm the molecule responsible for fractions 44 and 46 as more fractionation steps were needed and we had a little amount of the pertinent material. Some molecules could not be identified by MS, probably due to inherent properties determining peptide detectability/ionization efficiency (198). The fractions may have lacked some properties, such as the amount of basic residues, peptide length and hydrophobicity which have been reported as contributing toward peptide ionization and fragmentation. Such hydrophobicity could have been the case for fraction 2, having a 1.2 KDa molecular weight, as it was eluted in the hydrophilic part of the RP-HPLC; peptide hydrophobicity and

detectability hydrophobicity are selection criteria for peptide and proteomic studies as they have been widely reported as a determinant of ion detectability (199, 200). It was unclear whether the peptide was associated with better ionization just because of having higher hydrophobicity (201); other reports have affirmed that ionization efficiency becomes reduced for peptides eluting at both low and high organic concentrations (198).

The effect of net charge on peptide 'flyability' is further supported by considering peptide length, where shorter peptides appear to improve detectability; we did not know the charge or even the length of our undetected fractions and this could have influenced the ionization of our sequences. Larger amounts of material could facilitate enzymatic digestion with trypsin and thereby molecule ionization, as tryptic peptides with a lower average amount of basic residues are expected to produce a more complete set of fragments for identification (202). MS is usually used in positive ion mode; however, it has been reported that negative ion mode MS has improved sensitivity, identification and elucidation of organic compounds when being used in specific and sensitive cases (203).

All purified samples' results were sent for MS for later identification. Two of these samples were chosen for further work due to their greater signal intensity and clarity of MS data. The other Chapters of this thesis deal with in-depth evaluation and characterization of the purified and identified peptides obtained from fractions 36 and 45.

## **1.6. Conclusion**

RP-HPLC techniques ensured the effective purification of the fractions for evaluating their biological activity;

All the fractions obtained were evaluated against Gram-positive and Gram-negative bacteria; however, just 2 out of the 6 having antibacterial potential could be further analyzed.

This study showed that additional research is required to further elucidate the unknown fractions and identify the pertinent molecules. Fraction 2 had antibacterial activity against *M. luteus* and the other fractions against *P. aeruginosa*; further experimental approaches could help answer some of the questions raised. Other purification methods and means of analysis by MS should be tested. Larger

amounts of material are needed to effectively evaluate and develop all the required tests to discover the unknown sequences.

---

## 2. Chapter 2

# **Sarconesin: *Sarconesiopsis magellanica* blowfly larval excretions and secretions having antibacterial properties**

This Chapter reports a study aimed at characterizing the novel Sarconesin AMP purified from *S. magellanica* ES. The AMP's antimicrobial activity against various Gram-positive and Gram-negative bacteria was also evaluated.

### **2.1. Objectives**

1. Determining the isolated Sarconesin peptide primary structure and physicochemical properties;
2. Determining the previously characterized peptides' antibacterial activity against *Staphylococcus aureus*, *Pseudomonas aeruginosa*, *Escherichia coli* and *Micrococcus luteus*;
3. Analyzing the selected peptides' safety using cytotoxicity (CC) and hemolytic assays; and
4. Comparing the biological activity of the AMPs selected for synthesis with that of native AMPs.

### **2.2. Materials and Methods**

#### *2.2.1. Peptide purification*

The ES were partially purified by Sep-Pak C18 disposable columns for the first analysis; bound material was eluted with 80% ACN in acidified water and freeze-dried. *S. magellanica* hydrophobic ES (80%) were then lyophilized and reconstituted in 2mL trifluoroacetic acid (0.05% TFA). ES were purified by semi-preparative RP-HPLC using a C18 Jupiter column (10 $\mu$ m; 300A; 10mm x 250mm) at 2mL/min flowrate, as described previously (209). Fractions were collected manually, absorbance being monitored at 225nm. Each fraction's antibacterial activity was then determined. RP-HPLC (1mL/min flow rate) was used with fractions having antibacterial activity, using an analytical C18 Jupiter column (10 $\mu$ m; 300A;

4,6mm x 250mm). The Sarconesin gradient was open, ACN concentration ranging from 44% to 54%. Absorbance was monitored at 225nm, fractions were collected manually and antibacterial activity was tested.

### 2.2.2. Peptide synthesis

The sarconesin peptide was synthesized in solid phase according to Merrifield's technique (210), as modified by Houghten (211), using F-moc synthesis strategy. A Wang resin having 0.5 mmol / g substitution level was used as polymer support. TBTU (O-(benzotriazol-1-yl) - N,N,N',N'-tetramethyluronium tetrafluoroborate)/ HOBt (n-hydroxybenzotriazole) / N-methylmorpholine (NMM) in dimethylformamide (DMF ) at 0.3 M concentration with shaking for 5 minutes was used for activating F-moc-aa.

The resin-bound active ester was coupled to the aa chain, reacting for 30 minutes. The resin was washed with DMF for 1 min after each coupling. Removal of the FMOC protective group involved three 7-minute steps using 1,2-ethanedithiol with DMF for 1 minute. The cycle was repeated until the peptide chain was complete. The final peptide was cleaved from the resin and deprotected for 8 hours using 82.5% TFA, 5% phenol, 5% water, 5% thioanisole and 2.5% 1, 2-ethanedithiol (EDT). This was evaporated and the resulting product suspended in water and ACN for further purification by RP-HPLC (212).

### 2.2.3. Peptides' analytical RP-HPLC

Peptide purity was verified by analytical RP-HPLC and peptide mass was characterized by Liquid Chromatography - Mass Spectrometry/Mass Spectrometry (LC-MS/MS) on a LTQ-Orbitrap Velos hybrid mass spectrometer (Thermo Scientific) coupled to an Easy-nLCII liquid nano-chromatography system (Thermo Scientific).

### 2.2.4. Antimicrobial assays

A liquid growth inhibition assay was used for evaluating the fractions' antibacterial activity (213, 214). Lyophilized fractions were suspended in 500  $\mu$ L Milli-Q water; the assay was carried out using 96-well sterile plates. 20  $\mu$ L of the fractions were aliquoted into each well with 80  $\mu$ L of the bacterial dilution, at 100 $\mu$ L final volume. Bacteria were cultured in poor nutrient broth (PB) (1.0 g peptone in 100

mL water containing 86 mM NaCl at pH 7.4; 217 mOsm). Exponential growth phase cultures were diluted to  $5 \times 10^4$  CFU/mL (DO = 0.001) final concentration (144, 213, 215). Sterile water and PB were used as growth control and streptomycin was used as growth inhibition control. Microtiter plates were incubated for 18 h at 30°C; growth inhibition was determined by measuring absorbance at 595 nm. The assay for determining minimum peptide concentration required for 100% growth inhibition involved using a serial dilution in 96-well sterile plates at 100  $\mu$ L final volume (193, 194, 216); 20  $\mu$ L stock solution was used in each microtiter plate well at twofold serial dilution and added to 80  $\mu$ L of the bacterial dilution. The strains used were *Staphylococcus aureus* ATCC 29213, *S. epidermidis* ATCC 12228, *Escherichia coli* D31, *E. coli* DH5 $\alpha$ , *Pseudomonas aeruginosa* 27853, *Salmonella enterica* ATCC 13314 and *Micrococcus luteus* A270. Microbial growth was measured by monitoring OD at 595 nm and assays were performed in triplicate (PerkinElmer Victor 3TM 1420 multilabel, multitask plate reader). *S. aureus* bacterial growth curve with sarconesin MIC and  $\frac{1}{2}$  MIC was measured every 15 min for 1 h and then every hour for 12 hours. Graphs were background-corrected by subtracting the OD<sub>595</sub> for medium without bacteria (217, 218).

#### 2.2.5. Cytotoxicity

Sarconesin toxicity for VERO cells (African green monkey kidney fibroblast) was evaluated. Cells were obtained from the American Type Culture Collection (ATCC CCL81; Manassas, VA) and maintained in DMEM culture medium, supplemented with 10% heat-inactivated calf serum. CC was determined using an MTT colorimetric assay. Briefly, the cells were seeded in 96-well plates ( $2 \times 10^5$  cells/well) and cultured for 24 h at 37°C in a humidified atmosphere containing 5% CO<sub>2</sub>. Eight two-fold serial dilutions of peptide were performed with DMEM to give solutions having final concentrations ranging from 4.7 to 600  $\mu$ M. Varying concentrations were added and allowed to react with the cells for 48 h, followed by adding 20  $\mu$ L MTT (5 mg/mL in PBS) for another 4 h at 37°C. Formazan crystals were dissolved by adding 150  $\mu$ L isopropanol and incubating at room temperature until all crystals were dissolved. Absorbance was measured at 550 nm using a 96 well microplate ELISA reader. Cell survival was calculated using the following formula: survival (%) = (A<sub>550</sub> of peptide-treated cells / A<sub>550</sub> of peptide-untreated cells)\*100 (219).

### 2.2.6. Hemolytic activity

Fresh human red blood cells (hRBC) were washed 3 times with PBS (35 mM phosphate buffer, 0.15 M NaCl, pH 7.4) by centrifugation for 7 min at  $1000 \times g$ , and suspended in PBS at final 4% (v/v) concentration. Sarconesin solutions (serial 2-fold dilutions in PBS) were added to 100  $\mu$ L hRBC suspension at 200  $\mu$ L final volume and incubated for 1 h at 37°C. Hemoglobin release was monitored by measuring supernatant absorbance at 405 nm with a Microplate ELISA Reader. The hemolysis percentage was expressed in relation to a 100% lysis control (erythrocytes incubated with 0.1% Triton X-100); PBS was used as negative control

### 2.2.7. Mass spectrometry

Active antibacterial fractions were analyzed by (LC-MS/MS) on a LTQ-Orbitrap Velos hybrid mass spectrometer (Thermo Scientific) coupled to an Easy-nLCII liquid nano-chromatography system (Thermo Scientific). The chromatographic step involved automatically using 5  $\mu$ L of each sample on a C18 pre-column (100  $\mu$ m I.D.  $\times$  50 mm; Jupiter 10  $\mu$ m, Phenomenex Inc., Torrance, California, USA) coupled to a C18 analytical column (75  $\mu$ m I.D.  $\times$  100 mm; ACQUA 5  $\mu$ m, Phenomenex Inc.). The eluate was electro-sprayed at 2 kV and 200°C in positive ion mode. Mass spectra were acquired by FTMS analyzer; full scan (MS1) involved using 200-2,000 m/z (60,000 resolution at 400 m/z) as mass scan interval with the instrument operated in data dependent acquisition mode, the five most intense ions per scan being selected for fragmentation by collision-induced dissociation. The minimum threshold for selecting an ion for a fragmentation event (MS2) was set to 5,000 cps. The dynamic exclusion time used was 15 s, repeating at 30 s intervals.

### 2.2.8. Bioinformatics

MS/MS peak list files were submitted to an in-house version of the MASCOT server (Matrix Science, USA) and screened against the Uniprot database. PEAKS 8.5 (Bioinformatics Solutions Inc., Waterloo, Ontario, Canada) de novo sequencing/database search software was used for establishing sequences. Analysis involved 10 ppm error tolerance for precursor ions and 0.6 Da for fragment ions. Oxidation was considered a variable modification.

The sarconesin sequence was analyzed for similarities with the *L. sericata* and *L. cuprina* genome and transcriptome and also with other proteins registered in the National Center for Biotechnology (220) public database, using the Basic Local Alignment Search Tool (BLASTp), with default parameters (<http://blast.ncbi.nlm.nih.gov/>; accessed April 23<sup>rd</sup> 2018) (221). The PepCalc tool were used for calculating sequences' physical-chemical parameters (<http://pepcalc.com/>; accessed April 30<sup>th</sup> 2018). Gene Runner was used for nucleotide translation to protein and Seaview (222) and Boxshade ([http://www.ch.embnet.org/software/BOX\\_form.html](http://www.ch.embnet.org/software/BOX_form.html)) were used for making and formatting alignments' shaded background. The Chimera structure prediction tool (accessed through the European Bioinformatics Institute (<http://www.ebi.ac.uk/thornton-srv/databases/profunc/>; accessed April 30<sup>th</sup> 2018) was used for obtaining the 3D images of secondary structure.

#### 2.2.9. Circular dichroism

The peptide's far-UV (190-250nm) circular dichroism (223) spectrum was recorded on a Jasco J810 spectropolarimeter (Jasco Inc., Japan) at 25°C, using a 0.1cm path length quartz cell. All CD spectra were recorded after the accumulation of 4 runs and smoothed using a fast Fourier transform (FFT) filter to minimize background effects. The solvents used in the experiment were pure water and 10%, 30% and 50% v/v solutions of 2,2,2 TFE in water.

#### 2.2.10. Mechanism of action (MoA)

##### 2.2.10.1. Membrane integrity and esterase activity

Mid-log phase *E. coli* cells ( $2 \times 10^8$  CFU/mL) were incubated with or without MIC peptide solution at 37°C. Bacterial membrane integrity was measured by fluorometry and microscopy using propidium iodide (PI) at 60  $\mu$ M final concentration in the dark for 15 min, followed by measuring fluorescence with 485/620 nm excitation/emission wavelengths (224). Esterase activity involved transferring 180  $\mu$ L to a 96-well black plate to which was added 20  $\mu$ L of 250  $\mu$ M 5(6)-carboxyfluorescein diacetate (CFDA), incubated in the dark for 30 min, followed by measuring fluorescence with 485/535 nm excitation/emission wavelengths (225, 226). PI microscope slides were made by dropping melted 1% agarose (w/v) onto them; the dried culture was covered with a glass coverslip and observed by microscope after placing 20  $\mu$ L of the cells onto solidified agar pad for immobilization (227). Microscopy

involved using a Leica TCS SP8 confocal laser scanning electron microscope (SEM); the images were processed with Leica software LAS X.

#### 2.2.10.2. DNA staining

Treated and untreated bacterial cells were fixed on a slide, permeabilized with ethanol and stained with 4',6-diamidino-2-phenylindole (DAPI) to visualize the DNA using a confocal microscope.

#### 2.2.10.3. Gel retardation assay

Sarconesin binding to *E. coli* DH5 $\alpha$  genomic DNA (gDNA) was evaluated by a gel retardation assay (228). *E. coli* gDNA was extracted following the method described by Landry *et al.* (229). Seven two-fold increasing amounts of sarconesin (3.1 to 200  $\mu$ M) were incubated for 1 hour with 500 ng gDNA. The mixture was incubated for 1 hour at room temperature and analyzed by electrophoresis on 0.8 % agarose gel (226).

#### 2.2.11. Statistical analysis

GraphPad Prism software (version 7.00) was used for all statistical analysis. One-way ANOVA ( $\alpha = 0.05$ ) was used for comparing the bacterial growth curve following sarconesin treatment to that for untreated control. One-way ANOVA ( $\alpha = 0.05$ ) with Dunnett's multiple comparisons test was used for statistical comparison of combination treatment in toxicity assays (230, 231). GraphPad Prism analysis was used for obtaining the synthetic peptide's IC<sub>50</sub> data; non-linear regression parameters were mean  $\pm$  standard deviation, n= 3 (232) and the therapeutic index was defined as the IC<sub>50</sub>/MIC ratio (212, 233).

### 2.3. Results

#### 2.3.1. Peptide purification

ES material analyzed by RP-HPLC was lyophilized, suspended in water and its antibacterial activity tested. Antibacterial activity was quantified by plate growth inhibition assay using a Gram-positive *M. luteus* A270 bacteria as test-organism (Figure 19). Five of these fractions had antibacterial activity. Fractions 2, 3, 4 and 5 had anti-*P. aeruginosa* activity while the other compounds having no activity against *P. aeruginosa* were tested against Gram-positive *M. luteus*. Activity was found in fraction 1; fractions having antimicrobial activity were eluted at 8.1, 50.9, 51.7, 52.1 and 64.9 min and

chromatographed again in the same system with an analytic C18 column. All antimicrobial fractions were analyzed by MS; when compared through a preliminary database search, just fraction 3 had homogeneity with diptera proteins. Purification of this fraction revealed the 3.2 molecule, having antibacterial activity against *M. luteus*.

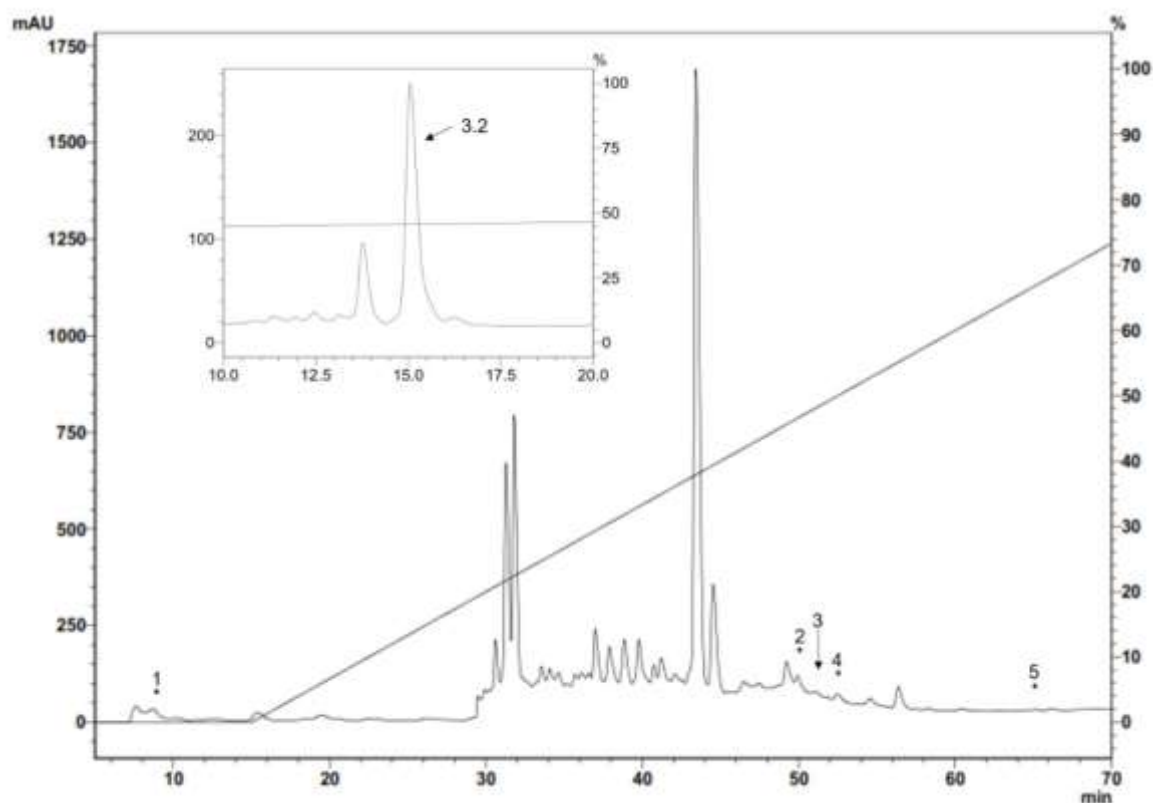


Figure 19. *S. magellanica* ES antimicrobial fractions eluted with 80% ACN from a Sep-Pak cartridge obtained from the first RP-HPLC purification step. Chromatography involved using a semi-preparative Jupiter C18 column (10 $\mu$ m; 300A; 10mm x 250mm) with a 0-80% ACN/0.05% TFA in H<sub>2</sub>O/0.05% TFA linear gradient for 60 min at 2 mL/min flowrate. Absorbance was monitored at 225 nm. The fractions indicated by an asterisk had antimicrobial activity and were eluted at 8.1, 50.9, 51.7, 52.1 and 64.9 min RT; fraction 3 (labelled with an arrow) was chromatographed again in the same system with an analytic Jupiter C18 column (10 $\mu$ m; 300A; 4.6mm x 250mm) and run in 44%-54% solution B for 60 min (inset). The eluted 3.2 fraction (i.e. sarconesin) had antibacterial activity and was purified.

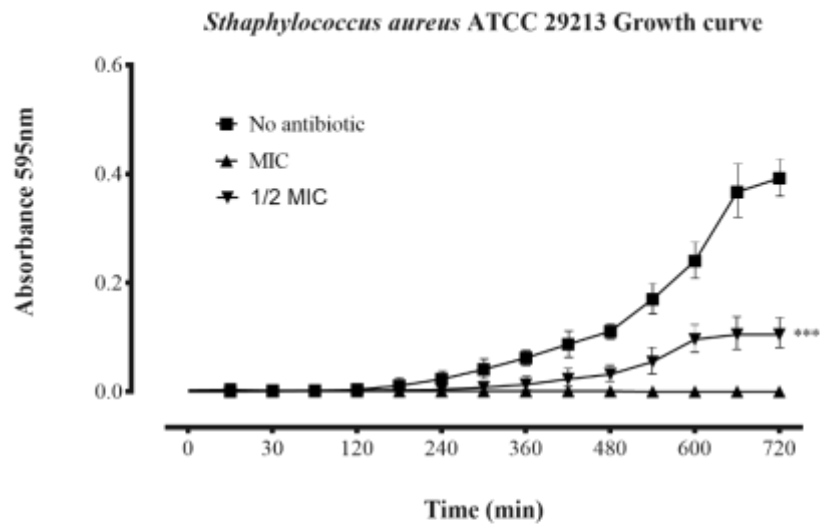
### 2.3.2. Antimicrobial assays

The peptides were studied regarding their potential for inhibiting Gram-positive and Gram-negative bacterial growth. Sarconesin MIC was the same (4.7  $\mu$ M) for *M. luteus* A270 and *P. aeruginosa* ATCC 27853; minimum MIC (1.2  $\mu$ M) was obtained for *S. aureus* ATCC 29213, *S. epidermidis* ATCC 12228 and *E. coli* D31; DH5 $\alpha$  MIC was 2.4  $\mu$ M (Table 3). The effect of sarconesin MIC was seen during *S. aureus*

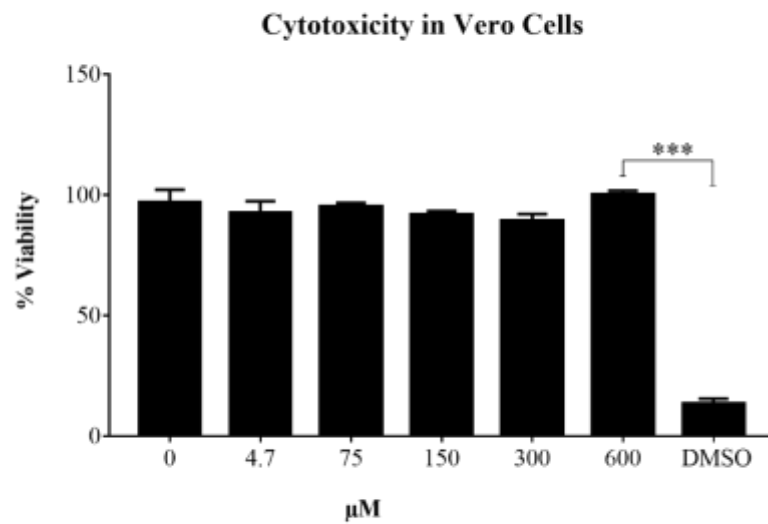
growth curve exponential phase which was reached after more than 180 min; incubation with  $\frac{1}{2}$  MIC revealed a decrease in bacterial growth (Figure 20A).

Table 4. Minimum inhibitory concentration (MIC); MIC refers to the concentration needed for achieving 100% inhibition of growth.

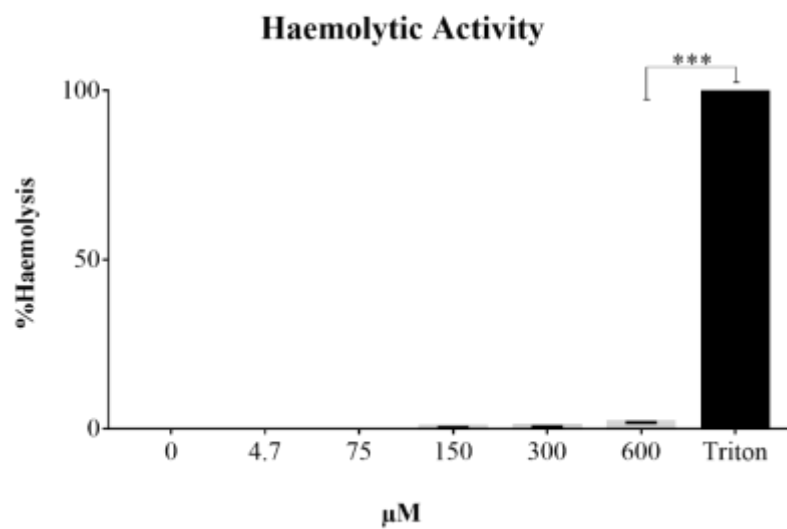
	<b>Strain</b>	<b>Sarconesin MIC</b>
Gram +	<i>M. luteus</i> A270	4.7 $\mu$ M
	<i>S. aureus</i> ATCC 29213	1.2 $\mu$ M
	<i>S. epidermidis</i> ATCC 12228	1.2 $\mu$ M
Gram -	<i>P. aeruginosa</i> ATCC 27853	4.7 $\mu$ M
	<i>E. coli</i> D31	2.4 $\mu$ M
	<i>E. coli</i> DH5 $\alpha$	2.4 $\mu$ M
	<i>S. enterica</i> ATCC 13314	2.4 $\mu$ M



A



B



C

Figure 20. Growth curve and toxicity assays. (A) Growth curve for *M. luteus* A270 incubated with sarconesin. Bacterial growth was inhibited and the antibacterial effect was detected during the exponential phase. (B) Sarconesin cytotoxicity regarding the VERO cell line and (C) hemolytic activity regarding fresh human RBC, showing very low toxicity, even at maximum 600  $\mu$ M concentration.

### 2.3.3. Toxicity

Sarconesin CC activity was tested against the Vero cell line (Figure 20B). No sign of CC was observed with sarconesin, even at the highest tested concentration, i.e. 600  $\mu$ M. Cell viability was 92% after exposure to sarconesin. The selectivity index was not calculated as no CC50 values were found in the maximum concentrations evaluated here. Very low (<2%) hemolytic activity was observed on incubating human RBC with sarconesin at the highest concentration tested (600  $\mu$ M) (Figure 20C).

### 2.3.4. Mass spectrometry

MS analysis of the sarconesin fraction revealed a molecule having 1,471.84 Da mass. The complete sarconesin aa sequence obtained by PEAKS de novo sequencing revealed a 13 aa sequence having a post-translational modification (PTM): TPm(+16)LLVGTKLDLR. Collision-induced dissociation spectrum from mass/charge (m/z) of its double-charged ion gave  $[M+2H]^{2+}$ , m/z 736.9266 (Figure 21). Characterizing the peptide's primary structure with the MASCOT tool gave the TPFLLVGTQIDLR sequence.

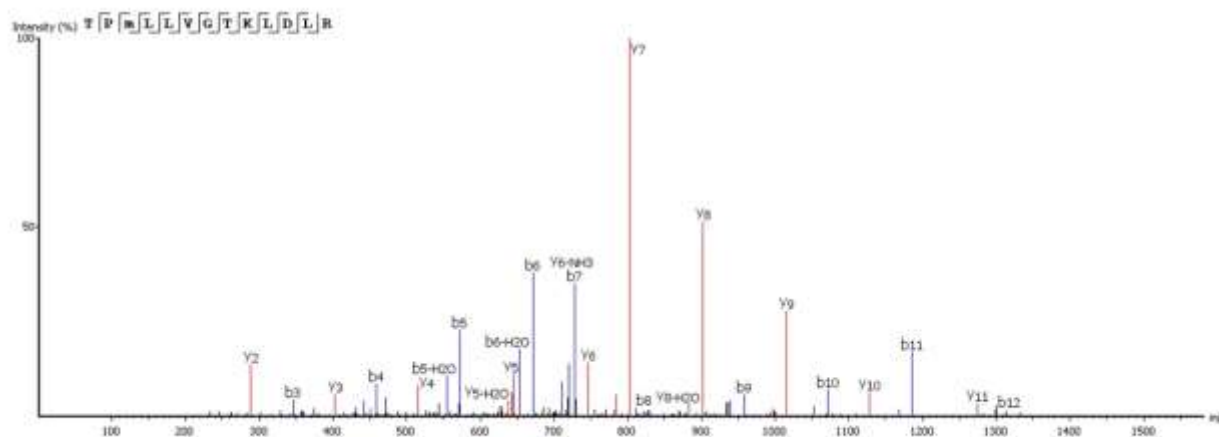
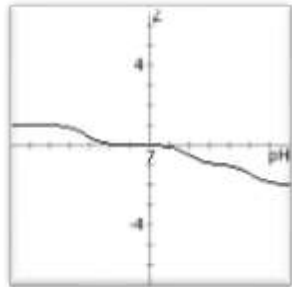


Figure 21. The complete sarconesin aa sequence was obtained by MS/MS fragmentation; representative de novo sequencing of sarconesin. CID spectrum from mass/charge (m/z) of its double-charged ion gave  $[M+2H]^{2+}$ , m/z 736.9266. The ions from y (red) and b (blue) series (marked at the top of the spectrum) represent the primary structure: TPm(+16)LLVGTKLDLR. The sequenced peptide's internal fragments whose ions were found in the spectrum are represented by standard aa letter code.

Proteomic and peptidomic bioinformatics tools were used for predicting sarconesin's significant physicochemical characteristics once the sequence was known. ExPASy's (SIB Bioinformatics Resource Portal) PepDraw and Pep-Calc.com sequence analysis yielded a potential peptide isoelectric point (pI), molar extinction coefficient and net charge (Table 4). The peptide was predicted to have one negatively-charged Asp aa residue and a positively-charged Arg residue, thereby contributing to the peptide's neutral characteristics (0 net charge). Four of the 13 aa were predicted to be hydrophobic (1 Ile, 3 Leu), suggesting sarconesin's poor water solubility. ExPASy's ProtParam tool predicted that the peptide would remain intact for up to 7.2 h in mammalian reticulocytes (*in vivo*), >20 hours in yeast and >10 hours in Gram-negative *E. coli* (*in vivo*). This would likely be due to a Thr (T) residue at the N-terminus.

Table 5. Physicochemical parameters calculated using ExPASy PepDraw and Pep-Calc.com (accessed April 30<sup>th</sup> 2018).

Peptide properties		
Sequence:	TPFLLVGTQIDLR	Net charge vs pH 
Length:	13	
Mass:	1471.8372	
Isoelectric point (pI):	6.42	
Net charge at pH 7:	0	
Hydrophobicity:	+8.87 Kcal * mol <sup>-1</sup>	
Estimated solubility:	poor water solubility	
Extinction coefficient 1:	0 M <sup>-1</sup> * cm <sup>-1</sup>	

### 2.3.5. Protein model

A search for TPFLVGTQIDLR in databases found matches with cell division control protein 42 (CDC42) sequences from humans, cows and fruit flies, having 100% sequence similarity. All sequences are referred to by their NCBI accession numbers (<https://www.ncbi.nlm.nih.gov/>) to minimize confusion: CDC42 cell division control protein 42 homologue OS=*Bos taurus* (Q2KJ93), CDC42\_HUMAN Chain A, structure of the Rho Family Gtp-binding protein Cdc42 in complex with the multifunctional regulator Rhogdi (gi|7245832|1DOA\_A), CDC42\_DROME CDC42 homologue

OS=*Drosophila melanogaster* GN=Cdc42 PE=1 SV=1 (P40793). The BLASTp 2.6.1+ tool for comparing the sequence obtained with those for other *Lucilia* species proteins found 69% identity with a similar sequence previously report as a Ras-related protein Rac1 [*Lucilia cuprina*, another blowfly from the Calliphoridae family]; GenBank: KNC23156.1.

Sarconesin sequence was sought in the genomes and transcriptomes reported for *L. cuprina* (genome ASM118794V1, transcriptome SRX907163) and *L. sericata* (genome ASM101483V1, transcriptome ERX614478, 3-4 day pupa transcriptome SRX087348). Sarconesin was found in all of them (*L. sericata* genome scaffold JXPF01028806.1 and transcriptomes ERR658157.22222021.1 and pupa SRR350018.17744834.1. *L. cuprina* genome scaffold JRES01000256.1 and transcriptome SRR1853100.27006533.2 (accessed May 16<sup>th</sup> 2018) (Figure 22A).

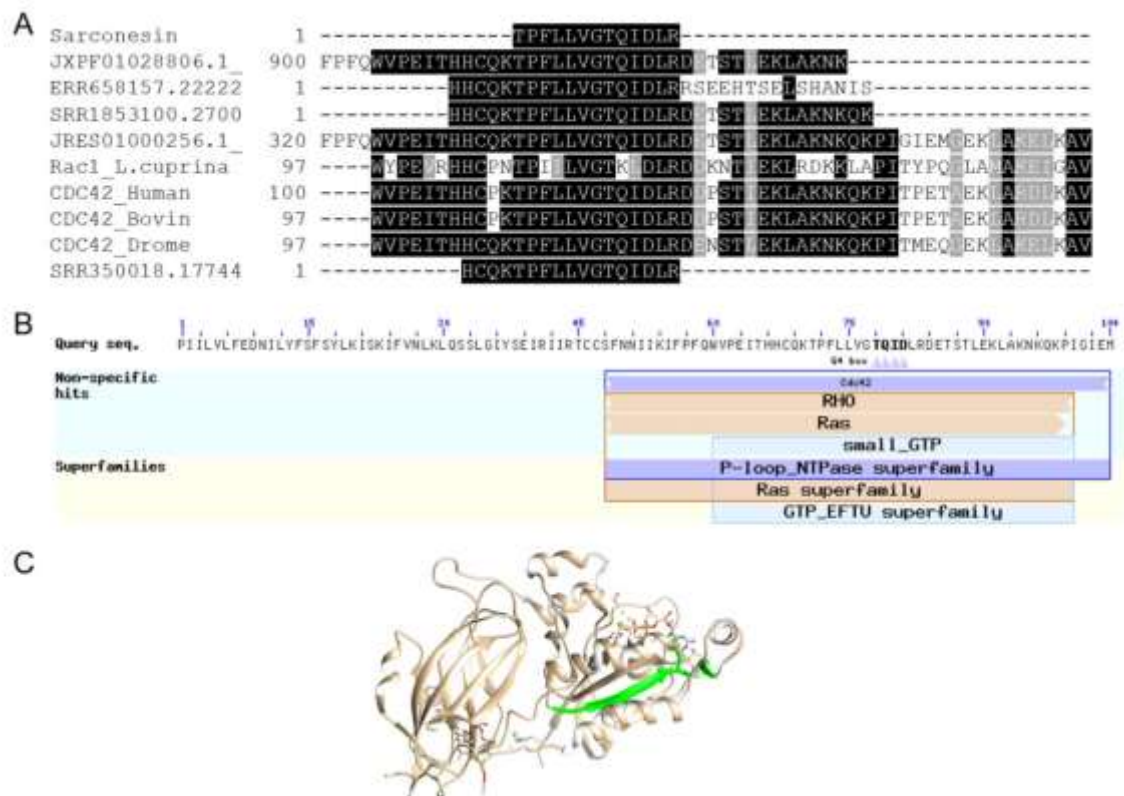


Figure 22. Sarconesin alignment and protein model. (A) Sarconesin multiple sequence alignment against selected proteins (<https://www.ncbi.nlm.nih.gov/>): CDC42 cell division control protein 42 homologue OS=*Bos taurus* (Q2KJ93), CDC42\_HUMAN Chain A, structure of the Rho family Gtp-binding protein Cdc42 in complex with the multifunctional regulator Rhogdi (gi|7245832|1DOA\_A), CDC42\_DROME Cdc42 homologue OS=*Drosophila melanogaster* GN=Cdc42 PE=1 SV=1 (P40793), Ras-related protein Rac1 [*Lucilia cuprina*] GenBank: KNC23156.1. Sarconesin has 100% sequence similarity with CDC proteins and 69% with Rac from *L. cuprina*. Translated sequences from *L. sericata*. Genome scaffold (JXPF01028806.1), transcriptomes

ERR658157.22222021.1 and pupa SRR350018.17744834.1 genome scaffold (JRES01000256.1) and *L. cuprina* transcriptome SRR1853100.27006533.2. (B) Conserved domains found in JXPf01028806.1 *L. sericata* Blastp, showing sarconesin as a conserved residue from the CDC42 domain. (C) Representative model of human CDC42 (PDB ID: 1DOA\_A). Sarconesin is encrypted in a site between residues 111 and 123 (234), which folds as a  $\beta$ -sheet.

The exon containing sarconesin in the JXPf01028806.1 scaffold (GenBank) was located and compared to other proteins by Blastp for determining which organisms had the greatest similarity with the gene. It was shown that this gene was mainly present in other Diptera species (*Stomoxys calcitrans* XP\_013103099.1, *Drosophila sechellia* XP\_002039460.1, *Musca domestica* XP\_005189222.1, *Anopheles gambiae* CAA93820.1 and *Ceratitis capitata* XP\_004518385.1), having 100% similarity. It was established that sarconesin formed part of a CDC42 conserved domain (Figure 22B). The sarconesin model was built using CDC42's known structure (PDB ID: 1DOA) since it has 100% identity with bovine CDC42 and a PDB model is available. Figure 22C shows the similarity model constructed for sarconesin.

#### 2.3.6. Circular dichroism

CD deconvolution software was not suitable for peptide analysis since it was designed for larger proteins (235), so the peptide's secondary structure analysis thus involved qualitatively comparing it to CD spectra obtained from known secondary structures in the pertinent literature. The peptide's CD spectra were obtained at 25°C in water and in TFE/water ranging from 0 to 50% v/v (Figure 23). The CD spectrum in water had a strong negative band around 208 nm and a moderate positive band around 190 nm. As TFE concentration increased, the negative band became less intense and the positive band became more intense, a shoulder appearing between 220 and 230 nm. TFE can aggregate itself around peptide molecules promoting the displacement of the solvation layer, thereby favoring the formation of intra-peptide hydrogen bonds, stabilizing the peptide's secondary-structure. CD spectra features suggested a mixture of 310-helix and  $\alpha$ -helix formations (236). The 310-helix proportion in water was favored and as TFE concentration in solution increased the  $\alpha$ -helix contribution also increased, suggesting that the  $\alpha$ -helix formation could be predominant in a low dielectric environment, as in a phospholipidic membrane.

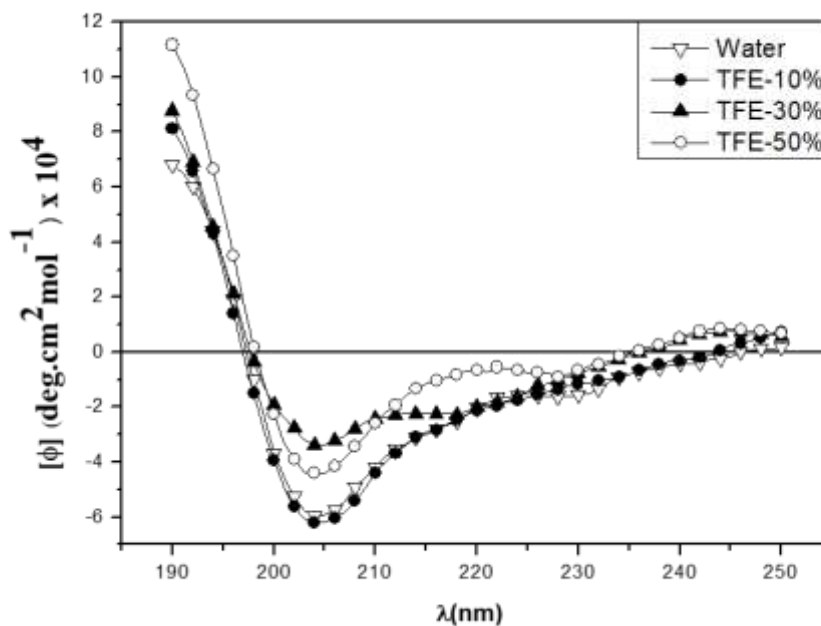


Figure 23. Sarconesin CD spectra in water and different TFE/water ratios.

### 2.3.7. Mechanism of action

#### 2.3.7.1. Membrane integrity and esterase activity

The red fluorescent dye propidium iodide (PI), which is kept on the outside of intact membranes, can penetrate damaged cell membranes and intercalate into nucleic acids. PI fluorescence intensity indicates the level of cell membrane integrity. In the absence of peptide, cells had no PI staining, indicating that membranes were intact (Figures 24 and 25). The percentage of PI-permeable *E. coli* cells increase after treatment with sarconesin; this suggested that the inner *E. coli* membrane became disrupted after sarconesin treatment. Altered esterase activity was observed when compared to bacterial control.

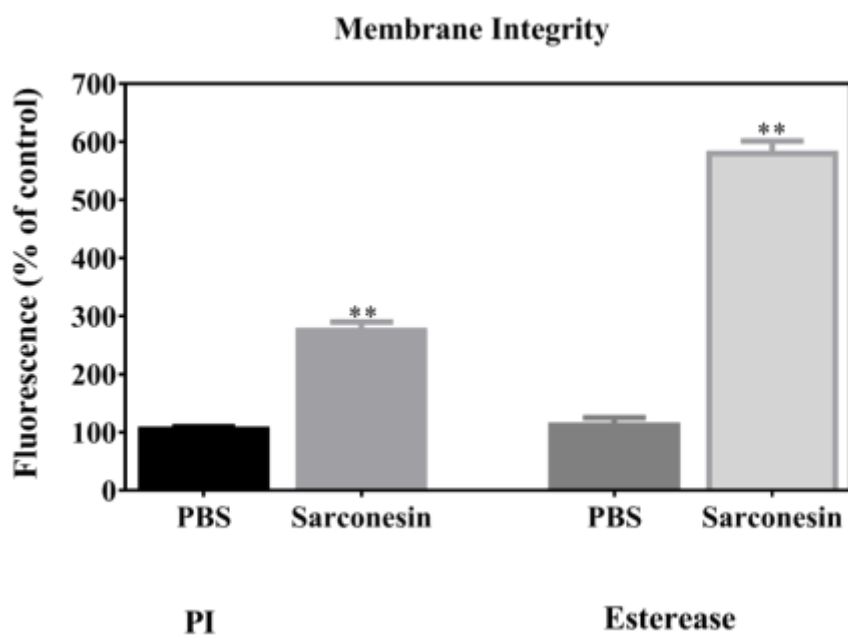


Figure 24. Representative image showing the change in mean fluorescence intensity of fluorescence probes PI and CFDA (esterase activity) in *E. coli*. Histogram represents changes in the mean  $\pm$  SD of PI and CFDA fluorescence, obtained from three independent experiments (\*\* $p < 0.05$  vs. control).

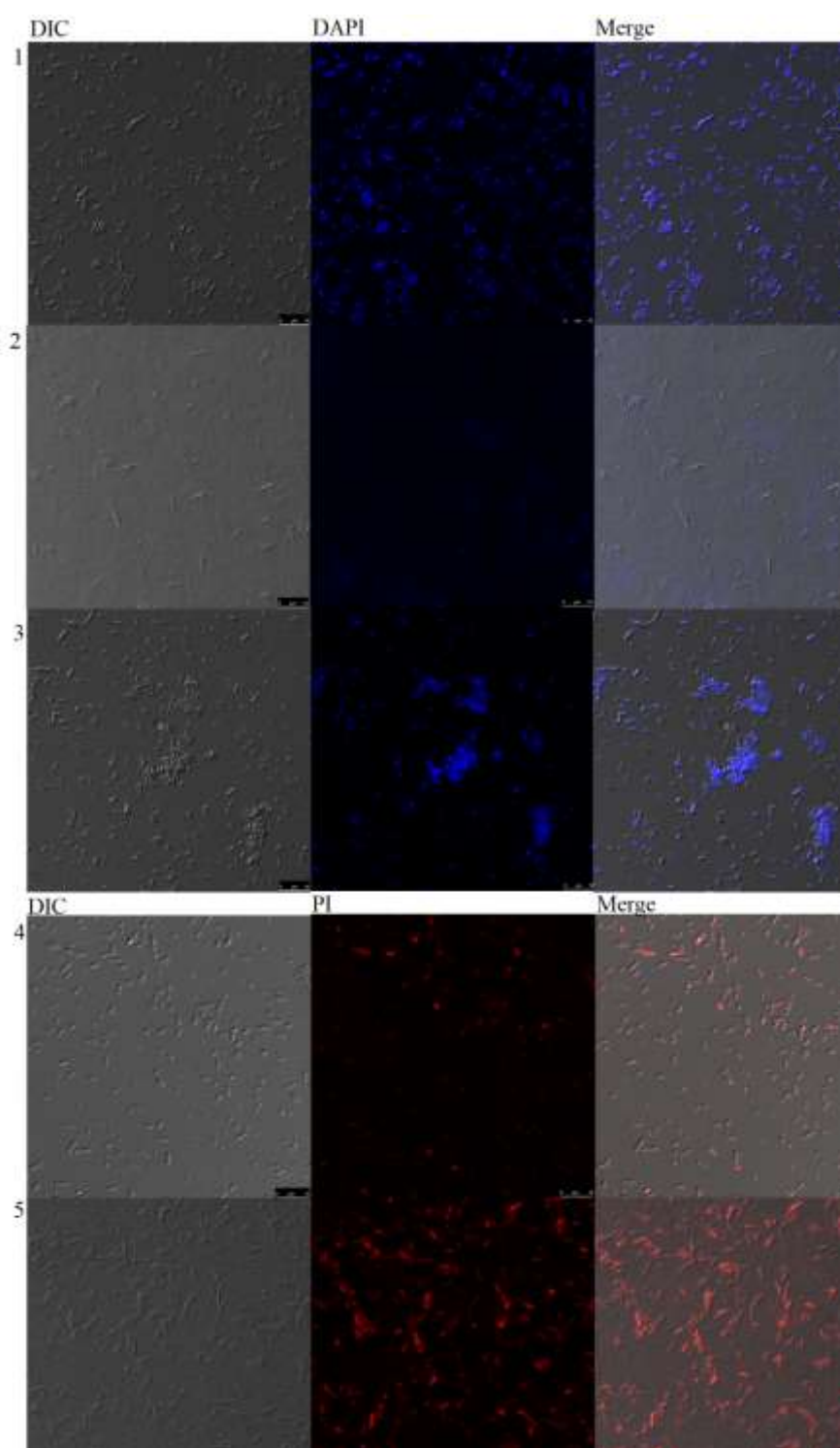


Figure 25. Confocal microscopy analysis of bacteria incubated with sarconesin. PBS-, ciprofloxacin- and sarconesin-treated bacteria stained with DAPI (1-3). PBS- and sarconesin-treated bacteria stained with PI (4-5).

### 2.3.7.2. DNA staining

Neither untreated bacteria nor sarconesin-treated bacteria showed DNA fluorescence, indicating that DNA did not become denatured by sarconesin treatment (Figure 25).

### 2.3.7.3. DNA gel retardation

Sarconesin's DNA-binding properties were examined by analyzing electrophoretic migration of DNA to clarify the molecular MoA. *E. coli* genomic DNA migration suppressed by sarconesin at 50, 100 and 200  $\mu\text{M}$  (Figure 26). This indicated that sarconesin could bind to bacterial DNA.

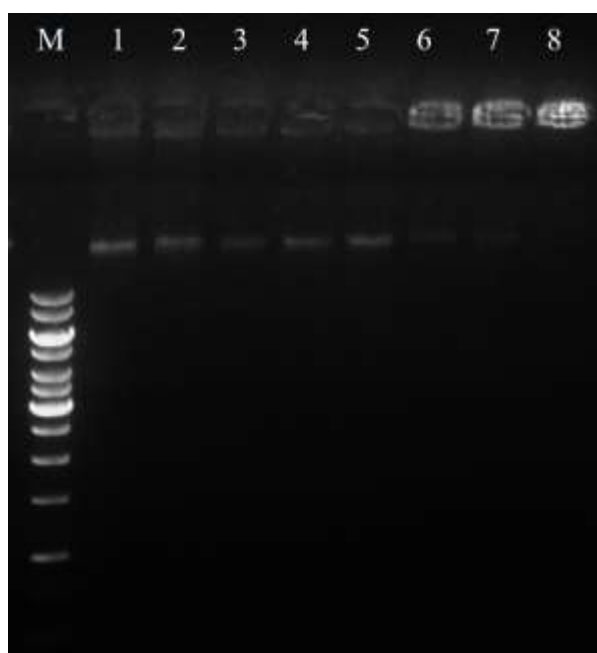


Figure 26. Sarconesin interaction with bacterial gDNA by gel migration assay. M: DNA marker GeneRuler 1Kb; 1-8: sarconesin concentrations were 0, 3.1, 6.25, 12.5, 25, 50, 100 and 200  $\mu\text{M}$ .

## 2.3.8. Synthetic sarconesin

### 2.3.8.1. Purifying synthetic sarconesin

Synthetic sarconesin was purified in RP-HPLC. Chromatography with sarconesin profile showed that the synthetic peptide was collected at TR=101 (Figure 27).

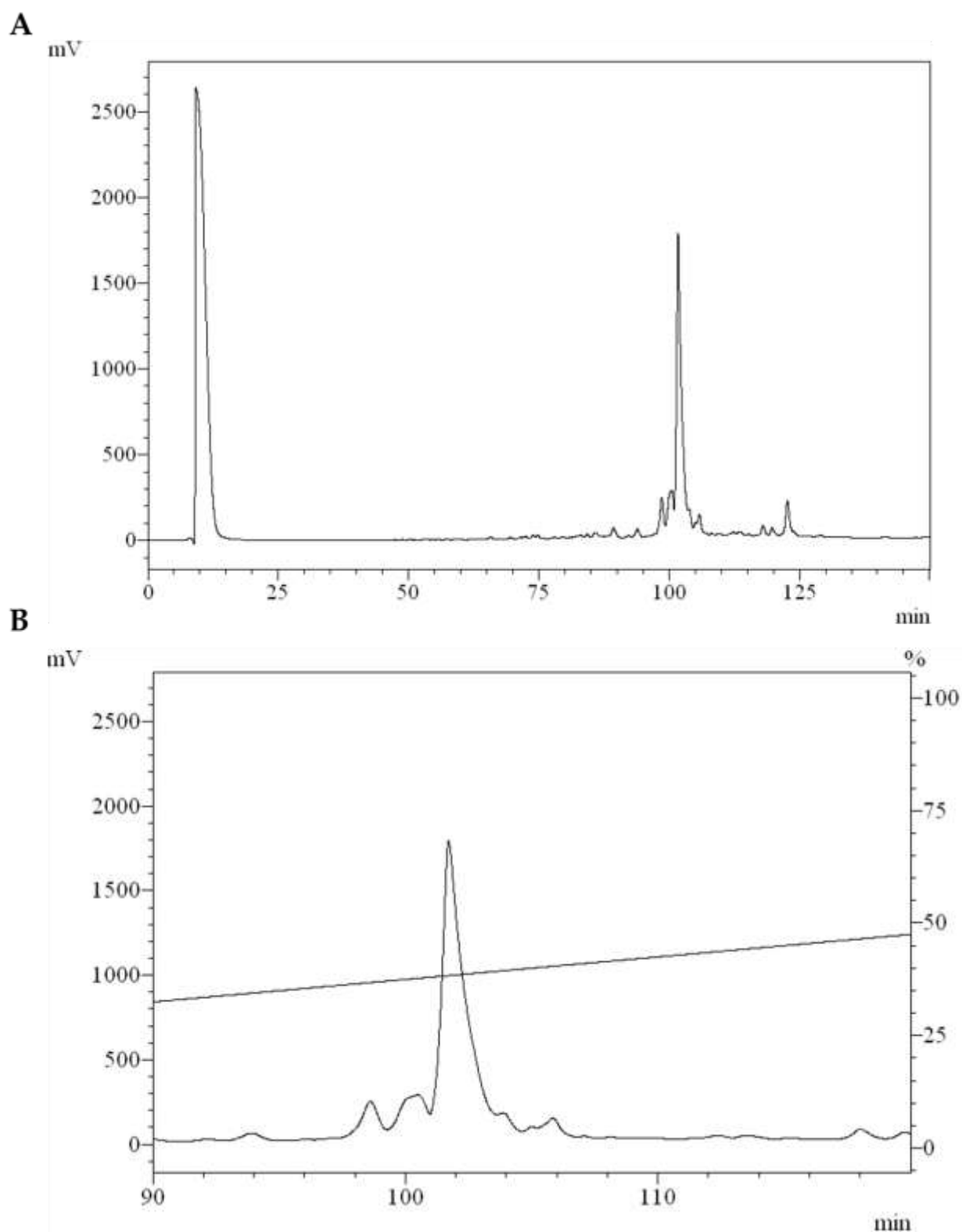


Figure 27. Chromatogram of RP-HPLC purification step from *S. magellanica* sarconesin synthetic peptide. Chromatography involved using a semi-preparative Jupiter C18 column (10 $\mu$ m; 300A; 10mm x 250mm) with a 0-80% ACN/H<sub>2</sub>O/0.05% TFA linear gradient for 120 min at 2 mL/min flow rate. Absorbance was monitored at 225 nm. Synthetic sarconesin was collected at TR=101 (Figure 9A), zoom image (B).

#### 2.3.8.2. Mass spectrometry

The complete synthetic sarconesin aa sequence was confirmed by MS (Figure 28).

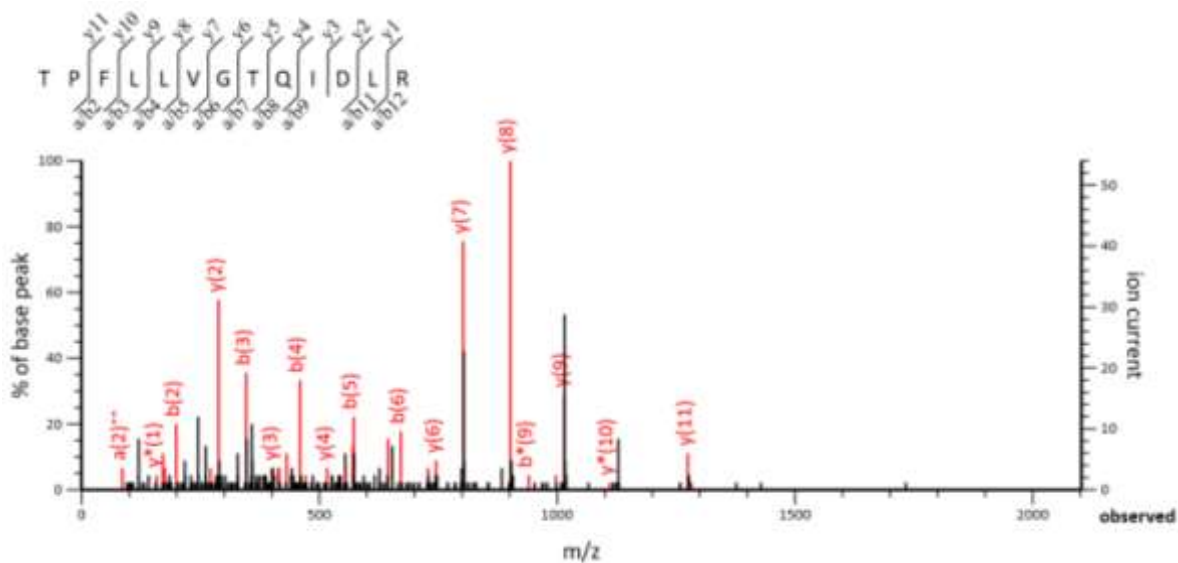


Figure 28. CID spectrum for sequenced synthetic sarconesin. The ions belonging to -y (red) series indicated at the top of the spectrum show the peptide's primary structure: TPFLLVGTQIDLR. Internal fragments of the sequenced peptide, whose ions were found in the spectrum, are represented by standard aa code letters.

### 2.3.8.3. Hemolytic activity

Its hemolytic activity was assessed to elucidate whether the synthetic peptide had any effect on hRBC at antimicrobial concentrations. No hemoglobin release was observed in the concentrations at which the peptide was active against bacteria and yeast; nevertheless, a statistically significant 10% hemolysis ( $SD \pm 0.03$ ) was obtained at 275  $\mu\text{M}$ ; a percentage hemolysis was also observed at higher concentrations. This suggested that sarconesin caused human erythrocyte lysis and may even be cytotoxic at concentrations higher than 275  $\mu\text{M}$ .  $IC_{50}$  is peptide concentration ( $\mu\text{M}$ ) giving 50% hemolysis after 1 h at 37°C, obtained by non-linear regression analysis, i.e. 1100  $\mu\text{M}$  (Figure 29).

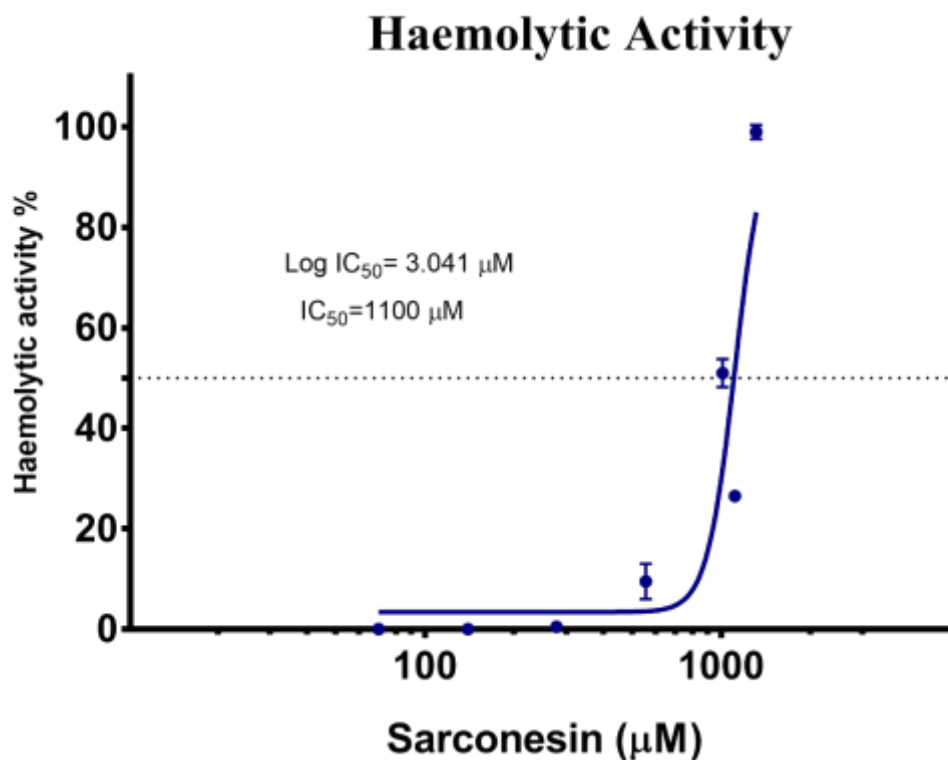


Figure 29. Synthetic sarconesin hemolytic activity after 1 hour treatment. The peptide's concentration-response curve for percentage hRBC lysis is shown. IC<sub>50</sub>=1100 µM dose-dependent hemolytic effect of sarconesin on hRBC. The control for 100% hemolysis was a sample of erythrocytes treated with 0.1% Triton-X 100. Peptide concentration is given in µM. GraphPad Prism was used for analyzing IC<sub>50</sub> data. Parameters: non-linear regression; (mean ± standard deviation, n= 3).

#### 2.3.8.4. Antimicrobial assay and therapeutic index (TI)

Synthetic sarconesin was tested for antimicrobial activity against three Gram-positive bacterial species, three Gram-negative bacterial species and one yeast species (Table 3). All the microorganisms tested were sensitive to the synthetic peptide which was active at concentrations beginning with 25 µM (Table 5). TI is the ratio of the IC<sub>50</sub> value (µM) to the geometric mean MIC value (µM) (237). High values indicate greater antimicrobial specificity; the highest one was obtained for *S. epidermidis* ATCC 12228 (TI 44), indicating that the peptide was selective.

Table 6. Synthetic sarconesin antimicrobial activity against different strains.

Strain		Synthetic MIC ( $\mu\text{M}$ )	TI.*
Gram +	<i>M. luteus</i> A270	>200	ND
	<i>S. aureus</i> ATCC 29213	50	22
	<i>S. epidermidis</i> ATCC 12228	25	44
Gram -	<i>P. aeruginosa</i> ATCC 27853	100	11
	<i>E. coli</i> D31	50	22
	<i>S. enterica</i> ATCC 13314	50	22
Yeast	<i>Candida albicans</i> MDM 8	50	22

\*MIC is the minimum inhibitory concentration ( $\mu\text{M}$ ) of peptide inhibiting bacterial growth after 18 h. TI is the ratio of the IC<sub>50</sub> value ( $\mu\text{M}$ ) to the geometric mean MIC value ( $\mu\text{M}$ ). High values indicate greater antimicrobial specificity.

## 2.4. Discussion

Bacterial resistance against antibiotics has created special interest in searching for new compounds as potential antimicrobial drugs which might be more effective in developing new therapeutic tools (51). This work led to finding a new sequence from *S. magellanica*; its antibacterial activity was screened, and its biochemical and structural properties were elucidated by sequence homology. One AMP responsible for the antibacterial activity previously reported in *S. magellanica* was found (76). Sarconesin was seen to have 1,471.8372 Da mass and similarity with Cdc42 and Rac proteins; the AMP was embedded in a site between human Cdc42 residues 111 and 123, folding as a  $\beta$ -sheet. A search for the peptide in AMPs database did not reveal any similarity with previously reported AMPs; however, this new peptide could be part of the family of linear AMPs (156).

The MIC obtained for sarconesin in this study suggested potent activity, similar to that previously reported for other peptides that are active below 32  $\mu\text{g}/\text{mL}$  concentration (238), the thanatin peptide has been shown to have a MIC below 2.5mM, highlighting the fact that sarconesin required less peptide to inhibit bacterial growth (205). This further supported the importance of new effective substances, knowing that several bacteria do become resistant after some days or even hours of exposure (239). The *S. aureus* growth curve showed that sarconesin has an effect in less than 180 minutes' incubation. It should be stressed that the fractions having antibacterial activity were absent in the peaks having the

greatest absorbance; this has already been observed in other work where defensin, dipterin (51) and lucifensin have been detected in very tiny peaks (45).

Sarconesin has C-terminal R and N-terminal T residues; when a search for homology was made, a K residue was found immediately before the N-terminal T, suggesting that it might be targeted by trypsin-like activity (240). The peptide so obtained could have resulted from some proteases and other enzymes in the ES, taking into account that our experimental procedure did not involve trypsin treatment (2); it has already been reported that ES have trypsin and chymotrypsin in their content (241, 242). Sarconesin could be a product of processing the Cdc42 or Rac protein and have other functions in the blowfly related to cell cycle; the derived sarconesin also has antibacterial activity. It is worth emphasizing that Rac's antimicrobial activity has not been reported before in Calliphoridae blowflies.

As sarconesin was also present in *S. scrofa* and the flies' food supplement was liver, it could be assumed that the peptide was a sub-product of CDC42 from *S. scrofa* and not from *S. magellanica*. However, sarconesin in other *Lucilia* species' transcriptome and genome showed that this peptide is present in such blowflies, maybe as a sub-product of Diptera. Indeed, multi-omics studies of maggots for LT usually involve using insects fed on bovine liver (243, 244). Sarconesin was also present in studies with maggots fed on sheep blood agar as supplement (144, 245). This exon was also searched through Blast to discard whether it had greater similarity with Diptera species than with *S. scrofa*. It was found to be more similar with Diptera species having different feeding habits and was also associated with a CDC42 conserved domain. Sarconesin was also found in pupa transcriptome having no contact with liver residue, showing that this peptide's origin could most likely be from the fly.

ES pH is usually 8–8.5 (i.e. in *Phaenicia sericata*) (246, 247) because of a waste product (ammonia), since ammonia increases wound pH, resulting in alkaline conditions which are unfavorable for many bacterial species (7, 8). Sarconesin's net charge would thus be negative as sarconesin is in ES and knowing that a protein's net charge is positive at pH below pI (248) (Table 4). This makes sarconesin an anionic peptide in ES in normal conditions. The MoA regarding bacteria could involve translocation across the membrane (the common mode of action for anionic peptides) (249), knowing that AMPs can function as direct antimicrobial compounds (250) and also as effector molecules induced upon microbial infection (138).

Sarconesin had 100% sequence similarity with different organisms' CDC42 protein and 69% identity with RAC from *L. cuprina*. Both proteins form part of the Rho-family GTPases (251); sarconesin may have a similar intracellular MoA, knowing that this protein's expression activates growth factors (252) and acts as a molecular switch by responding to exogenous and/or endogenous signals, relaying such signals to activate an intracellular biological pathway's downstream components (253). The PI assay confirmed a membrane disruption mechanism that has already been reported for other AMPs due to electrostatic interactions, which may be followed by hydrophobic patches' insertion into the nonpolar interior of the membrane bilayer (254), having a barrel-stave model for the channel pore similar to that for alamethicin as sarconesin has a 3<sub>10</sub>-helix conformation (255). Some morphological changes on bacteria were observed in the sarconesin PI experiment (Figure 25); these most likely occurred when the antimicrobial agent attacked the cell membrane, as previously reported by Hyde (256).

Sarconesin induced the release of 6-carboxyfluorescein, indicating an effect resulting from a transient destabilization of the bilayer upon initial interaction, a similar effect previously reported for the magainin-2 peptide (257). Bacterial DNA, when incubated with sarconesin and DAPI, did not become degraded and the gel retardation assay showed that sarconesin bound strongly to DNA *in vitro*, suggesting inhibiting intracellular functions via interference with DNA (258).

A selectivity index could not be established for the native peptide; nevertheless, no CC was found. These findings suggest this compound's appreciable selectivity against bacteria and, therefore, this observation may be an indicator of their safety as drugs for use with mammalian organisms. A hemolytic assay was performed to verify whether the peptide could disrupt human erythrocyte membranes to evaluate the peptide's pharmacological potential; the peptide had very low (<2%) hemolytic activity at 600  $\mu$ M final concentration. Hemolytic activity decreased to 0% at concentrations ranging between 600-300  $\mu$ M (Figure 20C). As expected, the peptide had no relevant toxic potential, even when tested at a concentration 128 times higher than that for *M. luteus* and *P. aeruginosa* MIC (i.e. 4.7 $\mu$ M), as sarconesin was identical to a conserved domain from CDC42 in human cells acting as a molecular switch for controlling a variety of eukaryotic processes (253).

Sarconesin may also have implications for wound healing. It has been reported in cell culture that ES from other necrophagous flies increase fibroblast proliferation for wound healing (259). Sarconesin

---

has specifically been reported as an angiogenesis biomarker of recovery after acute kidney injury, so it could be a good candidate for future wound evaluation activities (260). The Rho family also has wound-healing properties and GTPases role in epithelial remodeling during wound-healing and epithelial-mesenchymal transitions has also been reported (261). There is also evidence that Cdc42 plays a major role in wound healing regarding host defense against infection (262). Previously identified natural AMPs from insects are produced by bacteria, fungi, numerous invertebrates, vertebrates and plants and are usually associated with killing microbes, although they could also be involved in wound repair, inflammation, chemotaxis and cytokine activity (263).

The sequenced peptide's antibacterial potency was confirmed when evaluating synthetic sarconesin's bioactivity; nevertheless, synthetic sarconesin's MIC were higher than those obtained for native sarconesin. Differences between native and analogue synthetic peptides have previously been observed for surfactant protein B (SP-B) and Pg-AMP1, modified activity being obtained compared to that for natural protein. This was probably due to a peptide assuming several formations which may have great importance regarding its activity (264, 265). As synthetic peptides are formed as a TFA salt, it has been reported that counter-ions may also affect peptide and protein secondary structure; however, structural modifications have not significantly affected pediocin PA-1 antimicrobial activity (266, 267), though structural changes could have been caused by D-aa in the sequence. Living organisms use L-aa to synthesize proteins; a group of D-aa containing peptides (DAACPs) has been discovered in animals, having at least one of their residues isomerized to the D-form. It can change its biological functions due to such structural conversion (268) and could differentiate peptides just containing L-aa from those containing D-aa. Although this was not our stated purpose (i.e. to validate the sequenced peptide's antimicrobial potency), each peptide of interest must be examined individually, which can be extremely time-consuming (269).

Both native and synthetic sarconesin had lower MICs against Gram-positive bacteria; this was frequently reported as Gram-positive bacteria have only one membrane (the cytoplasmic membrane surrounding the cell) while Gram-negative bacteria have two: the cytoplasmic membrane and a peptidoglycan layer on the outer side of the cytoplasmic membrane (270). This may explain why *P. aeruginosa* ATCC 27853 required a higher dose of peptide.

None of the 25, 50, 100  $\mu\text{M}$  MIC concentrations for synthetic sarconesin had hemolysis, confirming that the peptide had interesting antimicrobial potential. Peptides having action on bacterial membranes are accompanied by hemolytic toxicity. Ideal therapeutic membrane-targeted antimicrobials should be selective against microbial cells and not affect mammalian cells (271). Some reported peptides, such as tetrameric Pg-AMP, have higher than 49.3% hemolysis at 100  $\mu\text{M}$ . Another example would be G8P analogous D-piscine IC<sub>50</sub> reported to be 55  $\mu\text{M}$  and sarconesin's IC<sub>50</sub> 1,100  $\mu\text{M}$  also suggesting that it had higher affinity for prokaryotic cell membranes (212, 272).

Large TI values indicate greater antimicrobial specificity. Sarconesin TI ranged from 11 to 44 for the tested strains. The modified AMPs D-piscidin 1 I9K had 3.2 TI and D-dermaseptin S4 L7K,A14 49 TI for *P. aeruginosa* (273); however, sarconesin TI for this same bacteria was 11. The potent native AMP gomesin has been reported to have TI values ranging from 0.15 to 0.61 for *S. aureus*, *E. coli* and *C. albicans*, showing sarconesin's therapeutic potential as it has higher TIs (237).

Several reports have demonstrated that after modifying some AMP analogues, their TI values and antimicrobial effect have become considerably increased, also reducing their hemolytic effect and reducing their sensitivity to proteases (212, 237, 274-279). It is well known that peptides are relatively sensitive toward proteolytic degradation (280) as *S. aureus* strains secrete aureolysin, staphopain A and staphopain B proteases involved in pathogenesis and resistance to host defense protein/peptides including complement factors and CAMPs<sub>46</sub> (281).

AMPs' therapeutic applications are limited by their sensitivity to proteases (282); some modifications, like blocking N- and C-termini and introducing D-aa improve their stability (274-278, 283, 284). Adding hydrophobic residues (W, Y, I, V) would help their interaction with lipid bilayer lipophilic regions to create pores or other destabilizing structures leading to membrane depolarization or local disruption and eventually bacterial cell death. Otherwise, adding or replacing aa for positively-charged residues (R, K) has been reported to considerably improve their biological activity (233, 285, 286), directing antimicrobial proteins to the negatively-charged bacterial cell wall and bacterial cytoplasmic membrane where they exert their antimicrobial effect.

It has been suggested that the C-terminus is responsible for the membrane interaction and pore formation, while the N-terminal region is important in bacteria-specific interaction and intracellular

components like DNA and RNA (287-290). Improved peptide screening and computational biology will promote peptide drug discovery; it would be interesting to optimize the sarconesin sequence and evaluate analog molecules to estimate whether its biological action and therapeutic effect can be increased.

## **2.5. Conclusion**

This chapter has reported a study regarding a small antimicrobial peptide which is a member of a new Rho family; it contains 13 residues and is active against Gram-positive and Gram-negative bacteria. The native peptide was purified from *S. magellanica* by RP-HPLC and characterized by aa sequencing. Further studies aimed at evaluating its activity against other bacteria, fungi, viruses and parasites are needed, as well as ascertaining its MoA and investigating its action regarding wound healing.

### 3. Chapter 3

## **Sarconesin II, a new antimicrobial peptide isolated from *Sarconesiopsis magellanica* excretions and secretions**

Chapter 3 describes the discovery of the AMP Sarconesin II. *S. magellanica* larval ES sarconesin II's antibacterial action and its MoA has been studied, isolated, characterized and evaluated, contributing towards the urgent need for developing new alternatives to antibiotics due to the increased incidence of multi-resistant bacteria. The discovery of new AMPs should provide an interesting and promising strategy and could result in a lower probability of the development of resistance regarding currently-used antibiotics.

### **3.1. Objective**

1. Determining the isolated peptide Sarconesin II primary structure and physicochemical properties;
2. Determining the previously characterized peptides' antibacterial activity against *Staphylococcus aureus*, *Pseudomonas aeruginosa*, *Escherichia coli* and *Micrococcus luteus*.
3. Analyzing the selected peptides' safety using cytotoxicity (CC) and hemolytic assays.

### **3.2. Materials and Methods**

#### *3.2.1. Bacterial strains*

The strains used were the multi-drug resistant *Pseudomonas aeruginosa* PA14, *P. aeruginosa* 27853, *Escherichia coli* MG1655, *E. coli* DH5 $\alpha$ , *Staphylococcus aureus* ATCC 29213 and *Micrococcus luteus* A270; they were obtained from the Butantan Institute's Special Laboratory for Applied Toxinology (LETA) (São Paulo, Brazil), while the resistant *P. aeruginosa* PA14 strain was kindly donated by Dr. Beny Spira (USP, Brazil).

#### *3.2.2. Antimicrobial assays*

MIC was assayed according to the standard method (296). Exponential growth phase cultures were diluted in poor nutrient broth (PB) at  $5 \times 10^4$  CFU/mL (DO = 0.001) final concentration (144, 213, 297).

The fractions' antimicrobial effects were evaluated by liquid growth inhibition assay, using 96-well sterile plates; 20  $\mu$ L serial dilutions of the fractions were incubated with bacteria at final 100  $\mu$ L volume. Sterile water, PB and streptomycin were used as growth and growth inhibition controls. The plates were incubated for 18 h at 30°C. Absorbance was measured at 595 nm (193).

Time-kill studies involved using a final inoculum of around  $1.5 \times 10^7$  CFU/mL at final 2 mL volume in a polypropylene tube. The samples and control were incubated at 37°C. Serial 100-fold dilutions were prepared in distilled water at each sampling time (0, 30, 120, 240, 360 and 420 min), where necessary. A 10  $\mu$ L aliquot of the diluted and/or undiluted sample plated in triplicate on LB agar were incubated for 24 h at 37°C; the colonies were counted. Activity was considered to be bactericidal when the original inoculum became reduced by  $\geq 3$  log CFU/mL (99.9%); bacteriostatic activity was defined as  $< 3$  log CFU/mL reduction in the original inoculum (298).

### 3.2.3. Acid and solid phase extraction

The ES were incubated with 2M acetic acid for five minutes and spun for 30 min at 4°C. The supernatant was eluted with Sep-Pack C18 cartridges (Waters Associates, Milford, MA, USA), using two ACN concentrations in water (0% and 80%). The hydrophobic part (80%) was lyophilized and reconstituted in 2 mL 0.05% TFA.

### 3.2.4. Peptide purification

RP-HPLC was used to fractionate the hydrophobic part of the ES, using a semi-preparative C18 Jupiter column (Phenomenex International, Torrance, CA, USA 10  $\mu$ m; 300 A; 10 mm  $\times$  250 mm), with a 0 to 80% elution gradient (60 min, 2mL/min flowrate). The fractions were manually collected and absorbance was monitored at 225 nm (299). The fractions' antibacterial activity was determined, and fractions eluted with 40% ACN were fractionated on an analytical Jupiter C18 column (10  $\mu$ m; 300A; 4.6 mm  $\times$  250 mm), at 30% to 45% ACN concentration (209). The purified fraction's (sarconesin II) antibacterial activity was evaluated against that of previously reported strains.

### 3.2.5. Toxicity

CC activity was evaluated against HeLa (human cervical carcinoma) cells kept in DMEM culture medium, supplemented with 10% heat-inactivated bovine serum and antibiotic-antimycotic solution (100 units/mL penicillin, 100 g/mL streptomycin and 25 g amphotericin B) in 5% CO<sub>2</sub> at 37°C (231). MTT assays were used to evaluate CC;  $5 \times 10^5$  cell/well were seeded in 96-well plate for 24 h and eight, two-fold serial dilutions of sarconesin II (starting at 100  $\mu$ M) were allowed to react with the cells for 24 h. 30% DMSO and medium were used as control (142). 5 mg/mL of MTT reagent were incubated for 4 hours at 37°C and dissolved with 150  $\mu$ L isopropanol. Absorbance was measured at 550 nm and CC

was determined, using the formula:  $CC\% = (\text{peptide treated cells}/\text{peptide untreated cells}) \times 100$  (295, 300).

Hemolytic activity was assessed using human erythrocytes. Cells were collected in 0.15 M citrate buffer, at pH7.4 and washed three times with PBS at final 4% (V/V) concentration. Eight two-fold serial dilutions of sarconesin II were evaluated at 100  $\mu\text{M}$  final concentration and incubated for 1 hour at 37°C. Hemolytic activity was determined by measuring absorbance (Abs) at 405 nm and calculated as a percentage of 100% lysis control (0.1% Triton X-100); % hemolysis =  $(\text{Abs sample} - \text{negative Abs}) / (\text{positive Abs} - \text{negative Abs})$  (301).

### 3.2.6. Mass spectrometry and sarconesin II identification

MS analysis involved using a LC-MS/MS on an LTQ-Orbitrap Velos hybrid mass spectrometer (Thermo Fisher Scientific, Waltham, MA, USA) coupled to an Easy-nLCII liquid nano-chromatography system (Thermo Scientific). The chromatographic step involved using 5  $\mu\text{L}$  of each sample on a C18 pre-column (100  $\mu\text{m}$  I.D.  $\times$  50 mm; Jupiter 10  $\mu\text{m}$ , Phenomenex Inc., Torrance, CA, USA) coupled to a C18 analytical column (75  $\mu\text{m}$  I.D.  $\times$  100 mm; ACQUA 5  $\mu\text{m}$ , Phenomenex Inc.). Samples had been previously concentrated in a vacuum centrifuge and diluted in 15  $\mu\text{L}$  0.1% FA. The eluate was electro-sprayed at 2 kV and 200°C in positive ion mode. Mass spectra were acquired by FTMS analyzer; full scan (MS1) involved using 200–2000  $m/z$  (60,000 resolution at 400  $m/z$ ) as mass scan interval with the instrument operated in data dependent acquisition mode. The five most intense ions per scan were selected for fragmentation by collision-induced dissociation. The minimum threshold for selecting an ion for a fragmentation event (MS2) was set to 5,000 cps (295).

MS/MS peak list files were screened against a bank database constructed with the *Lucilia* proteins obtained from UNIPROT and NCBI (220, 302) to determine their aa sequence. They were compared using PEAKS 8.5 search software (Bioinformatics Solutions Inc., Waterloo, ON, Canada), using the following parameters: oxidation considered as variable modification, 10 ppm precursor mass tolerance and 0.6 fragment ion mass tolerance (301).

### 3.2.7. Bioinformatics tools

The sarconesin II sequence was searched for similarity against *Calliphoridae* proteins registered in the National Center for Biotechnology (220) public database, using the Basic Local Alignment Search Tool (BLASTp) (303), with default parameters (304).

The antimicrobial peptide database APD (305) and the ClassAMP prediction tool were used for classifying AMPs (1).

Sequences' physical-chemical parameters were calculated using the Swiss Institute of Bioinformatics (SIB) website's ExPASy bioinformatics resource portal's ProtParam tool (306). The online

I-TASSER server available on the Yang Zhang laboratory website (307) was used to obtain a 3D image of peptide secondary structure (308).

The Chimera structure prediction tool (accessed through the European Bioinformatics Institute) was used to obtain the location of sarconesin II in the representative mitochondrial membrane ATP synthase subunit model (PDB ID: 2w6j) (234). The protein's molecular weight was calculated at the following link: <https://www.bioinformatics.org/sms/index.html>.

### 3.2.8. Circular dichroism

The peptide's far-UV (190–250 nm) CD spectrum was recorded on a Jasco J 810 spectropolarimeter (Jasco Inc., Tokyo, Japan) at 25°C, using a 0.1 cm path length quartz cell. CD spectra were recorded after accumulating 4 runs. The peptide was analyzed in pure water and 30, 70 and 100% *v/v* solutions of 2,2,2-trifluoroethanol (TFE) in water. Fast Fourier transform (FTF) was used to minimize background effects (309).

### 3.2.9. Mechanism of action (MoA)

#### 3.2.9.1. Membrane damage and esterase activity

The *E. coli* suspension ( $2 \times 10^8$  CFU/mL) was incubated with or without sarconesin II MIC solution at 37°C for 4 h. The cells were washed with PBS three times by spinning (2,000 rpm, 5 min) and bacterial membrane integrity was assessed by fluorometry and microscopy using propidium iodide (PI 60  $\mu$ M) for 15 min and measured with 485/620 nm excitation/emission wavelengths. PI microscope slides were prepared by placing 10  $\mu$ L of the mixture, covered with a glass coverslip, and observing them by microscope (226, 310). Microscopy involved using a TCS SP8 confocal laser SEM (Leica, Mannheim, Germany); Leica Application Suite X (LAS X) software was used to process the images. Esterase activity was evaluated by incubating in the dark, washing cells with 250  $\mu$ M 5(6)-carboxyfluorescein diacetate (CFDA) for 30 min, followed by measuring fluorescence at 485/535 nm excitation/emission wavelengths (226, 311).

#### 3.2.9.2. DNA binding activity and fluorescence microscopy

A gel retardation assay determined whether sarconesin II had DNA-binding activity. *E. coli* DNA was purified using the method described by Landry *et al.* (1993) (229); 500 ng gDNA were incubated for an hour with 25, 50 and 100  $\mu$ M sarconesin II. The mixtures were subjected to gel electrophoresis on 0.8% agarose gel (258). The previously washed peptide and bacterial cell mixtures were fixed on slides, permeabilized with ethanol, and stained with 4',6-diamidino 2-phenylindole (DAPI) for visualizing the DNA, using a confocal microscope.

### 3.2.9.3. Sarconesin II-treated *E. coli* cells total protein profiling

*E. coli* cells were grown in Luria-Bertani (281) medium and cell suspension turbidity was adjusted to final  $1 \times 10^8$  CFU/mL concentration, measuring bacterial suspension OD at 595 nm (OD<sub>595</sub>). After growth, cells were harvested by spinning at 4,000 g for 10 min at 4°C. The pellets were washed twice with PBS and  $10^8$  cells were suspended in 1 mL PB medium for further treatment at different sarconesin II concentrations (25, 50 and 100 µM) for 12 h at 37°C.

The samples were spun at 13,000 rpm for 3 min at 4°C; supernatants were discarded. This was followed by adding 225 µL lysis buffer (25 mM Tris-HCl, pH 7.5, 100 mM NaCl, 2.5 mM EDTA, 20 mM NaF, 1 mM Na<sub>3</sub>VO<sub>4</sub>, 10 mM sodium pyrophosphate, 0.5% Triton X-100, protease inhibitor cocktail) containing 30 mM IAM to the pellets with sonication in 3 bouts of 30 sec each on ice. The supernatants were collected by spinning at 14,000 rpm for 15 min at 4°C and stored at -20°C. Supernatant protein concentration was determined based on absorbance at 280 nm using a NanoDrop 2000 spectrophotometer (Thermo Fisher Scientific, Waltham, MA, USA).

*E. coli* cells' total protein profiling was carried out using 12% sodium dodecyl sulphate-polyacrylamide gel electrophoresis (SDS-PAGE). The samples were incubated with SDS-loading buffer at 90°C for 3 min before electrophoresis and then 25 µg of each sample was applied directly to the polyacrylamide gel. The total running time was 3 h at 120 V. The gel was then stained with silver nitrate or Coomassie Brilliant Blue R-250. Bacterial cells were incubated with streptomycin (a protein synthesis inhibitor) as positive control and incubated without antibacterial agents as negative control (312).

### 3.2.10. Determining cell morphology

#### 3.2.10.1. Gram assay

*E. coli* culture in logarithmic phase of growth was diluted to ~0.04 OD<sub>600</sub> and incubated for 4 h with sarconesin II at 37°C. Control PBS and peptide-treated cells were Gram-stained. Images were acquired using an IX81 microscope (Olympus, Tokyo, Japan), 100 × 1.35NA lens with Cell R software (167).

#### 3.2.10.2. Scanning electron microscopy (31)

Mid-log phase *E. coli* cells ( $1 \times 10^8$  CFU/mL) were incubated with MIC sarconesin II for 12 h at 37°C. The bacterial cells were then spun and washed three times with 0.1 M PBS (pH 7.2) and fixed overnight at 4°C with 2.5% glutaraldehyde. After washing twice with PBS, the cells were post-fixed on cover glasses with 1% osmium tetroxide (OsO<sub>4</sub>) in 0.2 M sodium cacodylate buffer for 1 h, dehydrated in a graded ethanol series (30%, 50%, 70%, 95% and 100%) for 15 min each time, and dried by the critical

point method drying from liquid CO<sub>2</sub>. Gold-palladium was sputtered on samples and observed by QUANTA 250 SEM (FEI, Hillsboro, OR, USA) at 12.5 kV (313).

### 3.2.11. Statistical analysis

GraphPad Prism software (version 7.00, La Jolla California USA) was used for all statistical analysis. One-way ANOVA was used for statistical comparison of combination treatment regarding toxicity assays, using  $\alpha = 0.05$  with Dunnett's multiple comparisons test. Data is presented as mean  $\pm$  standard deviation (SD).

## 3.3. Results

### 3.3.1. Purifying *S. magellanica* ES sarconesin

Larval ES crude extract RP-HPLC fractions were lyophilized, suspended in Milli-Q water and tested against *M. luteus*. The sarconesin II fraction having antibacterial activity was eluted at 43.7 min; this peak was collected and chromatographed in the same solvent system on an analytical C18 column (Figure 30).

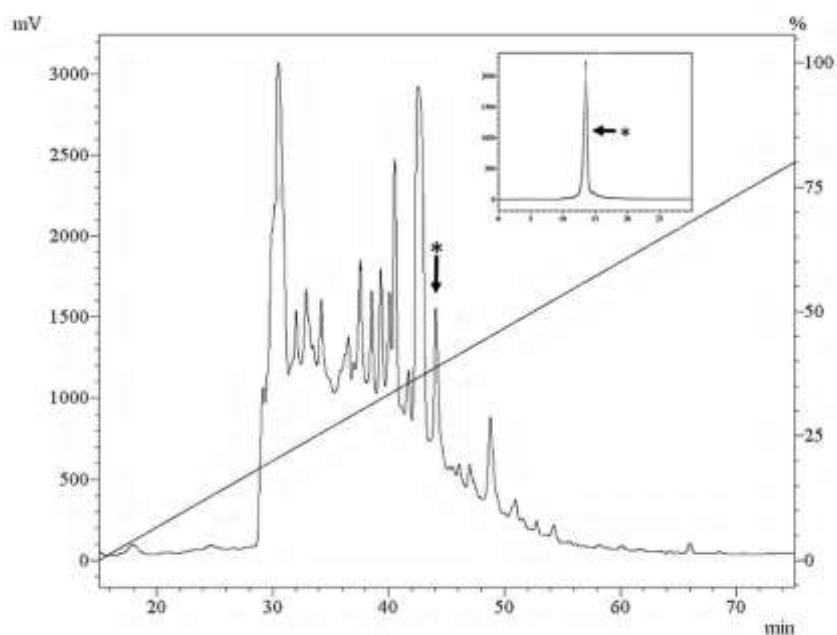


Figure 30. RP-HPLC profile of lyophilized larval ES crude extract at 225 nm eluted on a Jupiter C18 Column (10 mm  $\times$  250 mm, 10  $\mu$ m; 300  $\text{\AA}$ ), using a 0–80% B linear gradient for 80 min with solvent A (0.05% TFA/can) and solvent B (0.05% TFA/H<sub>2</sub>O) at 1.5 mL/min flowrate. Inset: sarconesin II fraction labelled with an asterisk was chromatographed in the same solvent system on a Jupiter C18 column (4.6 mm  $\times$  250 mm, 10  $\mu$ m; 300  $\text{\AA}$ ) using a 30%–45% B linear gradient for 60 min.

The sarconesin II fraction's antibacterial activity against Gram-positive and Gram-negative bacterial strains was evaluated once it had been purified. Sarconesin II MICs were 15.6  $\mu\text{M}$  for *P. aeruginosa* PA14, 7.8  $\mu\text{M}$  for *E. coli* MG1655 and *P. aeruginosa* ATCC 27853, 3.9  $\mu\text{M}$  for *E. coli* DH5 $\alpha$  and *S. aureus* ATCC 29213 and 1.9  $\mu\text{M}$  against *M. luteus* A270 (Table 6).

Table 7. Sarconesin II's antibacterial activity spectrum.

Microorganism	MIC ( $\mu\text{M}$ ) <sup>1</sup>
Gram-negative bacteria	
<i>Escherichia coli</i> K12 MG1655	7.8
<i>Escherichia coli</i> DH5 $\alpha$	3.9
<i>Pseudomonas aeruginosa</i> PA14	15.6
<i>Pseudomonas aeruginosa</i> ATCC 27853	7.8
Gram-positive bacteria	
<i>Staphylococcus aureus</i> ATCC 29213	3.9
<i>Micrococcus luteus</i> A270	1.9

<sup>1</sup> MIC, refers to the minimal peptide concentration without visible bacterial growth in a liquid medium.

### 3.3.2. Bacterial growth curve and toxicity

Exponentially grown  $10^7$  bacteria/mL were treated with sarconesin II for 7 h, sampling aliquots at different times, and plated on agar. Cell viability was determined by measuring colony forming units (CFU/mL). Sarconesin II MIC proved to be bactericidal against the *E. coli* reference strain after 4 h peptide exposure (Figure 31a).

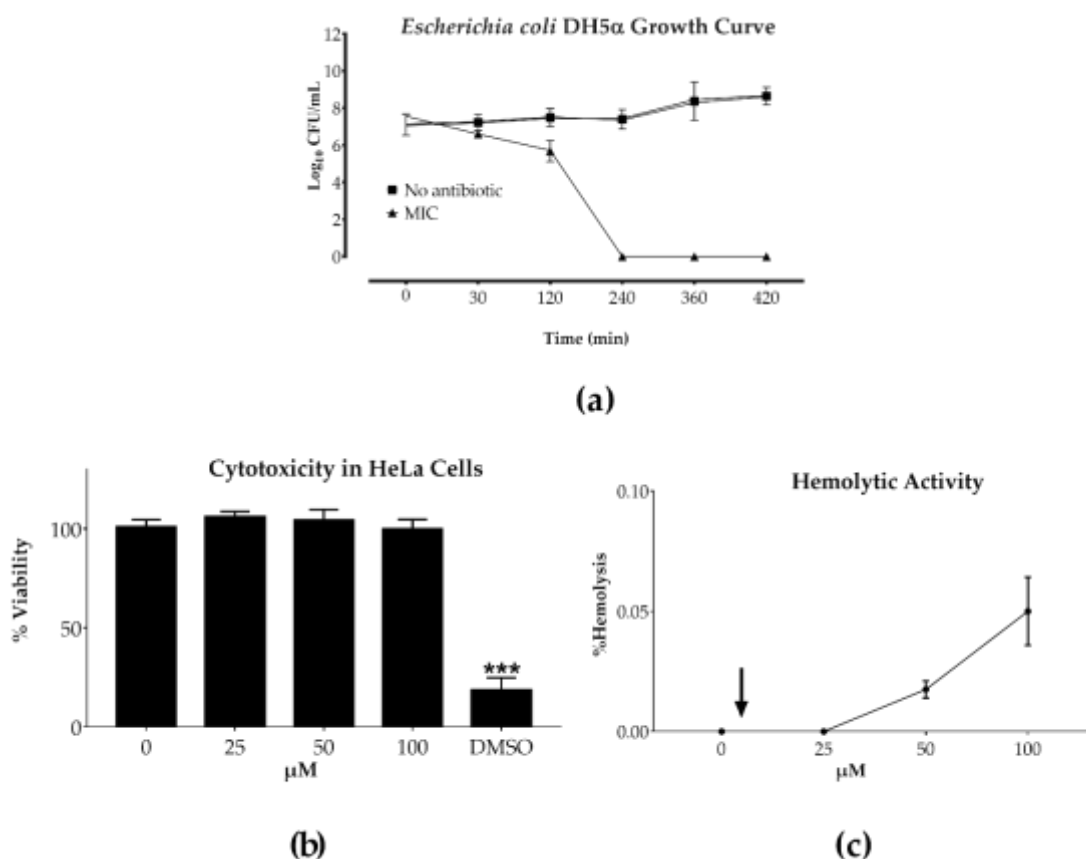


Figure 31. Sarconesin II's effect in toxicity assays. (a) Growth curve for *E. coli* DH5α incubated with sarconesin II MIC. Bacterial growth was inhibited at 240 min. (b) HeLa cell CC measured by MTT tetrazolium assay. Cells were incubated with sarconesin II at 25, 50 and 100 μM for 24 h. Untreated HeLa cells were used as negative control and HeLa cells treated with 30% DMSO were used as positive control. (c) Hemolytic activity against hRBC. Sarconesin II was tested at 25, 50 and 100 μM concentrations. PBS was added without peptide for determining 0% hemolysis. The arrow indicates the concentration at which the fraction had antimicrobial activity. The average of each experiment done in triplicate is presented in individual columns as mean ± SD. One-way ANOVA followed by post hoc Dunnett's multiple comparison test was used. \*\*\* $p < 0.001$ .

Toxicity assays were conducted with 25, 50 and 100 μM sarconesin II concentrations. An MTT proliferation assay was used to determine peptide CC, using the HeLa cell line. The compound had more than 95% cell viability at all concentrations (Figure 31b); the amount of formazan produced by living cells did not vary considerably, having no cytotoxic activity, even at the highest concentration tested here. Hemolytic activity was evaluated by determining the amount of human hemoglobin released after incubation with sarconesin II. None of the tested concentrations caused hemolysis (Figure 31c), indicating that sarconesin II had no toxicity.

### 3.3.3. Mass spectrometry and sarconesin II characterization

Sarconesin II's primary structure was obtained by MS/MS; PEAKS software was used to analyze the spectrum and revealed a 13 aa-long molecule, having a 1,439.67 Da mass, with VALTGLTVAEYFR aa sequence (Figure 32). The collision-induced dissociation (CID) spectrum from the mass/charge ( $m/z$ ) of its double-charged ion gave  $[M + 2H]^{2+}$ ,  $m/z$  720.3984.

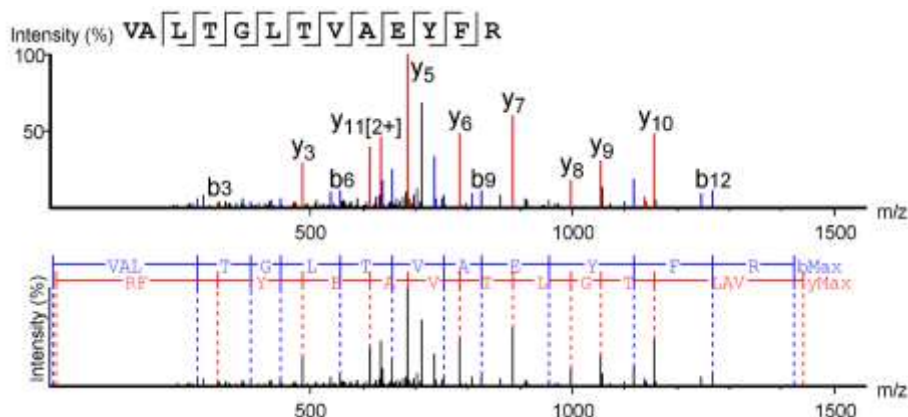


Figure 32. MS/MS fragmentation was used to obtain the complete sarconesin II aa sequence. The CID spectrum from mass/charge ( $m/z$ ) of its double-charged ion gave  $[M + 2H]^{2+}$ ,  $m/z$  720.3984. The ions from y (red) and b (blue) series (marked at the top of the spectrum) represent the primary structure: VALTGLTVAEYFR.

The ExPASy tool (SIB Bioinformatics Resource Portal) was used to obtain sarconesin II's physicochemical properties as the peptide sequence was known: i.e. theoretical isoelectric point (pI), molar extinction coefficient ( $\epsilon$ ) and grand average of hydropathicity (GRAVY) (Table 7). The sarconesin II instability index was calculated as 2.70, suggesting a stable peptide. The peptide was predicted to have a neutral charge because of having one basic positively-charged Arg (R) residue and one acid negatively-charged Glu (E) aa residue. The considered sequence's N-terminal was Val (V). The peptide was predicted to have seven out of 13 non-polar hydrophobic aa residues: two Ala (A), Leu (L), Val (V) and one Phe (F).

Table 8. Sarconesin II's theoretical physicochemical properties.

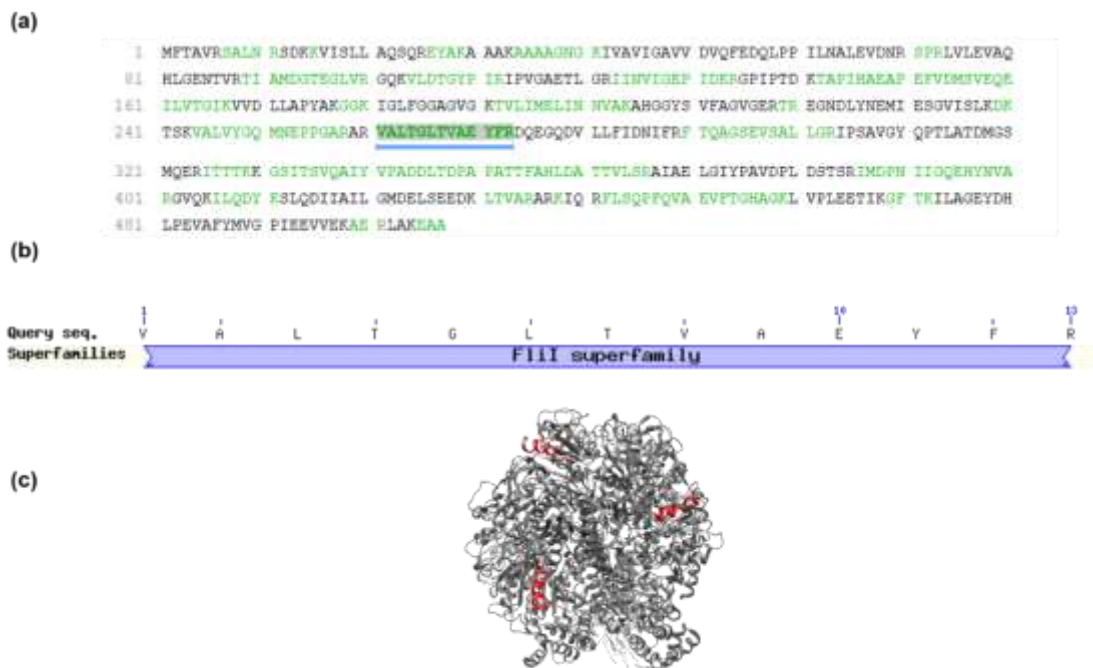
Peptide properties	
Sequence	VALTGLTVAEYFR
Length	13
Molecular weight	1439.67
Formula	$C_{67}H_{106}N_{16}O_{19}$
Theoretical isoelectric point (pI)	5.97
Net charge	0
Molar extinction coefficient ( $\epsilon$ )	1490 M <sup>-1</sup> cm <sup>-1</sup>
Instability index	2.70
Aliphatic index	120.00
Grand average of hydropathicity (GRAVY)	0.869

ExPASy's ProtParam tool was used for obtaining physicochemical parameters (306).

Sarconesin II's other four residues were polar uncharged aa: two Thr (T), one Gly (G) and Tyr (Y). Owing to a V aa residue at the N-terminal, estimated half-life *in vitro* suggested that the peptide would remain intact for up to 100 h in mammalian reticulocytes, >20 h in yeast (in vivo) and >10 h in *E. coli* (in vivo) (306).

A PEAKS DB database search revealed that the *S. magellanica* ES native peptide fraction might have been derived from the ATP synthase subunit beta, mitochondrial protein previously reported in *Lucilia cuprina*, another *Calliphoridae* blowfly (314): sequence ID: gi|1321322512, NCBI reference Sequence: XP\_023303742.1 and 507 aa total length. Sarconesin II was found to be between residues 260 and 274 long, covering 3% of the whole protein sequence (Figure 33a). Although the peptide was not submitted to trypsin digestion, the PEAKS software showed (in green) the probable cuts if such enzyme were used. The Arg preceding sarconesin II's N-terminal Val aa residue and the C-terminal Arg suggested trypsin cuts.

A BLAST search for *Calliphoridae* multiple sequence alignment (303) revealed sarconesin II's 100% matching identity with the mitochondrial ATP synthase subunit beta (Figure 33b), appearing as a putative conserved domain of the Fli-1 superfamily: flagellar biosynthesis/type III secretory pathway ATPase (Accession: c125576). Sarconesin II and the conserved domain also appeared in other organisms, such as *Homo sapiens* (Sequence ID: gi|179279|AAA51808.1), *Drosophila melanogaster* (gi|442614522|NP\_001259081.1) and *Mus musculus* (gi|31980648|NP\_058054.2). A representative model of the mitochondrial ATP synthase subunit beta (PDB ID: 2w6j) (Figure 33c) was built using Chimera to reveal sarconesin II localization, showing that it is exposed on ATPase surface (234).



---

Figure 33. Sarconesin II sequence and conserved domains. **(a)** Sarconesin II spectrum match indicated by a blue line below the mitochondrial KNC23160.1 ATP synthase subunit beta sequence [*Lucilia cuprina*]. Sarconesin II was found between residues 260 and 274, covering 3% of the whole protein sequence. Sequences in green represent tryptic peptides. **(b)** Sarconesin II sequence embedded in *Calliphoridae* multiple sequence alignment search (303) shows the putative conserved domain. Sarconesin II appears as an ATP synthase beta subunit protein conserved residue belonging to the Fli-1 superfamily. **(c)** Representative model of the mitochondrial ATP synthase subunit beta (PDB ID: 2w6j) built with Chimera (234). Sarconesin II is exposed on the surface (red).

Sarconesin II was also very similar in length to the ~13–20 aa of other higher vertebrates, such as frogs and rats, and also other arthropod AMPs (Table 8). The peptide had similar hydrophobicity ~40–69%, having a ~0–3 diverse net charge, like plantaricin having a neutral charge (305).

Table 9. Known antimicrobial peptides having similarity with sarconesin II, as identified in the Antimicrobial Peptide Database (APD2) (Wang *et al.*, 2009).

Peptide name	Sequence alignment	Source organism	APD identifier	Percentage similarity
Temporin-HN1 (14 aa)	+ A I L T T L A N W A R K F L V A + L T G L + T V A E Y F R	Frog <i>Odorrana hainanensis</i> (315)	AP01959	40%
H4-(86-100) (15 aa)	V V Y A L K R N G R T + + L Y G F + + V + A L + + T G L T V A E Y + F R	Rat (316)	AP02806	38.8%
CcAMP1 (17 aa)	M W I T N G + G V A N W Y F V L A R V A L T + G L T V A + E Y F + + + R	Stink bug <i>Coridius chinensis</i> (317)	AP02595	38.88%
Plantaricin DL3 (20 aa)	V G P G A I N A G + T Y L V S R E L F E R V + + + A + L T G L T + + V + A E Y F + R	Probiotic <i>Lactobacillus plantarum</i> DL3 (318)	AP02979	38.09%
VmCT1 (13 aa)	+ F L + G A L W N V A K S V F + V A L T G + L + T V A + E Y F R	Scorpion <i>Vaejovis mexicanus smithi</i> (319)	AP02216	37.5%

The Antimicrobial Peptide Database (APD) prediction tool was used to align sarconesin II (305).

### 3.3.4. Sarconesin II's secondary structure

Iterative Threading ASSEmblY Refinement (307) (307) and CD were used to predict and study sarconesin II structure. Figure 34a gives the CD spectra, giving a characteristic helix-coil transition spectrum where the peptide had random formation in water, characterized by a strong negative band at 200 nm, and becoming more structured as TFE concentration increased. The peptide had a characteristic alpha-helix spectrum in 100% TFE concentration, with some distortions which could might have been attributed to Tyr<sup>11</sup> aromatic contribution to the spectrum. Aromatic aa provided a positive contribution in 208 and 222 nm bands and a negative contribution in the 195 nm band (320).

Sarconesin II aa sequence was entered into I-TASSER, providing images of possible structures to further predict sarconesin II's secondary structure (308), giving a typical alpha-helix structure (Figure 34b). The 13 aa were strongly helical. Furthermore, when bioinformatics analysis was used to arrange the sequence in  $\alpha$ -helical wheels it had no hydrophobic face, as reported by the HeliQuest tool; it had a slightly opposite arrangement of hydrophilic and hydrophobic aa, characteristic of an amphipathic  $\alpha$ -helical peptide (Figure 34c).

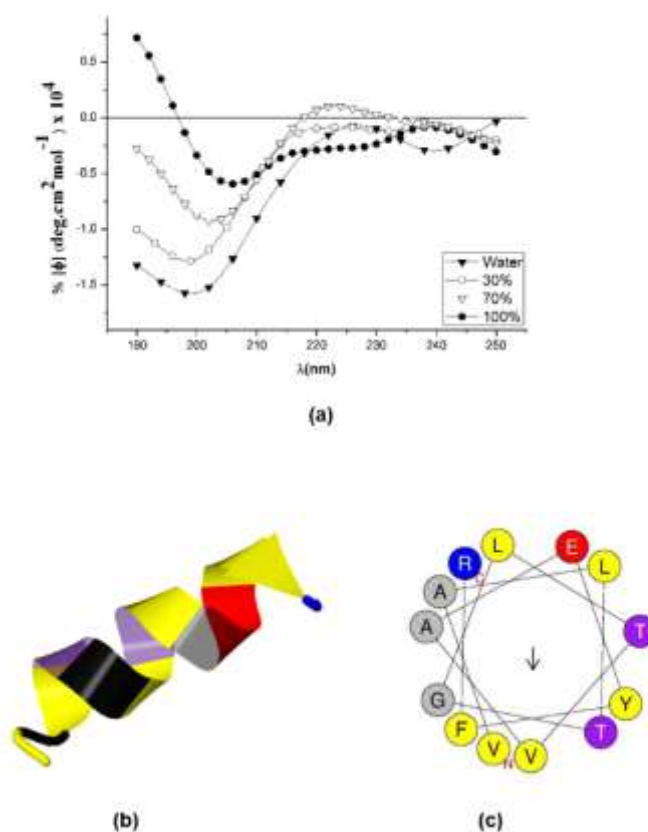


Figure 34. Sarconesin II secondary structure. (a) A Jasco-1500 CD spectrophotometer was used for measuring sarconesin II's CD spectrum. Sarconesin II CD spectra variation at 0%, 30%, 70% and 100% trifluoroethanol (TFE) concentrations (b). I-TASSER sarconesin II secondary structure gave an  $\alpha$ -helix, depicted in spiral ribbon format, using ordinary colors. (c) Computation of sarconesin II  $\alpha$ -helical wheel (321). No hydrophobic face reported. Note slightly opposite arrangement of hydrophobic (yellow) versus charged (red, blue) aa.

### 3.3.5. Mechanism of action (MoA)

#### 3.3.5.1. Membrane integrity

Red fluorescent dye propidium iodide (PI) and carboxyfluorescein diacetate (CFDA) assays were used to study disruption of the bacterial membrane by sarconesin II. PI penetrates damaged cell membranes and intercalates nucleic acids (226). PI fluorescent intensity indicated the level of cell membrane integrity as observed in cells without any treatment (PBS) where bacteria did not incorporate PI; treated cells had increased fluorescence when incubated with sarconesin II (Figure 35), suggesting disruption of the cells' inner membrane.

An alteration in sarconesin II esterase activity was observed when compared to bacterial control, since CFDA is cell permeant and fluorescent only after exposure to intracellular esterases, thereby confirming membrane alterations.

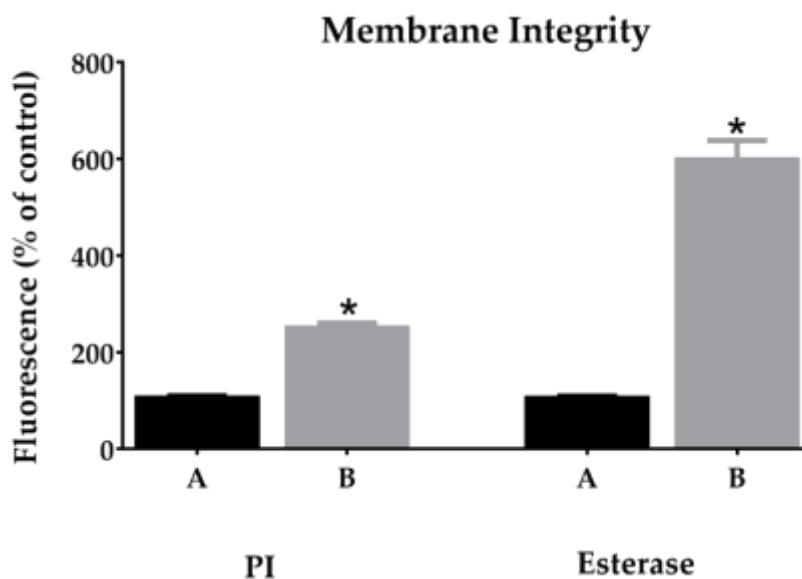


Figure 35. PI and esterase change mean fluorescence of bacteria treated with sarconesin II MIC concentration (B). PI incorporation showing membrane-damaged bacteria. Treated cells (B) showing increased PI and CFDA fluorescence when incubated with sarconesin II. Esterase activity determined by 5,6-carboxyfluorescein diacetate cleavage, expressed as a percentage of control PBS (A) activity. Data is expressed as mean  $\pm$  SD ( $n = 3$ ). \* $p < 0.001$ : significantly different from the control.

### 3.3.5.2. Sarconesin II effects on *E. coli* DNA and protein profile

Three sarconesin II concentrations were tested to evaluate whether sarconesin II interacted with bacterial DNA (bDNA) by analyzing the electrophoretic mobility of DNA bands with peptide on an agarose gel (Figure 36a). The bDNA in the gel retardation assay showed that sarconesin II became strongly bound to DNA *in vitro* because gDNA migration from *E. coli* became suppressed. Figure 36 shows that the peptide bound to the DNA and subtracted charges because it did not migrate, thereby suggesting inhibiting intracellular functions via interference with DNA.

Cells treated with or without sarconesin II were analyzed in 12% SDS-PAGE to further assess whether sarconesin II affected *E. coli* protein profile. The streptomycin control inhibiting protein synthesis gave no protein profile. Sarconesin II-treated bacteria had the same profile as that for bacteria with just PBS treatment, suggesting no peptide action on proteins (Figure 36b).

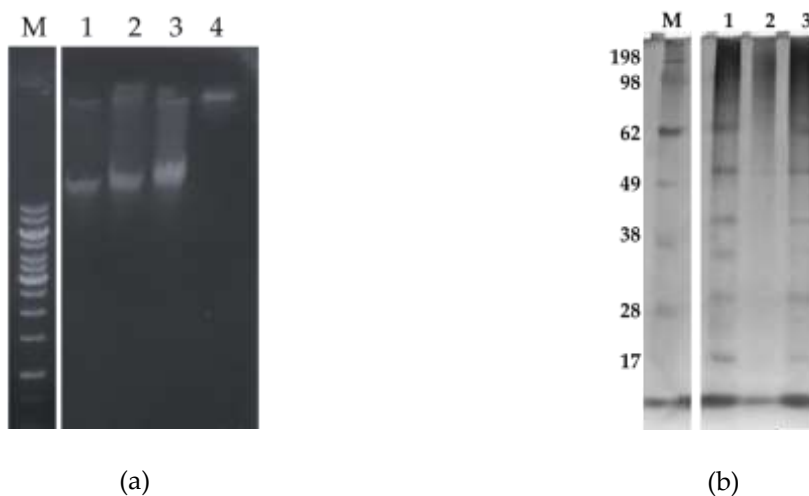


Figure 36. Assays for evaluating sarconesin II effects on *E. coli* DNA and proteins. **(a)** Gel retardation assay for evaluating sarconesin II effect on DNA. M, GeneRuler 1kb DNA ladder; 1–3. Sarconesin II concentrations were 0, 25, 50  $\mu\text{M}$ , showing proportionally suppressed migration regarding the increased amount of peptide compared to bDNA. The fourth concentration at 100  $\mu\text{M}$  showed that migration was suppressed, suggesting sarconesin II interaction with DNA. **(b)** Changes in protein profile for *E. coli* treated with sarconesin II. Cells treated with or without sarconesin II were washed and sonicated in lysis buffer and the protein profile was analyzed in 12% SDS-PAGE; proteins were visualized by silver nitrate staining. M, molecular weight marker (kDa) (SeeBlue Invitrogen). The streptomycin control (2) revealed no protein profile. There was no difference regarding sarconesin II (3)-treated bacteria compared to the PBS control (1) protein profile, suggesting no peptide action on proteins.

### 3.3.5.3. Fluorescence microscopy assays

Bacterial cytoplasmic membrane integrity was assessed with propidium iodide (PI) staining to investigate whether sarconesin II affected bacterial membrane. The cells had no PI staining in the absence of peptide, indicating that the membranes remained intact. By contrast, peptide-treated cells had intense red fluorescence, showing that sarconesin II could disrupt *E. coli* cell membrane, thereby confirming damaged bacterial membrane permeability (Figure 37).

4',6-diamidino-2 phenylindole (DAPI) fluorescent staining was used to evaluate the effect of sarconesin II by confocal microscopy. DAPI intercalates nucleic acids and yields blue fluorescence when observed in the whole image field. Figure 37 shows that cells treated with ciprofloxacin had less blue fluorescence (as the antibiotic promotes double-stranded DNA breakage). Sarconesin II-treated cells also had partial blue fluorescence, thus suggesting *E. coli* DNA fragmentation.

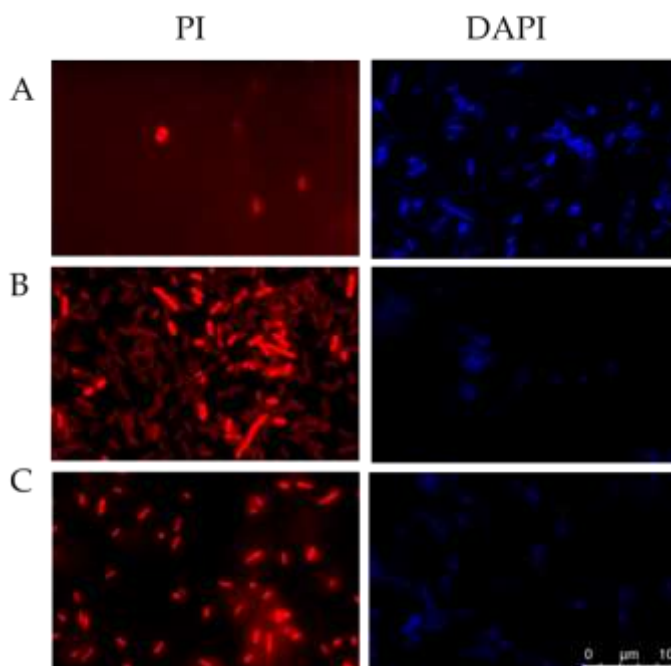
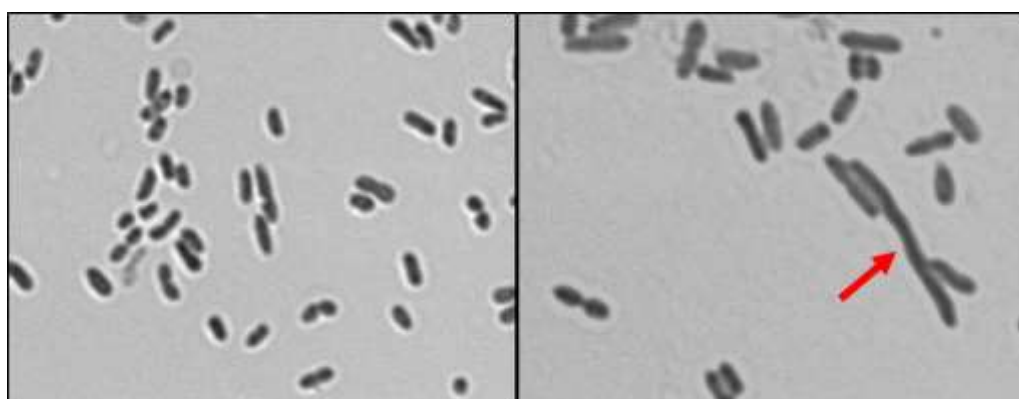


Figure 37. Fluorescence microscopy of *E. coli* cells incubated for 4 h at 37°C and stained with PI (322) or DAPI (blue). Untreated control cells, PBS (A), cells treated with sarconesin II (B), cells treated with ampicillin for PI or ciprofloxacin for DAPI (C). PI assay revealed bacterial membrane alteration when treated with sarconesin II and DAPI-stained cells had partial fluorescence, showing DNA fragmentation by sarconesin II.

### 3.3.6. Determining Cell Morphology

#### 3.3.6.1. Gram-stained *E. coli* cells

*E. coli* culture in logarithmic phase was incubated with or without peptide at 37°C to observe whether there were any morphological changes. Control PBS and peptide-treated cells were Gram-stained. Microscopic comparison of *E. coli* cell bacterial culture with sarconesin II revealed different morphologies. Figure 38 shows that cells were elongated due to a phenomenon commonly known as filamentation.



(a) (b)

Figure 38. Confocal microscopy image obtained from *E. coli* bacterial cultures incubated for 4 h with PBS (a) or sarconesin II (b). Cultures were obtained after 4 h incubation at 37°C. The arrow indicates filamentous cell morphology.

### 3.3.6.2. Examining bacterial membrane change by SEM

SEM (31) observations were made to further evaluate and confirm morphological changes detected after treatment with sarconesin II. *E. coli* cells were treated for 12 h with or without sarconesin II MIC. SEM preparations were fixed, dehydrated, coated with gold and examined by microscope. Figure 39A shows that non-treated *E. coli* cells had intact smooth surfaces, having typical morphological characteristics, remaining cylindrically shaped, turgid and smooth, while sarconesin II-treated cells underwent considerable structural changes. After treatment with the peptide, *E. coli* cells appeared as highly elongated, filamentous cells having several holes on their outer membrane (Figure 39B). The surface seemed to have been disrupted; other changes appeared to involve the formation of blebs on cell surface. This indicated that sarconesin II induced alterations in *E. coli* cell morphology.

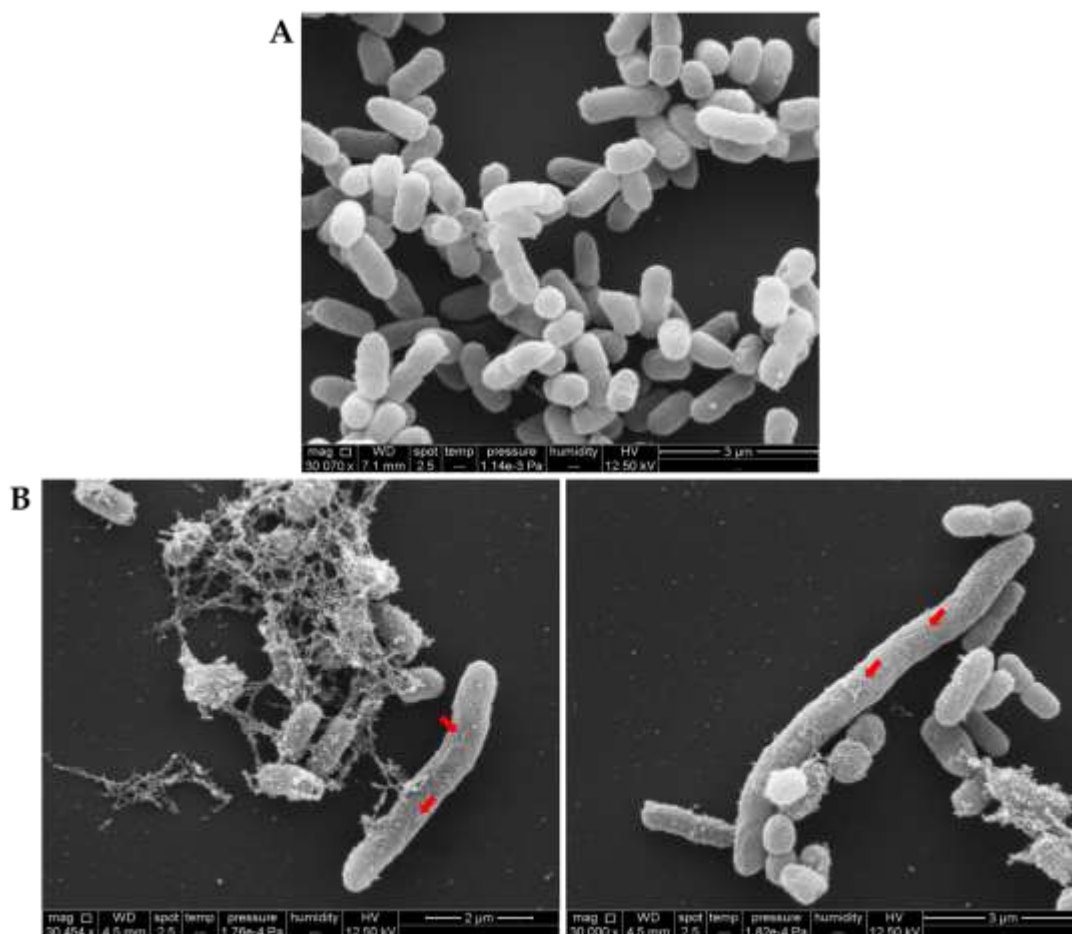


Figure 39. Sarconesin II MIC effect on *E. coli* bacterial membrane by SEM (31). Untreated *E. coli* (A) had a normal smooth surface, while treatment with sarconesin II (B) gave an elongated pattern, membrane

disruption and blebbing on the outer face (arrows). Some bacteria had variable length, rough cell surfaces or globular protrusions on their surfaces. These images revealed that sarconesin II could induce alterations in cell morphology.

### 3.4. Discussion

Antibiotic resistance constitutes one of the most pressing public health concerns worldwide; multicellular organism AMPs are considered part of a solution to this problem (323). This chapter has reported the isolation, characterization and MoA of an efficient AMP purified from *S. magellanica* third-instar larval ES (i.e. sarconesin II).

RP-HPLC results showed that *S. magellanica* ES could be separated into several fractions. The fraction having 43.7 min RT had antibacterial activity and was named sarconesin II. The *S. magellanica* ES profile looked similar to that previously reported for the same material, having a high peak, followed by sarconesin II sharing the same RT (295). Sarconesin II was further purified to confirm homogeneity, using the same chromatographic system (Figure 30).

Sarconesin II had good activity against Gram-negative and Gram-positive bacteria, including *E. coli* K12 MG1655 (Table 6) (324). *E. coli* is a Gram-negative bacteria which can use gene mutations and multidrug efflux pumps, resulting in multidrug resistance (325). Other promising native peptides, such as cecropin A, tenecin 1 and melittin from insects, and magainin II, pexiganan and LL-37 from vertebrates, have also been reported as being able to kill this strain (326). Other authors have reported AMP activity, having a MIC ranging from 40 to 150  $\mu\text{M}$ , regarding maize, lycotoxin I, lycotoxin II and magainin B against *E. coli* DH5 $\alpha$ . A 3.9  $\mu\text{M}$  MIC was obtained in the study described in this chapter using sarconesin II; a lower concentration was required for killing the bacteria compared to the range of previously reported AMPs (327-329).

Regarding sarconesin II activity against *P. aeruginosa*, this bacteria has previously been reported as being a microorganism developing high resistance to a variety of antibiotics, including aminoglycosides, quinolones and  $\beta$ -lactams (330). Many AMPs, including GL13K, LL-37, T9W, NLF20, cecropin P1, indolicidin, magainin II, nisin, ranalexin, melittin and defensin, have also had similarly potent antimicrobial effects against *P. aeruginosa* (322, 331-335). The  $\beta$ -defensin 3 AMP has been shown to have action against the multi-drug-resistant *P. aeruginosa* PA14, having a 32  $\mu\text{M}$  MIC, very close to the MIC found in our study (336).

Sarconesin II has been shown to have antimicrobial activity against Gram-positive bacteria, such as *S. aureus* and *M. luteus*. Previous studies have shown that AMPs have a broad range of antimicrobial activity against bacteria, parasites, fungi and viruses (337, 338). Two alloferons from the blowfly *Calliphora vicina* (the same *Calliphoridae* family as *S. magellanica*) are active against human influenza viruses A and B (339). The study reported here did not involve evaluating activity against other

microorganisms, but a high probability (0.96) of antiviral activity was found using *in silico* analysis (1); this could be interesting for future research, remembering that bactericidal antimicrobial agents are required to treat immunocompromised patients' infections and other diseases (340).

It is known that Gram-negative bacteria are more resistant to antimicrobial agents than Gram-positive bacteria due to their differing cell membranes (341). The sarconesin II requirement for killing Gram-negative bacteria thus had greater MICs than those obtained for Gram-positive bacteria, also demonstrating broad peptide activity killing both. Broad-spectrum AMPs have thus been suggested as an alternative to conventional antibiotics for combatting bacterial infections, as AMPs have rapid killing kinetics, low levels of induced resistance and low host toxicity (342-346). Time-kill studies (347) for evaluating sarconesin II antimicrobial activity against *E. coli* (Figure 31a) demonstrated that the peptide totally killed the bacterium after 240 min.

*E. coli* MIC, or the lowest concentration inhibiting visible bacterial growth, was found to be 3.9  $\mu\text{M}$ . MBC was not evaluated, but a higher drug concentration is probably required to kill bacteria completely (348). The MIC for the growth killing assay when plating the bacteria onto agar completely killed the bacteria after 4 h, suggesting that the MIC and the MBC could probably have been the same because sarconesin II caused death during the time evaluated, also suggesting a bactericidal MoA.

Faster action has been reported for other *Calliphoridae* family peptides (i.e. *L. sericata* lucifensin) than for sarconesin II. No bacteria-killing assay has been reported for lucifensin, but SEM images after a 60 min treatment showed the effects on bacterial membrane (45). Just one work was found reporting time-kill curves for *C. vicina* and *L. sericata* total ES against *E. coli*; both *Calliphoridae* had good bactericidal activity against *E. coli*, inhibiting growth over the first four hours (349).

Time-kill curves against MRSA ATCC 43300 have been reported regarding an insect defensin-like peptide DLP4 isolated from the black soldier fly *Hermetia illucens*, giving DLP2 1  $\times$  MIC killing effect in 8 h and 4  $\times$  MIC in 6 h (350). This suggested a faster effect for sarconesin II if increased MIC against bacteria were to be tested. As predicted *in silico*, the time that sarconesin II could remain stable without degradation in *E. coli* was 10 h (306); this could be enough time for complete sarconesin II action. It has been reported that some native drugs could gradually lose their effect after 24 h, and bacteria escaping drug action can multiply at a faster rate in suitable conditions (348). Sarconesin II action was seen to be faster than its degradation rate. It is known that AMPs' biological ability in serum may become largely reduced, thereby highlighting the importance of their transport and storage (351). Sarconesin II's instability index (123) suggested a stable peptide, an important role regarding any biological drug's application.

Encouragingly, concentrations where sarconesin II was active did not have any toxicity or hemolytic activity regarding either HeLa or erythrocyte cells, even when tested at concentrations 100 times higher than bacterial MIC (Figure 31), suggesting the compound's high selectivity. Nagarajan obtained similar results when testing the NN2\_0018 peptide which also has antibacterial activity against resistant bacteria (324). The recently discovered peptide LGH2 had low toxicity when evaluated against sheep RBC at 4  $\mu$ M (352). When evaluated at a concentration similar to that for sarconesin II (100  $\mu$ M) it had 100% hemolysis, while that for sarconesin II continued without having toxicity. Accordingly, sarconesin II lacked toxicity but did have potent antibacterial activity, making it a promising candidate for use in therapeutics.

The sarconesin II primary sequence obtained by HPLC-ESI-Orbitrap-MS had the same identity as that for the ATP synthase beta subunit protein conserved domain. Sarconesin II was also detected in the organisms of other larval extracts, as the BLAST search showed, and has been previously identified in research into human breast cancer MCF-7 and MDA-MB-231 cell lines, and as proteases in basidiomycete *Amanita virgineoides* (353, 354). Sarconesin II is a derivative of the subunit beta ATP synthase reported in a broad range of organisms. It is 13 aa long, making it a short sequence having ideal features for clinical use (329). Sarconesin II probably did not have any toxicity because it is part of an ATP protein's conserved domain which is found naturally in human cells and in all eukaryotic cells (353).

Sarconesin II was not subjected to tryptic cleavage but had particular trypsin cuts which may have involved proteolysis of the ATP synthase beta subunit protein having a 54.6 kDa molecular weight (<https://www.bioinformatics.org/sms/index.html>); the presence of a protein having this molecular weight was confirmed using the *S. magellanica* ES protein profile (185). This suggested that the protein could have been in previous contact with the enzyme, making sarconesin II a sub product of the protein. The 3D representative model also highlighted sarconesin II as being exposed on ATPase surface, facilitating the cutting. This has also been reported for sarconesin, knowing that the ES contain chymotrypsin and other enzymes (295). This suggests that proteins may play a role in blowflies' innate immunity during extracellular digestion, helping as a substrate for creating AMPs, probably because insect AMPs are secreted by fat body cells into the hemolymph (its action as humoral immunity factors has already been described) (355).

APD analysis revealed sarconesin II-similar AMPs and showed that all of them had antimicrobial activity against both Gram-negative and Gram-positive bacteria, having similar or higher MICs than sarconesin II. Moreover, VmCT1 (an  $\alpha$ -helical AMP from scorpions) has been reported as having activity against cancer cells (356, 357) and temporin-HN1 has been reported as having antifungal activity (315).

The study reported here found no sarconesin II toxicity against a breast cancer cell line; however, it could be interesting to test it against other cell lines and evaluate its antifungal activity.

APD gave sarconesin II 38.8% similarity with the H4-(86–100) peptide. This can be considered a good similarity percentage as the APD database contains 3,055 peptides. Similar percentages regarding other AMPs were found in the APD2 database, i.e. H4-(86–100) was reported as having 35.3% similarity with temporin-LTb (305). It should be stressed that sarconesin II had action on DNA, like the H4-(86–100) peptide which has been reported to cause an inhibitory effect on DNA gyrase (316).

The CD spectra indicated that sarconesin II had a random coil in water and adopted an  $\alpha$ -helical structure in 70% TFE (Figure 34a). This pattern indicated that sarconesin II was prone to assuming a specific conformation when interacting with membrane-mimicking agents like TFE or SDS. Alpha-helical characteristics are stronger in TFE. This agreed with TFE's known properties for promoting helical structures in peptides (358, 359). Peptide secondary structure was observed by I-TASSER and it has been reported that increased helix propensity also increases antimicrobial potency (285). AMPs having  $\alpha$ -helices are magainin, cecropin and cathelicidin; however, they can perform their functions through interactions with intracellular targets or by disturbing cell processes, as well as inhibiting cell wall, nucleic acid or protein synthesis (162).

An  $\alpha$ -helical structure has been found for other members of the Fli family (123). The sarconesin II sequence was arranged in  $\alpha$ -helical wheels by bioinformatics analysis to further characterize its structural properties, revealing a slightly opposite arrangement of hydrophobic aa (360); this is characteristic of amphipathic  $\alpha$ -helical peptides and is also known to be important in amphipathic arrangement (361). The ability to structure an  $\alpha$ -helix, without this arrangement is not sufficient to provide potent, broad-ranging, antimicrobial activity, as demonstrated by scrambled peptide P19(6|s) (362, 363). The importance of amphiphilic helices has been discussed regarding several AMPs, and it has previously been shown for another *Calliphoridae*, *Sarcophaga peregrina* (flesh fly), whose sarcotoxin IA and Pd peptides consist of two amphiphilic helices, having hydrophilic and hydrophobic faces (364–366).

Moreover, such hydrophobic arrangement can facilitate recognition of hydrophobic lipids on bacterial membranes. Sarconesin II has a C-terminal positively-charged Arg, frequently occurring in protein active or binding sites, giving a higher probability of interaction with negatively-charged non-protein atoms (367). Interestingly, some peptides have been classified as being glycine-rich; we cannot affirm that sarconesin II is part of this family, considering that it just has 13 aa, where Gly represents 7% of it. Glycine-rich peptides come mostly from insects and are active against Gram-negative bacteria (132, 174).

A mechanism for killing bacteria involving membrane disruption is probably particular for hydrophobic, moderate to strong amphipathic,  $\alpha$ -helical peptides, involving Arg, as found for sarconesin II and reported for AA230 arenicin-3 as an amphipathic molecule rich in Arg and hydrophobic aa (298). These characteristics have also been found for sapecin which has essential residues for membrane channel formation in its sequence, such as Asp and Arg. The opposite is true for plectasin where its sequence does not even have most of the hydrophobic residues at a specific site in the  $\alpha$ -helix chain (368).

Increased sarconesin II in esterase assays indicated bacterial membrane alteration; it has also been reported that esterase activity in *E. coli* therefore seems to function as a stress indicator rather than a viability parameter (225). After PI staining, sarconesin II-treated *E. coli* cells had increased fluorescence (Figures 35 and 37) since PI cannot diffuse into viable cells or dead cells having an intact membrane. PI confirmed sarconesin II entering *E. coli* cells and binding to DNA, thus confirming its action on the membrane. Knowing that PI stains dead cells as a result of porous membrane, other peptides have been reported such as NK-18, thereby showing the alteration of both; the outer and inner membrane were disturbed after treatment (369), as found for sarconesin II. The AMP cecropin has also been reported to induce inner membrane perturbation shown by high PI incorporation (370, 371). Bacteria's killing effect depends on membrane damage and inhibiting the membrane's functional proteins which can be critical for bacteria, even if there is no complete lysis (372).

This could imply that the peptides are not just only associated with the plasma membrane but can also enter cells. This prompted looking for an intracellular-targeting MoA for this peptide (373). Peptides affecting Gram-positive bacteria usually act on the membrane; however, no parameters enable discriminating between peptides acting on Gram-negative or Gram-positive bacteria. Malanovic *et al.*, (374) reported no apparent preference for targeting only Gram-positive or Gram-negative bacteria regarding hydrophobicity and aa residue charge and that AMP secondary structure could be identified when examining the APD (126).

One bactericidal drug mechanism concerns inducing DNA and protein damage (375). No action has been observed in proteins; sarconesin II DNA damage was perhaps caused by fragmentation, as shown by DAPI assay fluorescence (376, 377) or by sarconesin II interaction with and binding to bDNA during gel retardation assay. One of the better-studied peptides interacting with DNA is buforin II (378). Rondonin is another neutral peptide having a similar MoA regarding DNA as that for sarconesin II (193). Other authors have reported that AMPs such as insect defensins DPL2 and DLP4 have differential ability against differing species (as evidenced on agarose gel) regarding their binding to DNA, having variable binding for *E. coli* CVCC1515 or *S. typhimurium* ATCC 14028 (350). Tryptophan in the

sarconesin II sequence could also explain the double MoA on membrane and DNA, as this aa was shown to be involved in hydrophobic interactions with bacterial membranes and DNA (328).

Both MoA discovered for sarconesin II are probably important for increasing its antibacterial activity against Gram-negative and Gram-positive bacteria; this was also observed for NK-18 (329). Another example of double action is indolicidin which can kill bacteria, fungi and HIV. It has antifungal activity by causing cell membrane damage and also kills *E. coli* by penetrating cells and inhibiting DNA synthesis (372).

Morphological changes to the bacteria detected by SEM provided evidence that sarconesin II had an effect on *E. coli* cell membrane; a similar effect has been obtained for NK-18 (329). Its MoA has been related to cell membrane permeabilization. The Gram and SEM images revealed bacterial elongation; this morphology has also been found for indolicidin which inhibits DNA synthesis, leading to *E. coli* filamentation (379). This was indicative of cell division inhibition which, correlated with a lack of thymidine incorporation into cells, suggested that it was interacting with DNA (380). Once the peptide was internalized, it led to the formation of membrane vesicles (372). It is worth noting that the SEM images did not show complete membrane rupture and, as sarconesin II is an  $\alpha$ -helical peptide, it may have created pores on the membrane (372, 381).

Impaired bacterial cell division also depended on intracellular elastase-like serine protease activity which can proteolytically activate cathelicidins. Sarconesin II induced filamentation, resulting in the formation of filamentous bacteria having arrested septation (382). Such morphology indicated a bacterial stress response and has been observed in bacteria responding to damage from low doses of antibiotics, starvation and ROS and nitrogen species (383, 384). Furthermore, the appearance of filamentous cells first suggested an induced SOS repair system response via DNA damage, also called Sula-dependent filamentation (385, 386).

A second veto pathway responsive to DNA damage has also been identified in *E. coli*, known as the *sfi*-independent pathway causing filamentation in *sfi* cells via induction of the LexA regulon. (387). Hill *et al.*, have reported that LexA is necessary and also arrests DNA replication for inhibiting cell division. Sarconesin II might thus have induced filamentation in *E. coli* by inhibiting DNA synthesis (388).

Some AMPs have been reported as being membrane disruptive, such as alamethicin, magainin 2, cecropin and nisin, while some are membrane non-disruptive but do have internal action on DNA, RNA or proteins, i.e. buforin II, pleurocidin and PR39 (380). Sarconesin II could thus be a membrane non-disruptive peptide, also having internal action on DNA.

This chapter has thus provided a certain understanding of the whole sarconesin II antibacterial MoA. It could reasonably be assumed that sarconesin II's neutral, hydrophilic characteristics first

initiate an electrostatic interaction with the bacterial cell membrane's negatively-charged components. The peptide then induces outer and inner membrane permeabilization and depolarization, creating pores which the peptide can then use to enter cells. The budding or "wart"-formation can also lead to cell envelope destabilization, as seen by Gutschmann (389). Along with peptide internalization, sarconesin II could interact with DNA through electrostatic interaction, as found by Yang *et al.* (329). It would then spontaneously bind to DNA, causing filamentation in bacterial cells, inhibit cell repair function and lead to killing bacteria. As sarconesin II has two MoA it can easily kill Gram-positive and Gram-negative bacteria and is a potent AMP that might become a novel tool for combating resistant bacteria.

### 3.5. Conclusion

This chapter has described obtaining, characterizing and evaluating the antibacterial activity of a new *S. magellanica* larval ES-derived AMP named sarconesin II. It was obtained and purified using RP-HPLC. Sarconesin II fraction's antibacterial activity against Gram-positive and Gram-negative bacteria was demonstrated by MIC and measuring CFU. The peptide had no CC in the tests used here. Some of this AMP's relevant physicochemical characteristics obtained by MS/MS and spectrum analysis were: having a 13 aa sequence (VALTGLTVAEYFR), seven non-polar hydrophobic aa residues and another four polar uncharged aa (established predictively). It had a neutral charge because of having one basic positively-charged Arg (R) residue and one acid negatively-charged Glu (E) residue.

The PEAKS database search revealed that the native peptide fraction might have been derived from the ATP synthase  $\beta$  subunit, a mitochondrial protein previously reported in *Lucilia cuprina*. A BLAST search for *Calliphoridae* multiple sequence alignment revealed sarconesin II's 100% matching identity with the mitochondrial ATP synthase  $\beta$  subunit. This peptide's secondary structure had a characteristic  $\alpha$ -helix, predicted by I-TASSER and CD. The tests used to determine sarconesin II MoA on bacteria recorded disruption of the cells' inner membrane (PI), accompanied by alterations in sarconesin II's esterase activity, thereby confirming membrane alterations (CFDA), intracellular function inhibition via interference with DNA (DNA band electrophoretic mobility), without affecting the protein profile (SDS-PAGE), and damage to bacterial DNA (fluorescence microscopy). The peptide's effect on bacterial cell morphology (Gram staining) revealed elongation (i.e. filamentation), while using SEM demonstrated sarconesin II action on bacteria (having a highly elongated appearance) as filamentous cells having blebbing on their outer membrane. This AMP represents a new weapon for fighting against pathogenic microorganisms, acting mainly on both Gram-positive and Gram-negative bacteria, and showing so far good efficacy against an antibiotic-resistant pathogen such as *P. aeruginosa* PA14.

#### 4. Overall conclusions

Fractions from *S. magellanica* fly larval ES were isolated, characterized and analyzed for their antibacterial activity; all of the 67 were evaluated against Gram-positive and Gram-negative bacteria (using turbidimetry), but only 6 fractions had antibacterial activity.

When analyzing the sequence by MS, two fractions were selected from which it was possible to characterize and evaluate two new AMPs: sarconesin and sarconesin II;

*S. magellanica* AMPs had potent antibacterial activity and represent a new alternative for combating antibiotic resistance and are found in several organisms;

None of the AMPs reported here represent potential danger to mammalian cells, as no toxicity was seen;

These two new AMPs' MoA were shown to attack bacteria by affecting cell membrane and also internal structures as DNA;

Sarconesin has similarity with the CDC42 protein and sarconesin II with ATP synthase, are not toxic and their antimicrobial potential confirms them as good candidates for therapeutic drugs;

The tests involved in this work may help better understanding of the presence of antimicrobial substances in insects, their MoA and the development of potential new drugs.

## 5. References

1. Classamp. 2019 [March 7th 2019]. Available from: <http://www.bicnirrh.res.in/classamp/predict.php>.
2. Nigam Y, Dudley E, Bexfield A, Bond AE, Evans J, James J. The Physiology of Wound Healing by the Medicinal Maggot, *Lucilia sericata*. In: Simpson SJ, editor. *Advances in Insect Physiology*, Vol 39. *Advances in Insect Physiology*. 39. London: Academic Press Ltd-Elsevier Science Ltd; 2010. p. 39-81.
3. Bexfield A, Nigam Y, Thomas S, Ratcliffe NA. Detection and partial characterisation of two antibacterial factors from the excretions/secretions of the medicinal maggot *Lucilia sericata* and their activity against methicillin-resistant *Staphylococcus aureus* (MRSA). *Microbes Infect*. 2004;6(14):1297-304.
4. Mumcuoglu KY. Clinical applications for maggots in wound care. *American journal of clinical dermatology*. 2001;2(4):219-27.
5. Robinson W. Stimulation of healing in non-healing wounds: By Allantoin Occurring in Maggot Secretions and of Wide Biological Distribution. *The Journal of Bone & Joint Surgery JBJS*. 1935;17(2):267-71.
6. Gottrup F, Jorgensen B. Maggot debridement: an alternative method for debridement. *Eplasty*. 2011;11:e33.
7. Cazander G, van Veen KE, Bernards AT, Jukema GN. Do maggots have an influence on bacterial growth? A study on the susceptibility of strains of six different bacterial species to maggots of *Lucilia sericata* and their excretions/secretions. *J Tissue Viability*. 2009;18(3):80-7.
8. van der Plas MJ, Jukema GN, Wai SW, Dogterom-Ballering HC, Lagendijk EL, van Gulpen C, et al. Maggot excretions/secretions are differentially effective against biofilms of *Staphylococcus aureus* and *Pseudomonas aeruginosa*. *The Journal of antimicrobial chemotherapy*. 2008;61(1):117-22.
9. Church JC. The traditional use of maggots in wound healing, and the development of larva therapy (biosurgery) in modern medicine. *J Altern Complement Med*. 1996;2(4):525-7.
10. Thomas AM, Harding KG, Moore K. The structure and composition of chronic wound eschar. *Journal of wound care*. 1999;8(6):285-7.
11. Sherman RA, Hall MJ, Thomas S. Medicinal maggots: an ancient remedy for some contemporary afflictions. *Annual review of entomology*. 2000;45:55-81.
12. Wolff H, Hansson C. Rearing larvae of *Lucilia sericata* for chronic ulcer treatment--an improved method. *Acta dermato-venereologica*. 2005;85(2):126-31.
13. Spilsbury K, Cullum N, Dumville J, O'Meara S, Petherick E, Thompson C. Exploring patient perceptions of larval therapy as a potential treatment for venous leg ulceration. *Health expectations : an international journal of public participation in health care and health policy*. 2008;11(2):148-59.
14. Baer WS. The treatment of chronic osteomyelitis with the maggot (larva of the Blowfly). *J Bone Joint Surg*. 1931;13:438-75.
15. Robinson W, Norwood VH. The role of surgical maggots in the disinfection of osteomyelitis and other infected wounds. *J Bone Joint Surg Am*. 1933;15:409-12.

16. Weil GC, Simon RJ, Sweadner WR. A biological, bacteriological and clinical study of larval or maggot therapy in the treatment of acute and chronic pyogenic infections. *Am J Surg*. 1933;19(1):36-48.
17. Kerridge A, Lappin-Scott H, Stevens JR. Antibacterial properties of larval secretions of the blowfly, *Lucilia sericata*. *Medical and veterinary entomology*. 2005;19(3):333-7.
18. Cazander G, Pritchard DI, Nigam Y, Jung W, Nibbering PH. Multiple actions of *Lucilia sericata* larvae in hard-to-heal wounds: larval secretions contain molecules that accelerate wound healing, reduce chronic inflammation and inhibit bacterial infection. *BioEssays : news and reviews in molecular, cellular and developmental biology*. 2013;35(12):1083-92.
19. Hardy MA. The biology of scar formation. *Physical therapy*. 1989;69(12):1014-24.
20. Morgan C, Nigam Y. Naturally derived factors and their role in the promotion of angiogenesis for the healing of chronic wounds. *Angiogenesis*. 2013;16(3):493-502.
21. Nigam Y, Bexfield A, Thomas S, Ratcliffe NA. Maggot therapy: the science and implication for CAM part II-maggots combat infection. *Evidence-based complementary and alternative medicine : eCAM*. 2006;3(3):303-8.
22. Alexiadou K, Doupis J. Management of diabetic foot ulcers. *Diabetes therapy : research, treatment and education of diabetes and related disorders*. 2012;3(1):4-.
23. Bowler PG, Duerden BI, Armstrong DG. Wound microbiology and associated approaches to wound management. *Clinical microbiology reviews*. 2001;14(2):244-69.
24. Jaklic D, Lapanje A, Zupancic K, Smrke D, Gunde-Cimerman N. Selective antimicrobial activity of maggots against pathogenic bacteria. *Journal of medical microbiology*. 2008;57(Pt 5):617-25.
25. Chambers L, Woodrow S, Brown AP, Harris PD, Phillips D, Hall M, et al. Degradation of extracellular matrix components by defined proteinases from the greenbottle larva *Lucilia sericata* used for the clinical debridement of non-healing wounds. *Br J Dermatol*. 2003;148(1):14-23.
26. Prete PE. Growth effects of *Phaenicia sericata* larval extracts on fibroblasts: mechanism for wound healing by maggot therapy. *Life sciences*. 1997;60(8):505-10.
27. Telford G, Brown AP, Seabra RA, Horobin AJ, Rich A, English JS, et al. Degradation of eschar from venous leg ulcers using a recombinant chymotrypsin from *Lucilia sericata*. *Br J Dermatol*. 2010;163(3):523-31.
28. van der Plas MJ, van Dissel JT, Nibbering PH. Maggot secretions skew monocyte-macrophage differentiation away from a pro-inflammatory to a pro-angiogenic type. *PLoS one*. 2009;4(11):e8071.
29. Thomas S, Wynn K, Fowler T, Jones M. The effect of containment on the properties of sterile maggots. *British journal of nursing (Mark Allen Publishing)*. 2002;11(12 Suppl):S21-2, S4, S6 passim.
30. Young AR, Meeusen EN, Bowles VM. Characterization of ES products involved in wound initiation by *Lucilia cuprina* larvae. *Int J Parasitol*. 1996;26(3):245-52.
31. Giglioti R, Guimarães S, C.G. Oliveira-Sequeira T, David E, Brito L, Funes-Huacca M, et al. Proteolytic activity of excretory/secretory products of *Cochliomyia hominivorax* larvae (Diptera: Calliphoridae) 2016. 711-8 p.

32. Muharsini S, Sukarsih, Riding G, Partoutomo S, Hamilton S, Willadsen P, et al. Identification and characterisation of the excreted/secreted serine proteases of larvae of the Old World Screwworm Fly, *Chrysomya bezziana*. *International Journal for Parasitology*. 2000;30(6):705-14.
33. Schmidtchen A, Wolff H, Rydengard V, Hansson C. Detection of serine proteases secreted by *Lucilia sericata* in vitro and during treatment of a chronic leg ulcer. *Acta dermatovenereologica*. 2003;83(4):310-1.
34. Buchman J, Blair JE. Maggots and their use in the treatment of chronic osteomyelitis 1932. 177-90 p.
35. Wollina U, Liebold K, Schmidt WD, Hartmann M, Fassler D. Biosurgery supports granulation and debridement in chronic wounds--clinical data and remittance spectroscopy measurement. *International journal of dermatology*. 2002;41(10):635-9.
36. Robinson W. Stimulation of healing in non-healing wounds by allantoin in maggot secretions and of wide biological distribution. *J Bone Joint Surg Am*. 1935;17(2):267-71.
37. Harris LG, Nigam Y, Sawyer J, Mack D, Pritchard DI. *Lucilia sericata* chymotrypsin disrupts protein adhesin-mediated staphylococcal biofilm formation. *Applied and environmental microbiology*. 2013;79(4):1393-5.
38. Horobin AJ, Shakesheff KM, Woodrow S, Robinson C, Pritchard DI. Maggots and wound healing: an investigation of the effects of secretions from *Lucilia sericata* larvae upon interactions between human dermal fibroblasts and extracellular matrix components. *Br J Dermatol*. 2003;148(5):923-33.
39. Simmons SW. A Bactericidal Principle in Excretions of Surgical Maggots which Destroys Important Etiological Agents of Pyogenic Infections. *Journal of bacteriology*. 1935;30(3):253-67.
40. Pavillard ER, Wright EA. An antibiotic from maggots. *Nature*. 1957;180(4592):916-7.
41. Parnes A, Lagan KM. Larval therapy in wound management: a review. *International journal of clinical practice*. 2007;61(3):488-93.
42. Huberman L, Gollop N, Mumcuoglu KY, Breuer E, Bhusare SR, Shai Y, et al. Antibacterial substances of low molecular weight isolated from the blowfly, *Lucilia sericata*. *Medical and veterinary entomology*. 2007;21(2):127-31.
43. Hoffmann JA, Hetru C. Insect defensins: inducible antibacterial peptides. *Immunology today*. 1992;13(10):411-5.
44. Bulet P, Stocklin R. Insect antimicrobial peptides: structures, properties and gene regulation. *Protein and peptide letters*. 2005;12(1):3-11.
45. Cerovsky V, Zdarek J, Fucik V, Monincova L, Voburka Z, Bem R. Lucifensin, the long-sought antimicrobial factor of medicinal maggots of the blowfly *Lucilia sericata*. *Cellular and molecular life sciences : CMLS*. 2010;67(3):455-66.
46. Bexfield A, Bond AE, Roberts EC, Dudley E, Nigam Y, Thomas S, et al. The antibacterial activity against MRSA strains and other bacteria of a <500Da fraction from maggot excretions/secretions of *Lucilia sericata* (Diptera: Calliphoridae). *Microbes Infect*. 2008;10(4):325-33.

47. Arora S, Baptista C, Lim CS. Maggot metabolites and their combinatory effects with antibiotic on *Staphylococcus aureus*. *Ann Clin Microbiol Antimicrob*. 2011;10:6.
48. Daeschlein G, Mumcuoglu KY, Assadian O, Hoffmeister B, Kramer A. In vitro antibacterial activity of *Lucilia sericata* maggot secretions. *Skin pharmacology and physiology*. 2007;20(2):112-5.
49. Andersen AS, Sandvang D, Schnorr KM, Kruse T, Neve S, Joergensen B, et al. A novel approach to the antimicrobial activity of maggot debridement therapy. *J Antimicrob Chemother*. 2010;65(8):1646-54.
50. El Shazely B, Veverka V, Fucik V, Voburka Z, Zdarek J, Cerovsky V. Lucifensin II, a defensin of medicinal maggots of the blowfly *Lucilia cuprina* (Diptera: Calliphoridae). *Journal of medical entomology*. 2013;50(3):571-8.
51. Chernysh S, Gordya N, Suborova T. Insect Antimicrobial Peptide Complexes Prevent Resistance Development in Bacteria. *PloS one*. 2015;10(7):e0130788.
52. Andersen AS, Sandvang D, Schnorr KM, Kruse T, Neve S, Joergensen B, et al. A novel approach to the antimicrobial activity of maggot debridement therapy. *The Journal of antimicrobial chemotherapy*. 2010;65(8):1646-54.
53. Cerovsky V, Bem R. Lucifensins, the Insect Defensins of Biomedical Importance: The Story behind Maggot Therapy. *Pharmaceuticals*. 2014;7(3):251-64.
54. Yakovlev AY, Nesin AP, Simonenko NP, Gordya NA, Tulin DV, Kruglikova AA, et al. Fat body and hemocyte contribution to the antimicrobial peptide synthesis in *Calliphora vicina* R.-D. (Diptera: Calliphoridae) larvae. *In vitro cellular & developmental biology Animal*. 2017;53(1):33-42.
55. Gordya N, Yakovlev A, Kruglikova A, Tulin D, Potolitsina E, Suborova T, et al. Natural antimicrobial peptide complexes in the fighting of antibiotic resistant biofilms: *Calliphora vicina* medicinal maggots. *PloS one*. 2017;12(3):e0173559.
56. Chernysh S, Gordya N, Tulin D, Yakovlev A. Biofilm infections between *Scylla* and *Charybdis*: interplay of host antimicrobial peptides and antibiotics. *Infect Drug Resist*. 2018;11:501-14.
57. Cowan LJ, Stechmiller JK, Phillips P, Yang Q, Schultz G. Chronic Wounds, Biofilms and Use of Medicinal Larvae. *Ulcers*. 2013;2013:7.
58. Davis SC, Ricotti C, Cazzaniga A, Welsh E, Eaglstein WH, Mertz PM. Microscopic and physiologic evidence for biofilm-associated wound colonization in vivo. *Wound repair and regeneration : official publication of the Wound Healing Society [and] the European Tissue Repair Society*. 2008;16(1):23-9.
59. James GA, Swogger E, Wolcott R, Pulcini E, Secor P, Sestrich J, et al. Biofilms in chronic wounds. *Wound repair and regeneration : official publication of the Wound Healing Society [and] the European Tissue Repair Society*. 2008;16(1):37-44.
60. Leaper DJ, Schultz G, Carville K, Fletcher J, Swanson T, Drake R. Extending the TIME concept: what have we learned in the past 10 years?(\*). *International wound journal*. 2012;9 Suppl 2:1-19.

61. Harris LG, Bexfield A, Nigam Y, Rohde H, Ratcliffe NA, Mack D. Disruption of *Staphylococcus epidermidis* biofilms by medicinal maggot *Lucilia sericata* excretions/secretions. *The International journal of artificial organs*. 2009;32(9):555-64.
62. Cazander G, van de Veerdonk MC, Vandenbroucke-Grauls CM, Schreurs MW, Jukema GN. Maggot excretions inhibit biofilm formation on biomaterials. *Clin Orthop Relat Res*. 2010;468(10):2789-96.
63. van der Plas MJ, Dambrot C, Dogterom-Ballering HC, Kruithof S, van Dissel JT, Nibbering PH. Combinations of maggot excretions/secretions and antibiotics are effective against *Staphylococcus aureus* biofilms and the bacteria derived therefrom. *The Journal of antimicrobial chemotherapy*. 2010;65(5):917-23.
64. Pritchard DI, Brown AP. Degradation of MSCRAMM target macromolecules in VLU slough by *Lucilia sericata* chymotrypsin 1 (ISP) persists in the presence of tissue gelatinase activity. *International wound journal*. 2015;12(4):414-21.
65. Jiang K-c, Sun X-j, Wang W, Liu L, Cai Y, Chen Y-c, et al. Excretions/Secretions from Bacteria-Pretreated Maggot Are More Effective against *Pseudomonas aeruginosa* Biofilms. *PloS one*. 2012;7(11):e49815.
66. Kawabata T, Mitsui H, Yokota K, Ishino K, Oguma K, Sano S. Induction of antibacterial activity in larvae of the blowfly *Lucilia sericata* by an infected environment. *Medical and veterinary entomology*. 2010;24(4):375-81.
67. Dumville JC, Worthy G, Soares MO, Bland JM, Cullum N, Dowson C, et al. VenUS II: a randomised controlled trial of larval therapy in the management of leg ulcers. *Health technology assessment*. 2009;13(55):1-182, iii-iv.
68. Mariluis J, Mulieri P. The distribution of the Calliphoridae in Argentina (Diptera). *Revista de la Sociedad Entomológica Argentina*. 2003;62(1):85 - 97.
69. Pape T, Wolff M, Amat E. Los califóridos, éstridos, rinofóridos y sarcófágidos (Diptera: Calliphoridae, Oestridae, Rhinophoridae y Sarcophagidae) de Colombia. *Biota Colombiana*. 2004;5:201 - 8.
70. Figueroa-Roa L, Linhares AX. Sinantropia de los Calliphoridae (Diptera) de Valdivia, Chile. *Neotropical entomology*. 2002;31:233-9.
71. Mariluis JC, Peris SV. Datos para una sinopsis de los Calliphoridae neotropicales. *EOS-Revista Española de Entomología*. 1984;40:67-86.
72. James M. Catalogue of the diptera of the Americas South of United States, Sao Paulo, Museu de Zoologia da USP. Secretaria da Agricultura. Departamento de Zoologia.: S.N.; 1970. 88 p.
73. Goff ML. A fly for the prosecution: how insect evidence helps solve crimes. Harvard University Press. 2001:225.
74. Segura NA, Usaquen W, Sanchez MC, Chuairé L, Bello F. Succession pattern of cadaverous entomofauna in a semi-rural area of Bogota, Colombia. *Forensic science international*. 2009;187(1-3):66-72.
75. Segura N, Usaquén W, Sánchez M, Sánchez R, Chuairé L, Camacho G, et al. Curvas de crecimiento y desarrollo de los primeros insectos colonizadores (Diptera: Calliphoridae) sobre

cadáveres de cerdo *Sus scrofa* en Bogotá (Colombia). *Revista de Investigación Universidad de La Salle* 2005;5:129 - 40.

76. Diaz-Roa A, Gaona MA, Segura NA, Suarez D, Patarroyo MA, Bello FJ. *Sarconesiopsis magellanica* (Diptera: Calliphoridae) excretions and secretions have potent antibacterial activity. *Acta tropica*. 2014;136:37-43.

77. Cruz-Saavedra L, Diaz-Roa A, Gaona MA, Cruz ML, Ayala M, Cortes-Vecino JA, et al. The effect of *Lucilia sericata*- and *Sarconesiopsis magellanica*-derived larval therapy on *Leishmania panamensis*. *Acta Trop*. 2016;164:280-9.

78. Kuhn-Nentwig L, Nentwig W. *The Immune System of Spiders*. 2013. p. 81-91.

79. Vieira CS, Waniek PJ, Mattos DP, Castro DP, Mello CB, Ratcliffe NA, et al. Humoral responses in *Rhodnius prolixus*: bacterial feeding induces differential patterns of antibacterial activity and enhances mRNA levels of antimicrobial peptides in the midgut. *Parasites & vectors*. 2014;7:232.

80. Wirkner C, Huckstorf K. *The Circulatory System of Spiders*. 2013. p. 15-27.

81. Lackie AM. Immune mechanisms in insects. *Parasitology today*. 1988;4(4):98-105.

82. Lavine MD, Strand MR. Insect hemocytes and their role in immunity. *Insect biochemistry and molecular biology*. 2002;32(10):1295-309.

83. Brooks GT. *Comprehensive insect physiology, biochemistry and pharmacology*: Edited by G. A. Kerkut and L. I. Gilbert. Pergamon Press, Oxford. 1985. 13 Volumes. 8200 pp approx. £1700.00/\$2750.00. ISBN 0 08 026850 1. *Insect Biochemistry*. 1985;15(5):i-xiv.

84. Ratcliffe NA, Gagen SJ. Studies on the in vivo cellular reactions of insects: an ultrastructural analysis of nodule formation in *Galleria mellonella*. *Tissue & cell*. 1977;9(1):73-85.

85. Satyavathi VV, Minz A, Nagaraju J. Nodulation: an unexplored cellular defense mechanism in insects. *Cellular signalling*. 2014;26(8):1753-63.

86. Aguilar-Díaz H, Cossío-Bayúgar R. *Immune System and Its Relationships with Pathogens: Structure, Physiology, and Molecular Biology*. 2018.

87. Ratcliffe NA, Rowley AF. Cellular defense reactions of insect hemocytes in vitro: Phagocytosis in a new suspension culture system. *Journal of Invertebrate Pathology*. 1975;26(2):225-33.

88. Ratcliffe NA, Götz P. Functional studies on insect haemocytes, including non-self recognition. *Research in Immunology*. 1990;141(9):919-23.

89. Nappi AJ, Vass E, Frey F, Carton Y. Superoxide anion generation in *Drosophila* during melanotic encapsulation of parasites. *European journal of cell biology*. 1995;68(4):450-6.

90. Gillespie JP, Kanost MR, Trenczek T. Biological mediators of insect immunity. *Annual review of entomology*. 1997;42:611-43.

91. Soderhall K, Cerenius L. Role of the prophenoloxidase-activating system in invertebrate immunity. *Current opinion in immunology*. 1998;10(1):23-8.

92. Dunn PE. Humoral Immunity in Insects. *BioScience*. 1990;40(10):738-44.

93. Iwanaga S, Lee B. *Recent Advances in the Innate Immunity of Invertebrate Animals* 2005. 128-50 p.

- 
94. Binggeli O, Neyen C, Poidevin M, Lemaitre B. Prophenoloxidase Activation Is Required for Survival to Microbial Infections in *Drosophila*. *PLOS Pathogens*. 2014;10(5):e1004067.
  95. Dittmer NT, Suderman RJ, Jiang H, Zhu YC, Gorman MJ, Kramer KJ, et al. Characterization of cDNAs encoding putative laccase-like multicopper oxidases and developmental expression in the tobacco hornworm, *Manduca sexta*, and the malaria mosquito, *Anopheles gambiae*. *Insect biochemistry and molecular biology*. 2004;34(1):29-41.
  96. Gorman MJ, Wang Y, Jiang H, Kanost MR. *Manduca sexta* hemolymph proteinase 21 activates prophenoloxidase-activating proteinase 3 in an insect innate immune response proteinase cascade. *The Journal of biological chemistry*. 2007;282(16):11742-9.
  97. Shrestha S, Kim Y. Eicosanoids mediate prophenoloxidase release from oenocytoids in the beet armyworm *Spodoptera exigua*. *Insect biochemistry and molecular biology*. 2008;38(1):99-112.
  98. Hillyer JF, Christensen BM. Characterization of hemocytes from the yellow fever mosquito, *Aedes aegypti*. *Histochemistry and cell biology*. 2002;117(5):431-40.
  99. Rizki TM, Rizki RM, Bellotti RA. Genetics of a *Drosophila* phenoloxidase. *Molecular & general genetics : MGG*. 1985;201(1):7-13.
  100. Louradour I, Sharma A, Morin-Poulard I, Letourneau M, Vincent A, Crozatier M, et al. Reactive oxygen species-dependent Toll/NF- $\kappa$ B activation in the *Drosophila* hematopoietic niche confers resistance to wasp parasitism. *eLife*. 2017;6:e25496.
  101. Fujita AI. Lysozymes in insects: What role do they play in nitrogen metabolism?2004. 305-10 p.
  102. Zdybicka-Barabas A, Staczek S, Mak P, Skrzypiec K, Mendyk E, Cytrynska M. Synergistic action of *Galleria mellonella* apolipoprotein III and lysozyme against Gram-negative bacteria. *Biochimica et biophysica acta*. 2013;1828(6):1449-56.
  103. Whitten M, Sun F, Tew I, Schaub G, Soukou C, Nappi A, et al. Differential modulation of *Rhodnius prolixus* nitric oxide activities following challenge with *Trypanosoma rangeli*, *T. cruzi* and bacterial cell wall components. *Insect biochemistry and molecular biology*. 2007;37(5):440-52.
  104. Wu D, Cederbaum AI. Alcohol, oxidative stress, and free radical damage. *Alcohol research & health : the journal of the National Institute on Alcohol Abuse and Alcoholism*. 2003;27(4):277-84.
  105. Nita M, Grzybowski A. The Role of the Reactive Oxygen Species and Oxidative Stress in the Pathomechanism of the Age-Related Ocular Diseases and Other Pathologies of the Anterior and Posterior Eye Segments in Adults. *Oxidative medicine and cellular longevity*. 2016;2016:3164734-.
  106. Freeman BA, Crapo JD. Biology of disease: free radicals and tissue injury. *Laboratory investigation; a journal of technical methods and pathology*. 1982;47(5):412-26.
  107. Rivero A. Nitric oxide: an antiparasitic molecule of invertebrates. *Trends in parasitology*. 2006;22(5):219-25.
  108. Nehme NT, Liégeois S, Kele B, Giammarinaro P, Pradel E, Hoffmann JA, et al. A model of bacterial intestinal infections in *Drosophila melanogaster*. *PLoS pathogens*. 2007;3(11):e173-e.

109. Buchon N, Silverman N, Cherry S. Immunity in *Drosophila melanogaster*--from microbial recognition to whole-organism physiology. *Nature reviews Immunology*. 2014;14(12):796-810.
110. Kleino A, Silverman N. The *Drosophila* IMD pathway in the activation of the humoral immune response. *Developmental and comparative immunology*. 2014;42(1):25-35.
111. Valanne S, Wang J-H, Rämetsä M. The *Drosophila* Toll Signaling Pathway. *The Journal of Immunology*. 2011;186(2):649.
112. Kumar P, Kizhakkedathu JN, Straus SK. Antimicrobial Peptides: Diversity, Mechanism of Action and Strategies to Improve the Activity and Biocompatibility In Vivo. *Biomolecules*. 2018;8(1).
113. Elhag O, Zhou D, Song Q, Soomro AA, Cai M, Zheng L, et al. Screening, Expression, Purification and Functional Characterization of Novel Antimicrobial Peptide Genes from *Hermetia illucens* (L.). *PloS one*. 2017;12(1):e0169582.
114. Mylonakis E, Podsiadlowski L, Muhammed M, Vilcinskas A. Diversity, evolution and medical applications of insect antimicrobial peptides. *Philosophical transactions of the Royal Society of London Series B, Biological sciences*. 2016;371(1695).
115. Zhang L, Wang YW, Lu ZQ. Midgut immune responses induced by bacterial infection in the silkworm, *Bombyx mori*. *Journal of Zhejiang University Science B*. 2015;16(10):875-82.
116. Buchon N, Silverman N, Cherry S. Immunity in *Drosophila melanogaster*--from microbial recognition to whole-organism physiology. *Nat Rev Immunol*. 2014;14(12):796-810.
117. Romoli O, Saviane A, Bozzato A, D'Antona P, Tettamanti G, Squartini A, et al. Differential sensitivity to infections and antimicrobial peptide-mediated immune response in four silkworm strains with different geographical origin. *Scientific reports*. 2017;7(1):1048.
118. Mishra AK, Choi J, Moon E, Baek KH. Tryptophan-Rich and Proline-Rich Antimicrobial Peptides. *Molecules (Basel, Switzerland)*. 2018;23(4).
119. Hancock RE, Sahl HG. Antimicrobial and host-defense peptides as new anti-infective therapeutic strategies. *Nat Biotechnol*. 2006;24(12):1551-7.
120. Nguyen LT, Haney EF, Vogel HJ. The expanding scope of antimicrobial peptide structures and their modes of action. *Trends in biotechnology*. 2011;29(9):464-72.
121. Yi HY, Chowdhury M, Huang YD, Yu XQ. Insect antimicrobial peptides and their applications. *Applied microbiology and biotechnology*. 2014;98(13):5807-22.
122. Manzo G, Ferguson PM, Gustilo VB, Hind CK, Clifford M, Bui TT, et al. Minor sequence modifications in temporin B cause drastic changes in antibacterial potency and selectivity by fundamentally altering membrane activity. *Scientific reports*. 2019;9(1):1385.
123. Minamino T, Kazetani K-i, Tahara A, Suzuki H, Furukawa Y, Kihara M, et al. Oligomerization of the Bacterial Flagellar ATPase FliI is Controlled by its Extreme N-terminal Region. *Journal of Bacteriology*. 2006;188(3):510-9 p.
124. Leon-Calvijo MA, Leal-Castro AL, Almanzar-Reina GA, Rosas-Perez JE, Garcia-Castaneda JE, Rivera-Monroy ZJ. Antibacterial activity of synthetic peptides derived from lactoferricin against *Escherichia coli* ATCC 25922 and *Enterococcus faecalis* ATCC 29212. *Biomed Res Int*. 2015;2015:453826.

125. Yazici A, Ortucu S, Taskin M, Marinelli L. Natural-based Antibiofilm and Antimicrobial Peptides from Microorganisms. *Current topics in medicinal chemistry*. 2018;18(24):2102-7.
126. Wang G, Li X, Wang Z. APD2: the updated antimicrobial peptide database and its application in peptide design. *Nucleic acids research*. 2009;37(Database issue):D933-7.
127. Matsuyama K, Natori S. Purification of three antibacterial proteins from the culture medium of NIH-Sape-4, an embryonic cell line of *Sarcophaga peregrina*. *The Journal of biological chemistry*. 1988;263(32):17112-6.
128. Lambert J, Keppi E, Dimarcq JL, Wicker C, Reichhart JM, Dunbar B, et al. Insect immunity: isolation from immune blood of the dipteran *Phormia terranova* of two insect antibacterial peptides with sequence homology to rabbit lung macrophage bactericidal peptides. *Proc Natl Acad Sci U S A*. 1989;86(1):262-6.
129. Boulanger N, Bulet P, Lowenberger C. Antimicrobial peptides in the interactions between insects and flagellate parasites. *Trends in parasitology*. 2006;22(6):262-8.
130. Lehane MJ, Wu D, Lehane SM. Midgut-specific immune molecules are produced by the blood-sucking insect *Stomoxys calcitrans*. *Proc Natl Acad Sci U S A*. 1997;94(21):11502-7.
131. Rees JA, Moniatte M, Bulet P. Novel antibacterial peptides isolated from a European bumblebee, *Bombus pascuorum* (Hymenoptera, Apoidea). *Insect biochemistry and molecular biology*. 1997;27(5):413-22.
132. Bulet P, Hetru C, Dimarcq JL, Hoffmann D. Antimicrobial peptides in insects; structure and function. *Dev Comp Immunol*. 1999;23(4-5):329-44.
133. Hanzawa H, Shimada I, Kuzuhara T, Komano H, Kohda D, Inagaki F, et al. 1H nuclear magnetic resonance study of the solution conformation of an antibacterial protein, sapecin. *FEBS letters*. 1990;269(2):413-20.
134. Cornet B, Bonmatin JM, Hetru C, Hoffmann JA, Ptak M, Vovelle F. Refined three-dimensional solution structure of insect defensin A. *Structure*. 1995;3(5):435-48.
135. Landon C, Sodano P, Hetru C, Hoffmann J, Ptak M. Solution structure of drosomycin, the first inducible antifungal protein from insects. *Protein science : a publication of the Protein Society*. 1997;6(9):1878-84.
136. Fujiwara S, Imai J, Fujiwara M, Yaeshima T, Kawashima T, Kobayashi K. A potent antibacterial protein in royal jelly. Purification and determination of the primary structure of royalisin. *The Journal of biological chemistry*. 1990;265(19):11333-7.
137. Cerovsky V, Slaninova J, Fucik V, Monincova L, Bednarova L, Malon P, et al. Lucifensin, a novel insect defensin of medicinal maggots: synthesis and structural study. *Chembiochem*. 2011;12(9):1352-61.
138. Zhang Z, Wang J, Zhang B, Liu H, Song W, He J, et al. Activity of antibacterial protein from maggots against *Staphylococcus aureus* in vitro and in vivo. *International journal of molecular medicine*. 2013;31(5):1159-65.
139. Valachova I, Bohova J, Palosova Z, Takac P, Kozanek M, Majtan J. Expression of lucifensin in *Lucilia sericata* medicinal maggots in infected environments. *Cell and tissue research*. 2013;353(1):165-71.

140. Valachova I, Prochazka E, Bohova J, Novak P, Takac P, Majtan J. Antibacterial properties of lucifensin in *Lucilia sericata* maggots after septic injury. *Asian Pacific journal of tropical biomedicine*. 2014;4(5):358-61.
141. Kruglikova A, Chernysh S. Antimicrobial compounds from the excretions of surgical maggots, *Lucilia sericata* (Meigen) (Diptera, Calliphoridae). *Entomol Rev*. 2011;91:813-9.
142. Pinilla YT, Patarroyo MA, Velandia ML, Segura NA, Bello FJ. The effects of *Sarconesiopsis magellanica* larvae (Diptera: Calliphoridae) excretions and secretions on fibroblasts. *Acta tropica*. 2015;142:26-33.
143. Sherman RA. Mechanisms of maggot-induced wound healing: what do we know, and where do we go from here? *Evidence-based complementary and alternative medicine : eCAM*. 2014;2014:592419.
144. Poppel AK, Vogel H, Wiesner J, Vilcinskas A. Antimicrobial peptides expressed in medicinal maggots of the blow fly *Lucilia sericata* show combinatorial activity against bacteria. *Antimicrobial agents and chemotherapy*. 2015;59(5):2508-14.
145. Yi H-Y, Chowdhury M, Huang Y-D, Yu X-Q. Insect antimicrobial peptides and their applications. *Applied microbiology and biotechnology*. 2014;98(13):5807-22.
146. Hollmann A, Martinez M, Maturana P, Semorile LC, Maffia PC. Antimicrobial Peptides: Interaction With Model and Biological Membranes and Synergism With Chemical Antibiotics. *Frontiers in chemistry*. 2018;6:204-.
147. Aoki W, Ueda M. Characterization of Antimicrobial Peptides toward the Development of Novel Antibiotics. *Pharmaceuticals (Basel, Switzerland)*. 2013;6(8):1055-81.
148. Zhang L-j, Gallo RL. Antimicrobial peptides. *Current Biology*. 2016;26(1):R14-R9.
149. Leandro LF, Mendes CA, Casemiro LA, Vinholis AHC, Cunha WR, Almeida Rd, et al. Antimicrobial activity of apitoxin, melittin and phospholipase A2 of honey bee (*Apis mellifera*) venom against oral pathogens. *Anais da Academia Brasileira de Ciências*. 2015;87:147-55.
150. Yevtushenko DP, Romero R, Forward BS, Hancock RE, Kay WW, Misra S. Pathogen-induced expression of a cecropin A-melittin antimicrobial peptide gene confers antifungal resistance in transgenic tobacco. *Journal of experimental botany*. 2005;56(416):1685-95.
151. Findlay F, Proudfoot L, Stevens C, Barlow PG. Cationic host defense peptides; novel antimicrobial therapeutics against Category A pathogens and emerging infections. *Pathogens and global health*. 2016;110(4-5):137-47.
152. Brown KL, Hancock RE. Cationic host defense (antimicrobial) peptides. *Curr Opin Immunol*. 2006;18(1):24-30.
153. Bechinger B, Gorr SU. Antimicrobial Peptides: Mechanisms of Action and Resistance. *Journal of dental research*. 2017;96(3):254-60.
154. Toke O. Antimicrobial peptides: new candidates in the fight against bacterial infections. *Biopolymers*. 2005;80(6):717-35.
155. Yeaman MR, Yount NY. Mechanisms of antimicrobial peptide action and resistance. *Pharmacological reviews*. 2003;55(1):27-55.
156. Giuliani A, Pirri G, Nicoletto SF. Antimicrobial peptides: an overview of a promising class of therapeutics. *Current Medicinal Chemistry*. 2006;2(1):2449-66.

157. Sani MA, Separovic F. How Membrane-Active Peptides Get into Lipid Membranes. *Accounts of chemical research*. 2016;49(6):1130-8.
158. Zasloff M. Antimicrobial peptides of multicellular organisms. *Nature*. 2002;415(6870):389-95.
159. Ebenhan T, Gheysens O, Kruger HG, Zeevaert JR, Sathekge MM. Antimicrobial peptides: their role as infection-selective tracers for molecular imaging. *BioMed research international*. 2014;2014:867381-.
160. Brogden KA. Antimicrobial peptides: pore formers or metabolic inhibitors in bacteria? *Nature reviews Microbiology*. 2005;3(3):238-50.
161. Lee MT, Chen FY, Huang HW. Energetics of pore formation induced by membrane active peptides. *Biochemistry*. 2004;43(12):3590-9.
162. Brogden KA. Antimicrobial peptides: pore formers or metabolic inhibitors in bacteria? *Nat Rev Microbiol*. 2005;3(3):238-50.
163. Yang L, Harroun TA, Weiss TM, Ding L, Huang HW. Barrel-stave model or toroidal model? A case study on melittin pores. *Biophysical journal*. 2001;81(3):1475-85.
164. Yamaguchi S, Huster D, Waring A, Lehrer RI, Kearney W, Tack BF, et al. Orientation and dynamics of an antimicrobial peptide in the lipid bilayer by solid-state NMR spectroscopy. *Biophysical journal*. 2001;81(4):2203-14.
165. Matsuzaki K, Murase O, Fujii N, Miyajima K. An antimicrobial peptide, magainin 2, induced rapid flip-flop of phospholipids coupled with pore formation and peptide translocation. *Biochemistry*. 1996;35(35):11361-8.
166. Hallock KJ, Lee D-K, Ramamoorthy A. MSI-78, an analogue of the magainin antimicrobial peptides, disrupts lipid bilayer structure via positive curvature strain. *Biophysical journal*. 2003;84(5):3052-60.
167. Subbalakshmi C, Sitaram N. Mechanism of antimicrobial action of indolicidin. *FEMS microbiology letters*. 1998;160(1):91-6.
168. Otvos L, Jr. Antibacterial peptides and proteins with multiple cellular targets. *Journal of peptide science : an official publication of the European Peptide Society*. 2005;11(11):697-706.
169. Bahar AA, Ren D. Antimicrobial peptides. *Pharmaceuticals*. 2013;6(12):1543-75.
170. Brogden KA, Ackermann M, McCray PB, Jr., Tack BF. Antimicrobial peptides in animals and their role in host defences. *Int J Antimicrob Agents*. 2003;22(5):465-78.
171. Jenssen H, Hamill P, Hancock RE. Peptide antimicrobial agents. *Clin Microbiol Rev*. 2006;19(3):491-511.
172. Roudi R, Syn NL, Roudbary M. Antimicrobial Peptides As Biologic and Immunotherapeutic Agents against Cancer: A Comprehensive Overview. *Frontiers in Immunology*. 2017;8(1320).
173. Harris F, Dennison SR, Phoenix DA. Anionic antimicrobial peptides from eukaryotic organisms. *Curr Protein Pept Sci*. 2009;10(6):585-606.
174. Otvos L, Jr. Antibacterial peptides isolated from insects. *Journal of peptide science : an official publication of the European Peptide Society*. 2000;6(10):497-511.

175. Vilcinskas A. Anti-infective therapeutics from the Lepidopteran model host *Galleria mellonella*. *Current pharmaceutical design*. 2011;17(13):1240-5.
176. Pretzel J, Mohring F, Rahlfs S, Becker K. Antiparasitic peptides. *Advances in biochemical engineering/biotechnology*. 2013;135:157-92.
177. Tonk M, Vilcinskas A, Rahnamaeian M. Insect antimicrobial peptides: potential tools for the prevention of skin cancer. *Applied microbiology and biotechnology*. 2016;100(17):7397-405.
178. Chen Y, Mant CT, Farmer SW, Hancock RE, Vasil ML, Hodges RS. Rational design of alpha-helical antimicrobial peptides with enhanced activities and specificity/therapeutic index. *The Journal of biological chemistry*. 2005;280(13):12316-29.
179. Bhattacharjya S, Ramamoorthy A. Multifunctional host defense peptides: functional and mechanistic insights from NMR structures of potent antimicrobial peptides. *The FEBS journal*. 2009;276(22):6465-73.
180. Marshall SH, Arenas G. Antimicrobial peptides: A natural alternative to chemical antibiotics and a potential for applied biotechnology 2003.
181. WHO. 2018 [March 7th 2019]. Available from: <https://www.who.int/news-room/fact-sheets/detail/antibiotic-resistance>.
182. Mishra B, Reiling S, Zarena D, Wang G. Host defense antimicrobial peptides as antibiotics: design and application strategies. *Current opinion in chemical biology*. 2017;38:87-96.
183. O'Meara S, Al-Kurdi D, Ologun Y, Ovington LG. Antibiotics and antiseptics for venous leg ulcers. *The Cochrane database of systematic reviews*. 2010(1):CD003557.
184. Pinilla YT, Patarroyo MA, Bello FJ. *Sarconesiopsis magellanica* (Diptera: Calliphoridae) life-cycle, reproductive and population parameters using different diets under laboratory conditions. *Forensic science international*. 2013;233(1-3):380-6.
185. Pinilla YT, Moreno-Perez DA, Patarroyo MA, Bello FJ. Proteolytic activity regarding *Sarconesiopsis magellanica* (Diptera: Calliphoridae) larval excretions and secretions. *Acta tropica*. 2013;128(3):686-91.
186. Cruz M, Bello FJ. Establishment and characterization of an embryonic cell line from *Sarconesiopsis magellanica*. *Journal of insect science*. 2013;13:130.
187. Cruz M, Bello F. Características de cultivos celulares primarios derivados de *Sarconesiopsis magellanica* (Le Guillou, 1842) (Diptera: Calliphoridae). *Revista UDCA Actualidad & Divulgación Científica*. 2012;15(2):313 - 21.
188. Diaz-Roa A, Gaona MA, Segura NA, Suarez D, Patarroyo MA, Bello FJ. *Sarconesiopsis magellanica* (Diptera: Calliphoridae) excretions and secretions have potent antibacterial activity. *Acta Trop*. 2014;136:37-43.
189. Góngora J, Díaz-Roa A, Gaona MA, Corts-Vecino J, Bello F. Evaluación de la actividad antibacterial de los extractos de cuerpos grasos y hemolinfa derivados de la mosca *Sarconesiopsis magellanica* (Diptera: Calliphoridae). *Infectio*. 2015;19:3-9.
190. Góngora J, Díaz-Roa A, Ramírez-Hernández A, Cortés-Vecino J, Gaona MA, Patarroyo MA, et al. Evaluating the effect of *Sarconesiopsis magellanica* (diptera:

Calliphoridae) larvae-derived haemolymph and fat body extracts on chronic wounds in diabetic rabbits. *Journal of diabetes research*. 2015;270253.

191. Rueda LC, Ortega LG, Segura NA, Acero VM, Bello F. *Lucilia sericata* strain from Colombia: Experimental colonization, life tables and evaluation of two artificial diets of the blowfly *Lucilia sericata* (Meigen) (Diptera: Calliphoridae), Bogota, Colombia strain. *Biological research*. 2010;43(2):197-203.

192. Choi H, Aldrich JV. Comparison of methods for the Fmoc solid-phase synthesis and cleavage of a peptide containing both tryptophan and arginine. *Int J Pept Protein Res*. 1993;42(1):58-63.

193. Riciluca KC, Sayegh RS, Melo RL, Silva PI, Jr. Rondonin an antifungal peptide from spider (*Acanthoscurria rondoniae*) haemolymph. *Results in immunology*. 2012;2:66-71.

194. Silva PI, Jr., Daffre S, Bulet P. Isolation and characterization of gomesin, an 18-residue cysteine-rich defense peptide from the spider *Acanthoscurria gomesiana* hemocytes with sequence similarities to horseshoe crab antimicrobial peptides of the tachyplesin family. *The Journal of biological chemistry*. 2000;275(43):33464-70.

195. Chambers MC, Maclean B, Burke R, Amodei D, Ruderman DL, Neumann S, et al. A cross-platform toolkit for mass spectrometry and proteomics. *Nat Biotechnol*. 2012;30(10):918-20.

196. Perkins DN, Pappin DJ, Creasy DM, Cottrell JS. Probability-based protein identification by searching sequence databases using mass spectrometry data. *Electrophoresis*. 1999;20(18):3551-67.

197. Altschul SF, Gish W, Miller W, Myers EW, Lipman DJ. Basic local alignment search tool. *J Mol Biol*. 1990;215(3):403-10.

198. Jarnuczak AF, Lee DC, Lawless C, Holman SW, Evers CE, Hubbard SJ. Analysis of Intrinsic Peptide Detectability via Integrated Label-Free and SRM-Based Absolute Quantitative Proteomics. *Journal of proteome research*. 2016;15(9):2945-59.

199. Evers CE, Lawless C, Wedge DC, Lau KW, Gaskell SJ, Hubbard SJ. CONSeQuence: prediction of reference peptides for absolute quantitative proteomics using consensus machine learning approaches. *Molecular & cellular proteomics : MCP*. 2011;10(11):M110.003384.

200. Fusaro VA, Mani DR, Mesirov JP, Carr SA. Prediction of high-responding peptides for targeted protein assays by mass spectrometry. *Nature biotechnology*. 2009;27(2):190-8.

201. Tang K, Smith RD. Physical/chemical separations in the break-up of highly charged droplets from electrosprays. *Journal of the American Society for Mass Spectrometry*. 2001;12(3):343-7.

202. Gucinski AC, Dodds ED, Li W, Wysocki VH. Understanding and exploiting Peptide fragment ion intensities using experimental and informatic approaches. *Methods in molecular biology (Clifton, NJ)*. 2010;604:73-94.

203. Ghosh S, Challamalla P, Banji D. Negative ion mode mass spectrometry- an overview 2012. 1462-71 p.

204. Raposio E, Bortolini S, Maistrello L, Grasso DA. Larval Therapy for Chronic Cutaneous Ulcers: Historical Review and Future Perspectives. *Wounds : a compendium of clinical research and practice*. 2017;29(12):367-73.

205. Bulet P, Hetru C, Dimarcq JL, Hoffmann D. Antimicrobial peptides in insects; structure and function. *Developmental and comparative immunology*. 1999;23(4-5):329-44.
206. Brown KL, Hancock RE. Cationic host defense (antimicrobial) peptides. *Current opinion in immunology*. 2006;18(1):24-30.
207. O'Meara S, Al-Kurdi D, Ologun Y, Ovington LG, Martyn-St James M, Richardson R. Antibiotics and antiseptics for venous leg ulcers. *The Cochrane database of systematic reviews*. 2014(1):Cd003557.
208. Various-authors. *A Catalogue of the Diptera of the Americas south of the United States*. Museu de Zoologia, Departamento de Zoologia, Universidade de São Paulo. São Paulo: Departamento de Zoologia, Secretaria da Agricultura do Estado de São Paulo; 1966.
209. Hou F, Li J, Pan P, Xu J, Liu L, Liu W, et al. Isolation and characterisation of a new antimicrobial peptide from the skin of *Xenopus laevis*. *Int J Antimicrob Agents*. 2011;38(6):510-5.
210. Merrifield RB. Solid Phase Peptide Synthesis. I. The Synthesis of a Tetrapeptide. *Journal of the American Chemical Society*. 1963;85(14):2149-54.
211. Houghten RA. General method for the rapid solid-phase synthesis of large numbers of peptides: specificity of antigen-antibody interaction at the level of individual amino acids. *Proc Natl Acad Sci U S A*. 1985;82(15):5131-5.
212. Jiang Z, Vasil AI, Vasil ML, Hodges RS. "Specificity Determinants" Improve Therapeutic Indices of Two Antimicrobial Peptides Piscidin 1 and Dermaseptin S4 Against the Gram-negative Pathogens *Acinetobacter baumannii* and *Pseudomonas aeruginosa*. *Pharmaceuticals*. 2014;7(4):366-91.
213. Bulet P. Strategies for the discovery, isolation, and characterization of natural bioactive peptides from the immune system of invertebrates. *Methods in molecular biology* (Clifton, NJ). 2008;494:9-29.
214. Wiegand I, Hilpert K, Hancock RE. Agar and broth dilution methods to determine the minimal inhibitory concentration (MIC) of antimicrobial substances. *Nature protocols*. 2008;3(2):163-75.
215. Hetru C, Bulet P. Strategies for the isolation and characterization of antimicrobial peptides of invertebrates. *Methods in molecular biology* (Clifton, NJ). 1997;78:35-49.
216. Lorenzini DM, da Silva PI, Jr., Fogaca AC, Bulet P, Daffre S. Acanthoscurrin: a novel glycine-rich antimicrobial peptide constitutively expressed in the hemocytes of the spider *Acanthoscurria gomesiana*. *Developmental and comparative immunology*. 2003;27(9):781-91.
217. Magi G, Marini E, Facinelli B. Antimicrobial activity of essential oils and carvacrol, and synergy of carvacrol and erythromycin, against clinical, erythromycin-resistant Group A *Streptococci*. *Frontiers in microbiology*. 2015;6:165.
218. Velema WA, van der Berg JP, Hansen MJ, Szymanski W, Driessen AJM, Feringa BL. Optical control of antibacterial activity. *Nature Chemistry*. 2013;5:924.
219. Sayegh RS, Batista IF, Melo RL, Riske KA, Daffre S, Montich G, et al. Longipin: An Amyloid Antimicrobial Peptide from the Harvestman *Acutisoma longipes* (Arachnida: Opiliones) with Preferential Affinity for Anionic Vesicles. *PloS one*. 2016;11(12).

- 
220. NCBI. 2019 [March 7th 2019]. Available from: <https://www.ncbi.nlm.nih.gov/protein/?term=>.
221. Altschul SF, Madden TL, Schaffer AA, Zhang J, Zhang Z, Miller W, et al. Gapped BLAST and PSI-BLAST: a new generation of protein database search programs. *Nucleic acids research*. 1997;25(17):3389-402.
222. Gouy M, Guindon S, Gascuel O. SeaView Version 4: A Multiplatform Graphical User Interface for Sequence Alignment and Phylogenetic Tree Building. *Molecular Biology and Evolution*. 2010;27(2):221-4.
223. Dwyer DJ, Belenky PA, Yang JH, MacDonald IC, Martell JD, Takahashi N, et al. Antibiotics induce redox-related physiological alterations as part of their lethality. *Proc Natl Acad Sci U S A*. 2014;111(20):E2100-E9.
224. Faisal M, Saquib Q, Alatar AA, Al-Khedhairi AA, Ahmed M, Ansari SM, et al. Cobalt oxide nanoparticles aggravate DNA damage and cell death in eggplant via mitochondrial swelling and NO signaling pathway. *Biological research*. 2016;49(1):20.
225. Nocker A, Caspers M, Esveld-Amanatidou A, van der Vossen J, Schuren F, Montijn R, et al. Multiparameter viability assay for stress profiling applied to the food pathogen *Listeria monocytogenes* F2365. *Applied and environmental microbiology*. 2011;77(18):6433-40.
226. Yang N, Liu X, Teng D, Li Z, Wang X, Mao R, et al. Antibacterial and detoxifying activity of NZ17074 analogues with multi-layers of selective antimicrobial actions against *Escherichia coli* and *Salmonella enteritidis*. *Scientific reports*. 2017;7(1):3392.
227. Carretero GPB, Saraiva GKV, Cauz ACG, Rodrigues MA, Kiyota S, Riske KA, et al. Synthesis, biophysical and functional studies of two BP100 analogues modified by a hydrophobic chain and a cyclic peptide. *Biochimica et biophysica acta*. 2018;1860(8):1502-16.
228. Teng D, Wang X, Xi D, Mao R, Zhang Y, Guan Q, et al. A dual mechanism involved in membrane and nucleic acid disruption of AvBD103b, a new avian defensin from the king penguin, against *Salmonella enteritidis* CVCC3377. *Applied microbiology and biotechnology*. 2014;98(19):8313-25.
229. Landry BS, Dextraze L, Boivin G. Random amplified polymorphic DNA markers for DNA fingerprinting and genetic variability assessment of minute parasitic wasp species (Hymenoptera: Mymaridae and Trichogrammatidae) used in biological control programs of phytophagous insects. *Genome*. 1993;36(3):580-7.
230. Chaparro E, da Silva PIJ. Lacrain: the first antimicrobial peptide from the body extract of the Brazilian centipede *Scolopendra viridicornis*. *Int J Antimicrob Agents*. 2016;48(3):277-85.
231. Nan YH, Bang J-K, Jacob B, Park I-S, Shin SY. Prokaryotic selectivity and LPS-neutralizing activity of short antimicrobial peptides designed from the human antimicrobial peptide LL-37. *Peptides*. 2012;35(2):239-47.
232. Chen X, Zhang L, Wu Y, Wang L, Ma C, Xi X, et al. Evaluation of the bioactivity of a mastoparan peptide from wasp venom and of its analogues designed through targeted engineering 2018. 599-607 p.
233. Torres MT, Pedron CN, da Silva Lima JA, da Silva PIJ, da Silva FD, Oliveira VXJ. Antimicrobial activity of leucine-substituted decoralin analogs with lower hemolytic activity.

Journal of peptide science : an official publication of the European Peptide Society. 2017;23(11):818-23.

234. Pettersen EF, Goddard TD, Huang CC, Couch GS, Greenblatt DM, Meng EC, et al. UCSF Chimera--a visualization system for exploratory research and analysis. *Journal of computational chemistry*. 2004;25(13):1605-12.

235. Bochicchio B, Tamburro AM. Polyproline II structure in proteins: identification by chiroptical spectroscopies, stability, and functions. *Chirality*. 2002;14(10):782-92.

236. Berova NP, P.; Nakanishi, K.; Woody, R. *Comprehensive Chiroptical Spectroscopy: Applications in Stereochemical Analysis of Synthetic Compounds, Natural Products, and Biomolecules* 2012.

237. Fazio MA, Jouvencal L, Vovelle F, Bulet P, Miranda MT, Daffre S, et al. Biological and structural characterization of new linear gomesin analogues with improved therapeutic indices. *Biopolymers*. 2007;88(3):386-400.

238. Cézard C, Silva-Pires V, Mullié C, Sonnet P. Antibacterial peptides: a review 2011. 926-37 p.

239. Giacometti A, Cirioni O, Barchiesi F, Fortuna M, Scalise G. In-vitro activity of cationic peptides alone and in combination with clinically used antimicrobial agents against *Pseudomonas aeruginosa*. *The Journal of antimicrobial chemotherapy*. 1999;44(5):641-5.

240. Chay Pak Ting BP, Mine Y, Juneja LR, Okubo T, Gauthier SF, Pouliot Y. Comparative composition and antioxidant activity of Peptide fractions obtained by ultrafiltration of egg yolk protein enzymatic hydrolysates. *Membranes*. 2011;1(3):149-61.

241. Sandeman RM, Feehan JP, Chandler RA, Bowles VM. Tryptic and chymotryptic proteases released by larvae of the blowfly, *Lucilia cuprina*. *Int J Parasitol*. 1990;20(8):1019-23.

242. Telford G, Brown AP, Kind A, English JS, Pritchard DI. Maggot chymotrypsin I from *Lucilia sericata* is resistant to endogenous wound protease inhibitors. *Br J Dermatol*. 2011;164(1):192-6.

243. Sze SH, Dunham JP, Carey B, Chang PL, Li F, Edman RM, et al. A de novo transcriptome assembly of *Lucilia sericata* (Diptera: Calliphoridae) with predicted alternative splices, single nucleotide polymorphisms and transcript expression estimates. *Insect molecular biology*. 2012;21(2):205-21.

244. Anstead CA, Korhonen PK, Young ND, Hall RS, Jex AR, Murali SC, et al. *Lucilia cuprina* genome unlocks parasitic fly biology to underpin future interventions. *Nature communications*. 2015;6:7344.

245. Franta Z, Vogel H, Lehmann R, Rupp O, Goesmann A, Vilcinskas A. Next Generation Sequencing Identifies Five Major Classes of Potentially Therapeutic Enzymes Secreted by *Lucilia sericata* Medical Maggots. *BioMed Research International*. 2016;2016:8285428.

246. Erdmann GR. Antibacterial action of Myiasis-causing flies. *Parasitology today*. 1987;3(7):214-6.

247. Thomas S, Andrews AM, Hay NP, Bourgoise S. The anti-microbial activity of maggot secretions: results of a preliminary study. *Journal of tissue viability*. 1999;9(4):127-32.

- 
248. Shaw KL, Grimsley GR, Yakovlev GI, Makarov AA, Pace CN. The effect of net charge on the solubility, activity, and stability of ribonuclease Sa. *Protein science : a publication of the Protein Society*. 2001;10(6):1206-15.
249. Phoenix DA, Dennison SR, Harris F. Anionic Antimicrobial Peptides. *Antimicrobial Peptides*. 2013;doi: 10.1002/9783527652853.ch3.
250. Diamond G, Beckloff N, Weinberg A, Kisich KO. The roles of antimicrobial peptides in innate host defense. *Current pharmaceutical design*. 2009;15(21):2377-92.
251. Wennerberg K, Der CJ. Rho-family GTPases: it's not only Rac and Rho (and I like it). *Journal of Cell Science*. 2004;117(8):1301.
252. Higuchi M, Masuyama N, Fukui Y, Suzuki A, Gotoh Y. Akt mediates Rac/Cdc42-regulated cell motility in growth factor-stimulated cells and in invasive PTEN knockout cells. *Current Biology*. 2001;11(24):1958-62.
253. Johnson DI. Cdc42: An essential Rho-type GTPase controlling eukaryotic cell polarity. *Microbiology and molecular biology reviews : MMBR*. 1999;63(1):54-105.
254. Khamis AM, Essack M, Gao X, Bajic VB. Distinct profiling of antimicrobial peptide families. *Bioinformatics*. 2015;31(6):849-56.
255. Nagao T, Mishima D, Javkhlantugs N, Wang J, Ishioka D, Yokota K, et al. Structure and orientation of antibiotic peptide alamethicin in phospholipid bilayers as revealed by chemical shift oscillation analysis of solid state nuclear magnetic resonance and molecular dynamics simulation. *Biochimica et biophysica acta*. 2015;1848(11 Pt A):2789-98.
256. Hyde AJ, Parisot J, McNichol A, Bonev BB. Nisin-induced changes in *Bacillus* morphology suggest a paradigm of antibiotic action. *Proc Natl Acad Sci U S A*. 2006;103(52):19896-901.
257. Oren Z, Shai Y. Mode of action of linear amphipathic  $\alpha$ -helical antimicrobial peptides. *Peptide Science*. 1998;47(6):451-63.
258. Shi W, Li C, Li M, Zong X, Han D, Chen Y. Antimicrobial peptide melittin against *Xanthomonas oryzae* pv. *oryzae*, the bacterial leaf blight pathogen in rice. *Applied microbiology and biotechnology*. 2016;100(11):5059-67.
259. Polakovicova S, Polak S, Kuniakova M, Cambal M, Caplovicova M, Kozanek M, et al. The effect of salivary gland extract of *Lucilia sericata* maggots on human dermal fibroblast proliferation within collagen/hyaluronan membrane in vitro: transmission electron microscopy study. *Advances in skin & wound care*. 2015;28(5):221-6.
260. Titulaer MK. Candidate biomarker discovery for angiogenesis by automatic integration of Orbitrap MS1 spectral- and X!Tandem MS2 sequencing information. *Genomics, proteomics & bioinformatics*. 2013;11(3):182-94.
261. Van Aelst L, Symons M. Role of Rho family GTPases in epithelial morphogenesis. *Genes & development*. 2002;16(9):1032-54.
262. Lee K, Boyd KL, Parekh DV, Kehl-Fie TE, Baldwin HS, Brakebusch C, et al. Cdc42 promotes host defenses against fatal infection. *Infection and immunity*. 2013;81(8):2714-23.
263. Ratcliffe N, Azambuja P, Mello CB. Recent advances in developing insect natural products as potential modern day medicines. *Evidence-based complementary and alternative medicine : eCAM*. 2014;2014:904958.

264. Ryan MA, Akinbi HT, Serrano AG, Perez-Gil J, Wu H, McCormack FX, et al. Antimicrobial activity of native and synthetic surfactant protein B peptides. *Journal of immunology (Baltimore, Md : 1950)*. 2006;176(1):416-25.
265. Tavares LS, Rettore JV, Freitas RM, Porto WF, Duque AP, Singulani Jde L, et al. Antimicrobial activity of recombinant Pg-AMP1, a glycine-rich peptide from guava seeds. *Peptides*. 2012;37(2):294-300.
266. Gaussier H, Morency H, Lavoie MC, Subirade M. Replacement of trifluoroacetic acid with HCl in the hydrophobic purification steps of pediocin PA-1: a structural effect. *Applied and environmental microbiology*. 2002;68(10):4803-8.
267. Sikora K, Jaskiewicz M, Neubauer D, Bauer M, Bartoszewska S, Baranska-Rybak W, et al. Counter-ion effect on antistaphylococcal activity and cytotoxicity of selected antimicrobial peptides. *Amino Acids*. 2018;50(5):609-19.
268. Bai L, Sheeley S, Sweedler J. Analysis of Endogenous C-Amino Acid-Containing Peptides in Metazoa2009. 7-24 p.
269. Griffiths J. Hunting the elusive D-amino acid. *Analytical Chemistry*. 2008;80(9):3070-.
270. Vega Chaparro SC, Valencia Salguero JT, Martinez Baquero DA, Rosas Perez JE. Effect of Polyvalence on the Antibacterial Activity of a Synthetic Peptide Derived from Bovine Lactoferricin against Healthcare-Associated Infectious Pathogens. *Biomed Res Int*. 2018;2018:5252891.
271. Xin P, Sun Y, Kong H, Wang Y, Tan S, Guo J, et al. A unimolecular channel formed by dual helical peptide modified pillar[5]arene: correlating transmembrane transport properties with antimicrobial activity and haemolytic toxicity. *Chemical communications (Cambridge, England)*. 2017;53(83):11492-5.
272. Yeung AT, Gellatly SL, Hancock RE. Multifunctional cationic host defence peptides and their clinical applications. *Cellular and molecular life sciences : CMLS*. 2011;68(13):2161-76.
273. Jiang Z, Vasil AI, Vasil ML, Hodges RS. "Specificity Determinants" Improve Therapeutic Indices of Two Antimicrobial Peptides Piscidin 1 and Dermaseptin S4 Against the Gram-negative Pathogens *Acinetobacter baumannii* and *Pseudomonas aeruginosa*. *Pharmaceuticals (Basel, Switzerland)*. 2014;7(4):366-91.
274. Saravanan R, Bhunia A, Bhattacharjya S. Micelle-bound structures and dynamics of the hinge deleted analog of melittin and its diastereomer: implications in cell selective lysis by D-amino acid containing antimicrobial peptides. *Biochimica et biophysica acta*. 2010;1798(2):128-39.
275. Oren Z, Hong J, Shai Y. A repertoire of novel antibacterial diastereomeric peptides with selective cytolytic activity. *The Journal of biological chemistry*. 1997;272(23):14643-9.
276. Wang G. Determination of solution structure and lipid micelle location of an engineered membrane peptide by using one NMR experiment and one sample. *Biochimica et biophysica acta*. 2007;1768(12):3271-81.
277. Molchanova N, Hansen PR, Franzyk H. Advances in Development of Antimicrobial Peptidomimetics as Potential Drugs. *Molecules (Basel, Switzerland)*. 2017;22(9).

278. Di Grazia A, Cappiello F, Cohen H, Casciaro B, Luca V, Pini A, et al. D-Amino acids incorporation in the frog skin-derived peptide esculentin-1a(1-21)NH<sub>2</sub> is beneficial for its multiple functions. *Amino Acids*. 2015;47(12):2505-19.
279. Yoshida M, Hinkley T, Tsuda S, Abul-Haija YM, McBurney RT, Kulikov V, et al. Using Evolutionary Algorithms and Machine Learning to Explore Sequence Space for the Discovery of Antimicrobial Peptides. *Chem*. 2018;4(3):533-43.
280. Giuliani A, Pirri G, Nicoletto SF. Antimicrobial peptides: an overview of a promising class of therapeutics. *Central European Journal of Biology*. 2007;2(1):1-33.
281. Kasetty G, Papareddy P, Kalle M, Rydengard V, Morgelin M, Albiger B, et al. Structure-activity studies and therapeutic potential of host defense peptides of human thrombin. *Antimicrobial agents and chemotherapy*. 2011;55(6):2880-90.
282. Oliva R, Chino M, Pane K, Pistorio V, De Santis A, Pizzo E, et al. Exploring the role of unnatural amino acids in antimicrobial peptides. *Scientific reports*. 2018;8(1):8888.
283. Manabe T, Kawasaki K. D-form KLKLLLLLKLK-NH<sub>2</sub> peptide exerts higher antimicrobial properties than its L-form counterpart via an association with bacterial cell wall components. *Scientific reports*. 2017;7:43384.
284. Huang J, Hao D, Chen Y, Xu Y, Tan J, Huang Y, et al. Inhibitory effects and mechanisms of physiological conditions on the activity of enantiomeric forms of an alpha-helical antibacterial peptide against bacteria. *Peptides*. 2011;32(7):1488-95.
285. Porto W, Silva O, Franco O. Prediction and rational design of antimicrobial peptides, in *Protein Structure2019*.
286. Torres M, Pedron C, de Araujo I, da Silva Junior P, D. Silva F, Junior V. Decoralin Analogs with Increased Resistance to Degradation and Lower Hemolytic Activity2017. 18-23 p.
287. Lata S, Sharma BK, Raghava GPS. Analysis and prediction of antibacterial peptides. *BMC bioinformatics*. 2007;8:263-.
288. Sitaram N, Nagaraj R. Host-defense antimicrobial peptides: importance of structure for activity. *Current pharmaceutical design*. 2002;8(9):727-42.
289. Matsuzaki K, Nakamura A, Murase O, Sugishita K, Fujii N, Miyajima K. Modulation of magainin 2-lipid bilayer interactions by peptide charge. *Biochemistry*. 1997;36(8):2104-11.
290. Torrent M, Nogues VM, Boix E. A theoretical approach to spot active regions in antimicrobial proteins. *BMC bioinformatics*. 2009;10:373.
291. Pinilla Beltran YT, Segura NA, Bello FJ. Synanthropy of Calliphoridae and Sarcophagidae (Diptera) in Bogota, Colombia. *Neotropical entomology*. 2012;41(3):237-42.
292. Gongora J, Diaz-Roa A, Ramirez-Hernandez A, Cortes-Vecino JA, Gaona MA, Patarroyo MA, et al. Evaluating the effect of *Sarconesiopsis magellanica* (Diptera: Calliphoridae) larvae-derived haemolymph and fat body extracts on chronic wounds in diabetic rabbits. *J Diabetes Res*. 2015;2015:270253.
293. Diaz-Roa A, Gaona MA, Segura NA, Ramirez-Hernandez A, Cortes-Vecino JA, Patarroyo MA, et al. Evaluating *Sarconesiopsis magellanica* blowfly-derived larval therapy and comparing it to *Lucilia sericata*-derived therapy in an animal model. *Acta Trop*. 2016;154:34-41.

294. Laverde-Paz MJ, Echeverry MC, Patarroyo MA, Bello FJ. Evaluating the anti-leishmania activity of *Lucilia sericata* and *Sarconesiopsis magellanica* blowfly larval excretions/secretions in an in vitro model. *Acta tropica*. 2018;177:44-50.
295. Diaz-Roa A, Patarroyo MA, Bello FJ, Da Silva PI, Jr. Sarconesin: *Sarconesiopsis magellanica* Blowfly Larval Excretions and Secretions With Antibacterial Properties. *Front Microbiol*. 2018;9:2249.
296. CLSI. Methods for Dilution Antimicrobial Susceptibility Tests for Bacteria that Grow Aerobically, Approved Standard, 9th ed., CLSI document M07-A9. Clinical and Laboratory Standards Institute, 950 West Valley Road, Suite 2500, Wayne, Pennsylvania 19087, USA. 2012.
297. Hetru C, Bulet P. Strategies for the isolation and characterization of antimicrobial peptides of invertebrates. *Methods in molecular biology*. 1997;78:35-49.
298. Umerska A, Strandh M, Cassisa V, Matougui N, Eveillard M, Saulnier P. Synergistic Effect of Combinations Containing EDTA and the Antimicrobial Peptide AA230, an Arenicin-3 Derivative, on Gram-Negative Bacteria. *Biomolecules*. 2018;8(4).
299. Bulet P. Strategies for the discovery, isolation, and characterization of natural bioactive peptides from the immune system of invertebrates. *Methods in molecular biology*. 2008;494:9-29.
300. Moghaddam MM, Barjini KA, Ramandi MF, Amani J. Investigation of the antibacterial activity of a short cationic peptide against multidrug-resistant *Klebsiella pneumoniae* and *Salmonella typhimurium* strains and its cytotoxicity on eukaryotic cells. *World journal of microbiology & biotechnology*. 2014;30(5):1533-40.
301. Segura-Ramírez PJ, Silva Júnior PI. *Loxosceles gaucho* Spider Venom: An Untapped Source of Antimicrobial Agents. *Toxins*. 2018;10(12):522.
302. Uniprot. 2019 [March 7th 2019]. Available from: [www.uniprot.org](http://www.uniprot.org).
303. Blast. 2019 [March 7th 2019]. Available from: <https://blast.ncbi.nlm.nih.gov/Blast.cgi>.
304. Altschul SF, Madden TL, Schaffer AA, Zhang J, Zhang Z, Miller W, et al. Gapped BLAST and PSI-BLAST: a new generation of protein database search programs. *Nucleic Acids Res*. 1997;25(17):3389-402.
305. Antimicrobial-peptide-database. 2019 [April 7th 2019]. Available from: [http://aps.unmc.edu/AP/prediction/prediction\\_main.php](http://aps.unmc.edu/AP/prediction/prediction_main.php).
306. Expasy. [March 7th 2019]. Available from: <http://web.expasy.org/protparam/>.
307. i-Tasser. 2019 [March 7th 2019]. Available from: <http://zhanglab.ccmb.med.umich.edu/I-TASSER/>.
308. Yang J, Yan R, Roy A, Xu D, Poisson J, Zhang Y. The I-TASSER Suite: protein structure and function prediction. *Nat Methods*. 2015;12(1):7-8.
309. Lopes Alves F, Oliva M, Miranda A. Conformational and biological properties of *Bauhinia bauhinioides* kallikrein inhibitor fragments with bradykinin-like activities 2015.
310. Carretero GPB, Saraiva GKV, Cauz ACG, Rodrigues MA, Kiyota S, Riske KA, et al. Synthesis, biophysical and functional studies of two BP100 analogues modified by a

- hydrophobic chain and a cyclic peptide. *Biochim Biophys Acta Biomembr.* 2018;1860(8):1502-16.
311. Li L, Song X, Yin Z, Jia R, Li Z, Zhou X, et al. The antibacterial activity and action mechanism of emodin from *Polygonum cuspidatum* against *Haemophilus parasuis* in vitro. *Microbiological research.* 2016;186-187:139-45.
312. Zou L, Lu J, Wang J, Ren X, Zhang L, Gao Y, et al. Synergistic antibacterial effect of silver and ebselen against multidrug-resistant Gram-negative bacterial infections. *EMBO molecular medicine.* 2017;9(8):1165-78.
313. Yamamoto D, Hernandez RT, Liberatore AM, Abe CM, Souza RB, Romao FT, et al. *Escherichia albertii*, a novel human enteropathogen, colonizes rat enterocytes and translocates to extra-intestinal sites. *PloS one.* 2017;12(2):e0171385.
314. Anstead CA, Korhonen PK, Young ND, Hall RS, Jex AR, Murali SC, et al. *Lucilia cuprina* genome unlocks parasitic fly biology to underpin future interventions. *Nat Commun.* 2015;6:7344.
315. Wang H, Yu Z, Hu Y, Li F, Liu L, Zheng H, et al. Novel antimicrobial peptides isolated from the skin secretions of Hainan odorous frog, *Odorrana hainanensis*. *Peptides.* 2012;35(2):285-90.
316. Lemaire S, Trinh TT, Le HT, Tang SC, Hincke M, Wellman-Labadie O, et al. Antimicrobial effects of H4-(86-100), histogranin and related compounds--possible involvement of DNA gyrase. *The FEBS journal.* 2008;275(21):5286-97.
317. LI Shang-Wei ZB-S, DU Juan. Isolation, purification, and detection of the antimicrobial activity of the antimicrobial peptide CcAMP1 from *Coridius chinensis* (Hemiptera: Dinidoridae). *Acta Entomologica Sinica.* 2015;58(6):610-6.
318. Lv X, Lin Y, Jie Y, Sun M, Bolin Z, Bai F, et al. Purification, characterization, and action mechanism of plantaricin DL3, a novel bacteriocin against *Pseudomonas aeruginosa* produced by *Lactobacillus plantarum* DL3 from Chinese Suan-Tsai 2017.
319. Ramirez-Carretero S, Quintero-Hernandez V, Jimenez-Vargas JM, Corzo G, Possani LD, Becerril B, et al. Gene cloning and functional characterization of four novel antimicrobial-like peptides from scorpions of the family Vaejovidae. *Peptides.* 2012;34(2):290-5.
320. Webb RL. *Circular Dichroism and the Conformational Analysis of Biomolecules* Edited by Gerald D. Fasman. Plenum Press, New York and London. 1996. ix + 738 pp. 17 × 25.5 cm. ISBN 0-306-45152-5. \$125.00. *Journal of Medicinal Chemistry.* 1996;39(26):5285-6.
321. Heliquet. 2019 [March 7th 2019]. Available from: <http://heliquet.ipmc.cnrs.fr>.
322. Papareddy P, Kasetty G, Kalle M, Bhongir RK, Morgelin M, Schmidtchen A, et al. NLF20: an antimicrobial peptide with therapeutic potential against invasive *Pseudomonas aeruginosa* infection. *The Journal of antimicrobial chemotherapy.* 2016;71(1):170-80.
323. Yu G, Baeder DY, Regoes RR, Rolff J. Predicting drug resistance evolution: insights from antimicrobial peptides and antibiotics. *Proceedings Biological sciences.* 2018;285(1874).
324. Nagarajan D, Nagarajan T, Roy N, Kulkarni O, Ravichandran S, Mishra M, et al. Computational antimicrobial peptide design and evaluation against multidrug-resistant clinical isolates of bacteria. *The Journal of biological chemistry.* 2018;293(10):3492-509.

- 
325. Aeschlimann JR. The role of multidrug efflux pumps in the antibiotic resistance of *Pseudomonas aeruginosa* and other gram-negative bacteria. Insights from the Society of Infectious Diseases Pharmacists. *Pharmacotherapy*. 2003;23(7):916-24.
326. Rodriguez-Rojas A, Moreno-Morales J, Mason AJ, Rolff J. Cationic antimicrobial peptides do not change recombination frequency in *Escherichia coli*. *Biology letters*. 2018;14(3).
327. Duvick JP, Rood T, Rao AG, Marshak DR. Purification and characterization of a novel antimicrobial peptide from maize (*Zea mays* L.) kernels. *J Biol Chem*. 1992;267(26):18814-20.
328. Sousa DA, Porto WF, Silva MZ, da Silva TR, Franco OL. Influence of Cysteine and Tryptophan Substitution on DNA-Binding Activity on Maize alpha-Hairpinin Antimicrobial Peptide. *Molecules (Basel, Switzerland)*. 2016;21(8).
329. Yan J, Wang K, Dang W, Chen R, Xie J, Zhang B, et al. Two hits are better than one: membrane-active and DNA binding-related double-action mechanism of NK-18, a novel antimicrobial peptide derived from mammalian NK-lysin. *Antimicrobial agents and chemotherapy*. 2013;57(1):220-8.
330. Hancock RE, Speert DP. Antibiotic resistance in *Pseudomonas aeruginosa*: mechanisms and impact on treatment. *Drug Resist Updat*. 2000;3(4):247-55.
331. Dosler S, Karaaslan E. Inhibition and destruction of *Pseudomonas aeruginosa* biofilms by antibiotics and antimicrobial peptides. *Peptides*. 2014;62:32-7.
332. Zhu X, Ma Z, Wang J, Chou S, Shan A. Importance of Tryptophan in Transforming an Amphipathic Peptide into a *Pseudomonas aeruginosa*-Targeted Antimicrobial Peptide. *PloS one*. 2014;9(12):e114605.
333. Giacometti A, Cirioni O, Barchiesi F, Fortuna M, Scalise G. In-vitro activity of cationic peptides alone and in combination with clinically used antimicrobial agents against *Pseudomonas aeruginosa*. *J Antimicrob Chemother*. 1999;44(5):641-5.
334. Hirt H, Gorr SU. Antimicrobial peptide GL13K is effective in reducing biofilms of *Pseudomonas aeruginosa*. *Antimicrobial agents and chemotherapy*. 2013;57(10):4903-10.
335. Wnorowska U, Niemirowicz K, Myint M, Diamond SL, Wróblewska M, Savage PB, et al. Bactericidal activities of cathelicidin LL-37 and select cationic lipids against the hypervirulent *Pseudomonas aeruginosa* strain LESB58. *Antimicrobial agents and chemotherapy*. 2015;59(7):3808-15.
336. Lin P, Li Y, Dong K, Li Q. The Antibacterial Effects of an Antimicrobial Peptide Human beta-Defensin 3 Fused with Carbohydrate-Binding Domain on *Pseudomonas aeruginosa* PA14. *Current microbiology*. 2015;71(2):170-6.
337. Mallapragada S, Wadhwa A, Agrawal P. Antimicrobial peptides: The miraculous biological molecules. *Journal of Indian Society of Periodontology*. 2017;21(6):434-8.
338. Nijnik A, Hancock R. Host defence peptides: antimicrobial and immunomodulatory activity and potential applications for tackling antibiotic-resistant infections. *Emerging health threats journal*. 2009;2:e1.
339. Chernysh S, Kim SI, Bekker G, Pleskach VA, Filatova NA, Anikin VB, et al. Antiviral and antitumor peptides from insects. *Proc Natl Acad Sci U S A*. 2002;99(20):12628-32.

- 
340. Oh D, Sun J, Nasrolahi Shirazi A, LaPlante KL, Rowley DC, Parang K. Antibacterial activities of amphiphilic cyclic cell-penetrating peptides against multidrug-resistant pathogens. *Molecular pharmaceutics*. 2014;11(10):3528-36.
341. Richter MF, Hergenrother PJ. The challenge of converting Gram-positive-only compounds into broad-spectrum antibiotics. *Annals of the New York Academy of Sciences*. 2019;1435(1):18-38.
342. Pooi Yin C, Khanum R. Antimicrobial peptides as potential anti-biofilm agents against multi-drug resistant bacteria2017.
343. Hirt H, Gorr S-U. Antimicrobial Peptide GL13K Is Effective in Reducing Biofilms of *Pseudomonas aeruginosa*2013.
344. Henriksen JR, Etzerodt T, Gjetting T, Andresen TL. Side chain hydrophobicity modulates therapeutic activity and membrane selectivity of antimicrobial peptide mastoparan-X. *PloS one*. 2014;9(3):e91007.
345. Almaaytah A, Mohammed GK, Abualhajjaa A, Al-Balas Q. Development of novel ultrashort antimicrobial peptide nanoparticles with potent antimicrobial and antibiofilm activities against multidrug-resistant bacteria. *Drug Des Devel Ther*. 2017;11:3159-70.
346. Cardoso MH, Ribeiro SM, Nolasco DO, de la Fuente-Nunez C, Felicio MR, Goncalves S, et al. A polyalanine peptide derived from polar fish with anti-infectious activities. *Sci Rep*. 2016;6:21385.
347. Rudilla H, merlos A, Sans E, Fusté E, Sierra J, Zalacain A, et al. New and old tools to evaluate new antimicrobial peptides2018. 522 p.
348. Misra R, Sahoo SK. Antibacterial activity of doxycycline-loaded nanoparticles. *Methods in enzymology*. 2012;509:61-85.
349. Barnes KM, Gennard DE, Dixon RA. An assessment of the antibacterial activity in larval excretion/secretion of four species of insects recorded in association with corpses, using *Lucilia sericata* Meigen as the marker species. *Bull Entomol Res*. 2010;100(6):635-40.
350. Li Z, Mao R, Teng D, Hao Y, Chen H, Wang X, et al. Antibacterial and immunomodulatory activities of insect defensins-DLP2 and DLP4 against multidrug-resistant *Staphylococcus aureus*. *Scientific reports*. 2017;7(1):12124.
351. Hu F, Wu Q, Song S, She R, Zhao Y, Yang Y, et al. Antimicrobial activity and safety evaluation of peptides isolated from the hemoglobin of chickens. *BMC microbiology*. 2016;16(1):287.
352. He J, Luo X, Jin D, Wang Y, Zhang T. Identification, Recombinant Expression, and Characterization of LHG2, a Novel Antimicrobial Peptide of *Lactobacillus casei* HZ1. *Molecules (Basel, Switzerland)*. 2018;23(9).
353. Liang S-S, Wang T-N, Tsai E-M. Analysis of Protein-Protein Interactions in MCF-7 and MDA-MB-231 Cell Lines Using Phthalic Acid Chemical Probes2014. 20770-88 p.
354. Yuan X, Zhu M, Tian G, Zhao Y, Zhao L, Ng TB, et al. Biochemical characteristics of a novel protease from the basidiomycete *Amanita virgineoides*. *Biotechnology and applied biochemistry*. 2017;64(4):532-40.
355. Hoffmann JA. The immune response of *Drosophila*. *Nature*. 2003;426(6962):33-8.

356. Pedron CN, Andrade GP, Sato RH, Torres MT, Cerchiaro G, Ribeiro AO, et al. Anticancer activity of VmCT1 analogs against MCF-7 cells. *Chemical biology & drug design*. 2018;91(2):588-96.
357. Ramírez-Carretero S, Quintero-Hernandez V, María Jiménez-Vargas J, Corzo G, Possani L, Becerril B, et al. Gene cloning and functional characterization of four novel antimicrobial-like peptides from scorpions of the family Vaejovidae 2012. 290-5 p.
358. Formaggio F, Toniolo C. Electronic and vibrational signatures of peptide helical structures: A tribute to Anton Mario Tamburro. *Chirality*. 2010;22 Suppl 1:E30-9.
359. Juba M, Porter D, Dean S, Gillmor S, Bishop B. Characterization and Performance of Short Cationic Antimicrobial Peptide Isomers 2013.
360. Da F, Joo H-S, Cheung G, E. Villaruz A, Rohde H, Luo X-X, et al. Phenol-Soluble Modulin Toxins of *Staphylococcus haemolyticus* 2017.
361. Fernández-Vidal M, Jayasinghe S, Ladokhin AS, White SH. Folding amphipathic helices into membranes: amphiphilicity trumps hydrophobicity. *Journal of molecular biology*. 2007;370(3):459-70.
362. Giangaspero A, Sandri L, Tossi A. Amphipathic alpha helical antimicrobial peptides. *Eur J Biochem*. 2001;268(21):5589-600.
363. Tossi A, Sandri L, Giangaspero A. Amphipathic, alpha-helical antimicrobial peptides. *Biopolymers*. 2000;55(1):4-30.
364. Iwai H, Nakajima Y, Natori S, Arata Y, Shimada I. Solution conformation of an antibacterial peptide, sarcotoxin IA, as determined by <sup>1</sup>H-NMR. *European journal of biochemistry*. 1993;217(2):639-44.
365. Buhroo Z, Ma Kashmir I, Bhat, Na Kashmir I, Ganai, And Kashmir J, et al. Antimicrobial peptides from insects with special reference to silkworm *Bombyx mori* L: A review 2018.
366. Memarpoor-Yazdi M, Zardini H, Asoodeh A. A Novel Antimicrobial Peptide Derived from the Insect *Paederus dermatitis* 2012.
367. J. Betts M, Russell R. Amino-Acid Properties and Consequences of Substitutions. *Bioinformatics for Geneticists: A Bioinformatics Primer for the Analysis of Genetic Data: Second Edition* 2007. p. 311-42.
368. Kristian Erlin Nygaard M, Schou Andersen A, Kristensen H-H, Krogfelt KA, Fojan P, Wimmer R. The insect defensin lucifensin from *Lucilia sericata* 2012. 277-82 p.
369. Kainz K, Tadic J, Zimmermann A, Pendl T, Carmona-Gutierrez D, Ruckenstein C, et al. Methods to Assess Autophagy and Chronological Aging in Yeast. *Methods in enzymology*. 2017;588:367-94.
370. Diaz-Achirica P, Prieto S, Ubach J, Andreu D, Rial E, Rivas L. Permeabilization of the mitochondrial inner membrane by short cecropin-A-melittin hybrid peptides. *Eur J Biochem*. 1994;224(1):257-63.
371. Chen HM, Chan SC, Lee JC, Chang CC, Murugan M, Jack RW. Transmission electron microscopic observations of membrane effects of antibiotic cecropin B on *Escherichia coli*. *Microsc Res Tech*. 2003;62(5):423-30.

- 
372. Bahar AA, Ren D. Antimicrobial peptides. *Pharmaceuticals (Basel)*. 2013;6(12):1543-75.
373. Hamley IW. *Small Bioactive Peptides for Biomaterials Design and Therapeutics*. *Chem Rev*. 2017;117(24):14015-41.
374. Malanovic N, Lohner K. *Antimicrobial Peptides Targeting Gram-Positive Bacteria*. *Pharmaceuticals (Basel, Switzerland)*. 2016;9(3):59.
375. Kohanski MA, Dwyer DJ, Hayete B, Lawrence CA, Collins JJ. A common mechanism of cellular death induced by bactericidal antibiotics. *Cell*. 2007;130(5):797-810.
376. Hwang D, Lim Y-H. Resveratrol antibacterial activity against *Escherichia coli* is mediated by Z-ring formation inhibition via suppression of FtsZ expression. *Scientific reports*. 2015;5:10029.
377. Kumar A, Pandey AK, Singh SS, Shanker R, Dhawan A. Engineered ZnO and TiO<sub>2</sub> nanoparticles induce oxidative stress and DNA damage leading to reduced viability of *Escherichia coli*. *Free radical biology & medicine*. 2011;51(10):1872-81.
378. Viridi AS, Singh N. *Antimicrobial Peptides and Polyphenols: Implications in Food Safety and Preservation*. In: Juneja VK, Dwivedi HP, Sofos JN, editors. *Microbial Control and Food Preservation: Theory and Practice*. New York, NY: Springer New York; 2017. p. 117-52.
379. Hsu C-H, Chen C, Jou M-L, Lee AY-L, Lin Y-C, Yu Y-P, et al. Structural and DNA-binding studies on the bovine antimicrobial peptide, indolicidin: Evidence for multiple conformations involved in binding to membranes and DNA. *PLoS Pathogens*. 2005;1(12):4053-64 p.
380. Hale JD, Hancock RE. Alternative mechanisms of action of cationic antimicrobial peptides on bacteria. *Expert Rev Anti Infect Ther*. 2007;5(6):951-9.
381. Shai Y. Mode of action of membrane active antimicrobial peptides. *Biopolymers*. 2002;66(4):236-48.
382. El-Hajj ZW, Newman EB. How much territory can a single *E. coli* cell control? *Frontiers in microbiology*. 2015;6:309-.
383. Poole K. Bacterial stress responses as determinants of antimicrobial resistance. *The Journal of antimicrobial chemotherapy*. 2012;67(9):2069-89.
384. Shapiro RS. Antimicrobial-induced DNA damage and genomic instability in microbial pathogens. *PLoS pathogens*. 2015;11(3):e1004678-e.
385. Walters R, Piddock L, Wise R. The effect of mutations in the SOS response on the kinetics of quinolone killing. *Antonie van Leeuwenhoek*. 1990;58(6):863-73 p.
386. Kawarai T, Wachi M, Ogino H, Furukawa S, Suzuki K, Ogihara H, et al. SulA-independent filamentation of *Escherichia coli* during growth after release from high hydrostatic pressure treatment. *Applied microbiology and biotechnology*. 2004;64(2):255-62.
387. Hill TM, Sharma B, Valjavec-Gratian M, Smith J. *sfi*-independent filamentation in *Escherichia coli* is *lexA* dependent and requires DNA damage for induction. *J Bacteriol*. 1997;179(6):1931-9.
388. Lutkenhaus J. Regulation of cell division in *E. coli*. *Trends in genetics : TIG*. 1990;6(1):22-5.
389. Gutschmann T. Interaction between antimicrobial peptides and mycobacteria. *Biochim Biophys Acta*. 2016;1858(5):1034-43.



## 6. Additional files

### 6.1. Publications

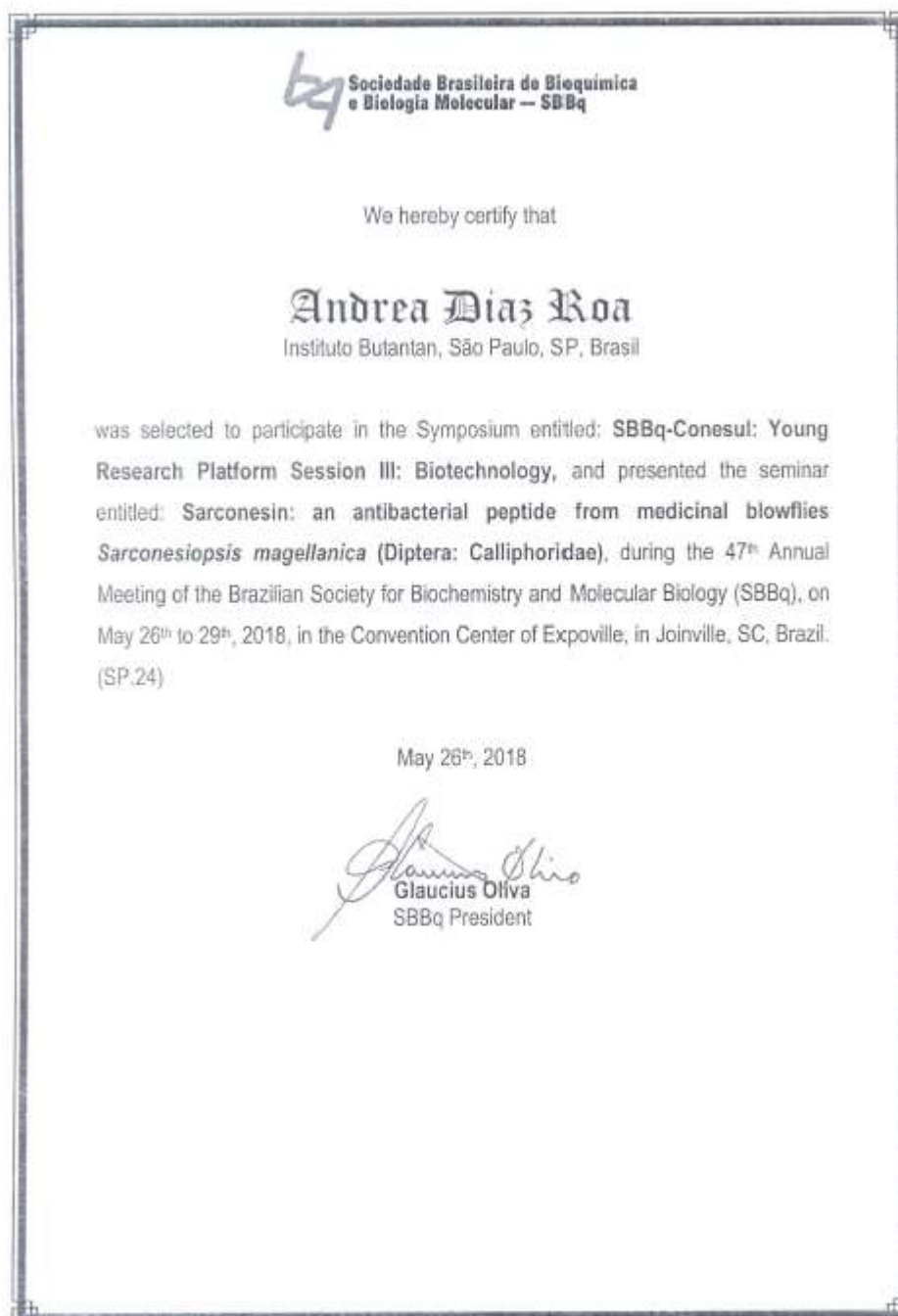
1. Sarconesin: *Sarconesiopsis magellanica* (Diptera: Calliphoridae) blowfly larval excretions and secretions with antibacterial properties. Díaz-Roa A, Patarroyo MA, Bello FJ, Da Silva PI Jr. *Front Microbiol.* 2018 Sep 28;9:2249. doi: 10.3389/fmicb.2018.02249. eCollection 2018. PMID: 30323791 Free PMC Article <https://www.ncbi.nlm.nih.gov/pubmed/30323791>
2. Sarconesin II, a New Antimicrobial Peptide Isolated from *Sarconesiopsis magellanica* Excretions and Secretions. Andrea Díaz-Roa, Abraham Espinoza-Culupú, Orlando Torres-García, Monamaris M. Borges, Ivan N. Avino, Flávio L. Alves, Antonio Miranda, Manuel A. Patarroyo, Pedro I. da Silva Jr., Felio J. Bello. *Molecules.* 2019 May 31;24(11). pii: E2077. doi: 10.3390/molecules24112077.

## 6.2. Awards

National Entomology award "HERNÁN ALCARAZ VIECO" 2018: Sarconesin: *Sarconesiopsis magellanica* (Diptera: Calliphoridae) blowfly larval excretions and secretions with antibacterial properties. Authors: Andrea Díaz-Roa, Manuel A. Patarroyo, Felio J. Bello and Pedro L da, Silva Junior.



Jovem Cientista SBBq-Conesul award. 47a Reunião Anual da SBBq, Joinville, Santa Catarina, 26 - 29 May 2018.



Jovem Cientista third place award Ph.D category. 47a Reunião Científica Anual do Instituto Butantan, São Paulo, Brazil, 5 – 7 december 2018.



## 6.3. Oral presentations



Certificamos que:

**Díaz-Roa A, Patarroyo MA, Bello da Silva Junior PI,**

apresentou o trabalho "How can a disgusting fly save your life" na 20ª Reunião Científica Anual do Instituto Butantan, **100 anos da Gripe Espanhola - Imagine o Mundo sem Vacinas**, realizada em São Paulo, Brasil de 5 a 7 de dezembro de 2018.

/



SIXTY-SIXTH  
ANNUAL MEETING  
November 5-9, 2017  
The Baltimore Convention Center | Baltimore, Maryland USA

## Certificate of Presentation

This certificate recognizes that:

**Andrea Diaz Roa**

Presented:

Sarconesin: a new antibacterial peptide from blowfly *Sarconesiopsis magellanica* (Diptera: Calliphoridae) larval excretions & secretions

**American Society of Tropical Medicine and Hygiene**

66<sup>th</sup> Annual Meeting  
November 5 – 9, 2017  
Baltimore Convention Center  
Baltimore, Maryland USA

*Patricia F. Walker, MD, DTM&H*

ASTMH President

*David Church*

ASTMH Scientific Program Chair

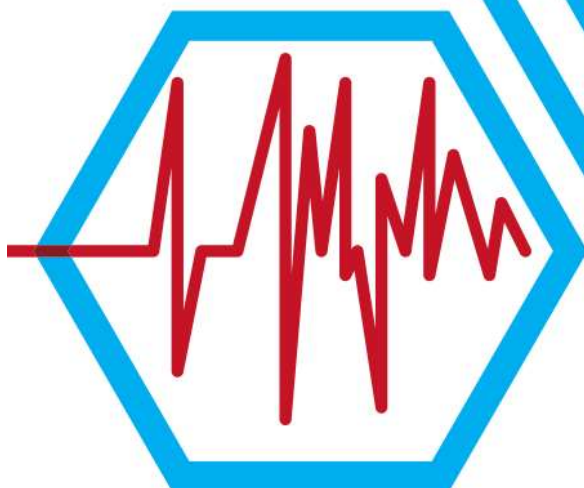
*Karen A. Jaramila*

ASTMH Executive Director



Instituto Butantan,  
ciência e saúde

19<sup>a</sup> rca **ib** reunião científica  
anual 2017



Certificamos que

**Diaz\_Roa A, Diaz\_Roa  
A, Patarroyo MA, Bello  
FJ, da Silva Junior PI**

apresentou o trabalho  
"Antibacterial properties of a  
peptide isolate from fly larvae  
*Sarconesiopsis magellanica*  
(Diptera: Calliphoridae)"  
na 19<sup>a</sup> Reunião Científica  
Anual do Instituto Butantan  
realizada em São Paulo, Brasil,  
de 29/11 a 1/12 de 2017.



Renato Mancini Astray  
Presidente da 19<sup>a</sup> Reunião Científica  
Anual do Instituto Butantan



Ana Maria Moura  
Diretora da Divisão de  
Desenvolvimento Científico



**Asociación Colombiana de Ciencias Biológicas**

PERSONERÍA JURÍDICA 05547 - Diciembre 16 de 1974  
N.º. 805.014.676-1

1965-2016 "51 años promoviendo el Desarrollo, Investigación,  
Enseñanza y Divulgación de las Ciencias Biológicas"



Armenia, 21 de octubre de 2016

EL COMITÉ ORGANIZADOR DEL LI CONGRESO NACIONAL DE CIENCIAS BIOLÓGICAS

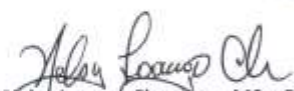
HACE CONSTAR QUE:

**CONGRESO  
NACIONAL DE**

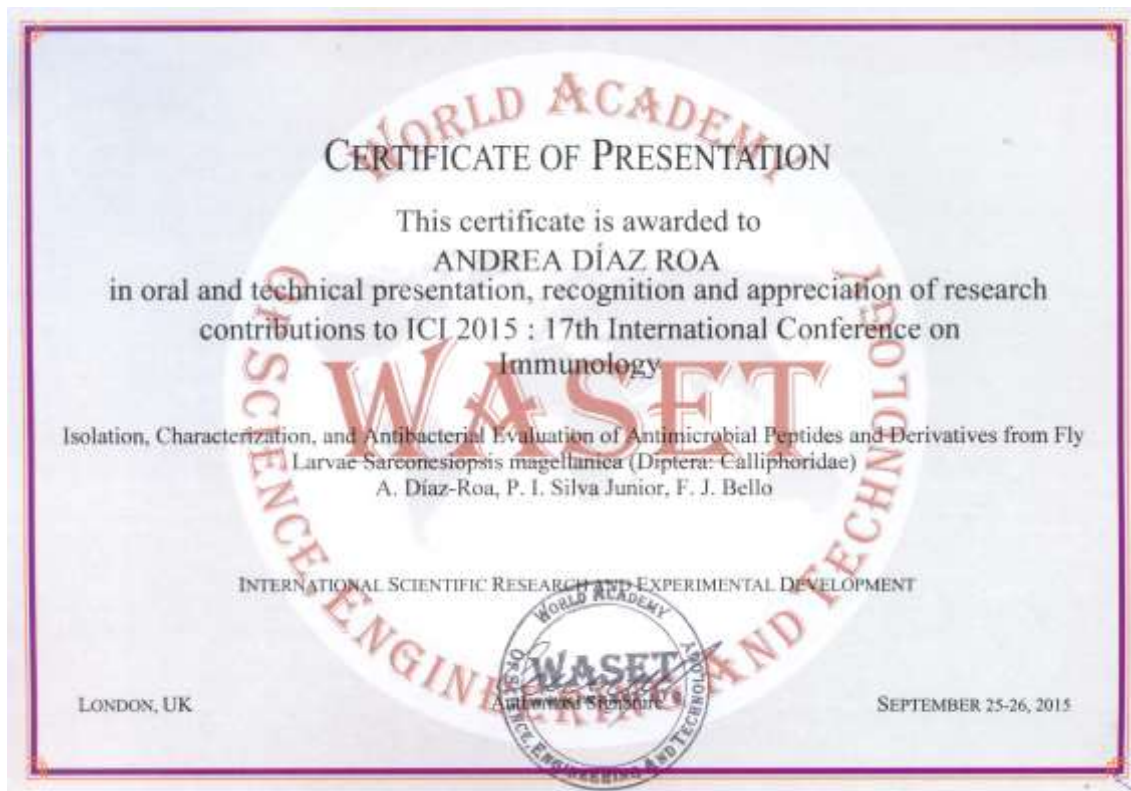
Andrea Díaz-Roa, Fello Bello García, Pedro Da Silva Jr., presentaron el trabajo Aislamiento y evaluación antibacterial de fracciones proteicas derivadas de larvas de la mosca *Sarconesiopsis magellanica* (Diptera: Calliphoridae), en modalidad Oral en el LI Congreso Nacional de Ciencias Biológicas, que tuvo lugar en el Centro Cultural Metropolitano de Convenciones de la ciudad de Armenia (Quindío-Colombia), durante los días 18 al 21 de octubre de 2016.

**BIOLÓGICAS**

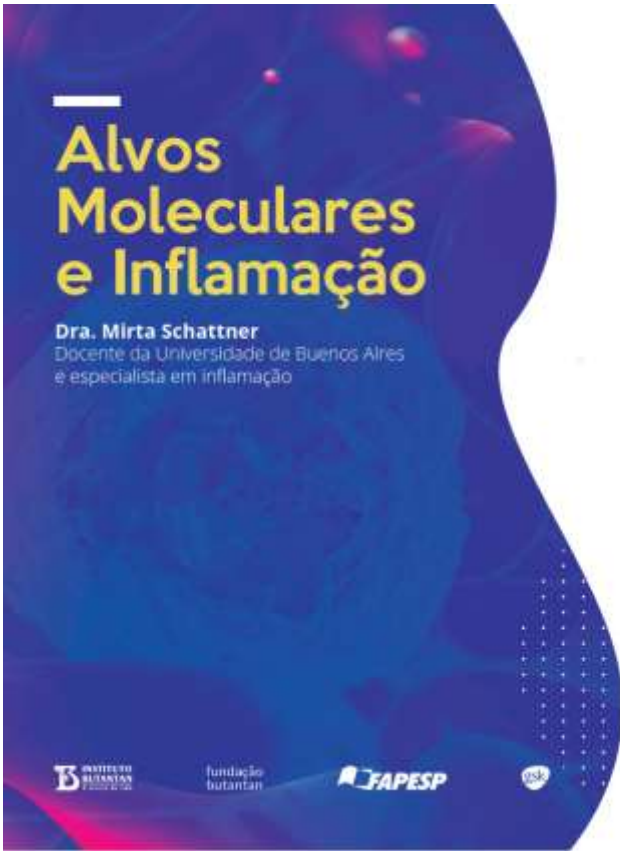
**Armenia, Quindío**

  
Nelsy Loango Chamorro MSc, PhD.  
Presidente Comité Organizador  
LI Congreso ACCB 2016

Calle 23AN No. 19-47 casa 16 - Armenia, Quindío, Móvil: 310 846 77 10  
[www.asociacióncolombianadecienciasbiologicas.org](http://www.asociacióncolombianadecienciasbiologicas.org)



## 6.4. Courses



**Alvos Moleculares e Inflamação**

**Dra. Mirta Schattner**  
Docente da Universidade de Buenos Aires e especialista em inflamação

**centre of excellence in new target discovery**

Declaramos para os devidos fins, que

**Andrea Díaz Roa**

participou do curso **Alvos Moleculares e Inflamação** no Instituto Butantan, realizado nos dias 21, 22 e 23 de Maio de 2019 das 09h às 17h, na Avenida Vital Brasil, 1500.

São Paulo, 29 de maio de 2019.

**ANA MARIA CHADZINSKI-TAVAZI**  
Coordenadora do CENID

**LINDA BERNARDES**  
Gerente de Difusão do CENID

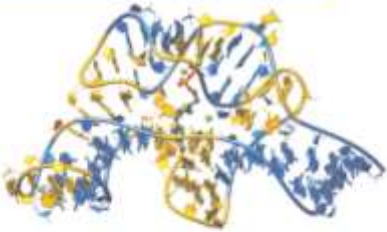
**ISABEL CORREIA BATISTA**  
Coordenadora do evento

**INSTITUTO BUTANTAN** **FUNDAÇÃO BUTANTAN** **FAPESP** **USP**

**IX Escola de Modelagem Molecular em Sistemas Biológicos**

Registro no CAPES sob o número 31036015001  
Registro nº: 2102 - Folha: 47 - Livro: 2

**EMSB**  
LNCC, de 20 a 24  
Agosto 2018  
www.emsb.lncc.br



**CERTIFICADO**

**Andrea Díaz Roa**

Participou na **IX Escola de Modelagem Molecular em Sistemas Biológicos**, realizada no período de 20 a 24 de agosto de 2018, no Laboratório Nacional de Computação Científica - LNCC/MCTIC, do minicurso prático com 06 horas de duração,

**MÉTODOS DE DOCKING RECEPTOR-LIGANTE.**

Petrópolis, 24 de agosto de 2018

**Laurent E. Dardenne**  
P/ Comissão Organizadora

**Abimael Fernando Dourado Loula**  
Coordenador da Pós-Graduação e Aperfeiçoamento - COPGA  
PO 787/2017

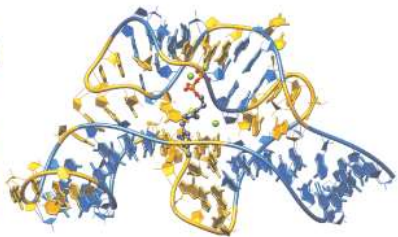
**LABORATÓRIO NACIONAL DE COMPUTAÇÃO CIENTÍFICA**  
Av. Celso Vargas, 333 - Guatanduba - Petrópolis, RJ  
Tel.: 24 2233-6130 - www.lncc.br

**INSTITUTO DA QUÍMICA, TECNOLOGIA, INOVAÇÃO E COOPERAÇÕES**

IX Escola de Modelagem Molecular em Sistemas Biológicos

Registro no CAPES sob o número 31036015001  
Registro nº.: 2197 Folha: 49 Livro: 2

**9 EMSB**  
LNCC, de 20 a 24  
Agosto 2018  
www.emmsb.lncc.br



**CERTIFICADO**

**Andrea Díaz Roa**

Participou na **IX Escola de Modelagem Molecular em Sistemas Biológicos**, realizada no período de 20 a 24 de agosto de 2018, no Laboratório Nacional de Computação Científica - LNCC/MCTIC, do minicurso prático com 06 horas de duração,

**Predição de Estruturas de Proteínas: Modelagem Comparativa e Ab initio.**

Petrópolis, 24 de agosto de 2018

  
**Laurent E. Dardenne**  
P/ Comissão Organizadora

  
**Abimael Fernando Dourado Loula**  
Coordenador da Pós-Graduação e Aperfeiçoamento - COPGA  
PO 787/2017

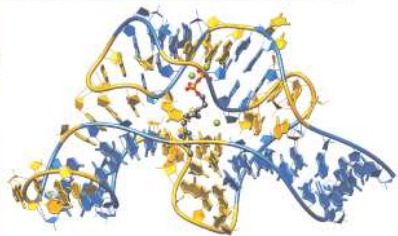
**Laboratório Nacional de Computação Científica**  
Av. Getúlio Vargas, 333 - Quitandinha - Petrópolis, RJ  
Tel.: 24 2233-6150 - www.lncc.br

IX Escola de Modelagem Molecular em Sistemas Biológicos

Registro no CAPES sob o número 31036015001  
Registro nº.: 2150 Folha: 48 Livro: 2

**9 EMSB**  
LNCC, de 20 a 24  
Agosto 2018  
www.emmsb.lncc.br



**CERTIFICADO**

**Andrea Díaz Roa**

Participou na **IX Escola de Modelagem Molecular em Sistemas Biológicos**, realizada no período de 20 a 24 de agosto de 2018, no Laboratório Nacional de Computação Científica - LNCC/MCTIC, do minicurso prático com 06 horas de duração,

**ASPECTOS PRÁTICOS DA TRIAGEM VIRTUAL EM LARGA ESCALA E DESEMPENHO RACIONAL DE FÁRMACOS.**

Petrópolis, 24 de agosto de 2018

  
**Laurent E. Dardenne**  
P/ Comissão Organizadora

  
**Abimael Fernando Dourado Loula**  
Coordenador da Pós-Graduação e Aperfeiçoamento - COPGA  
PO 787/2017

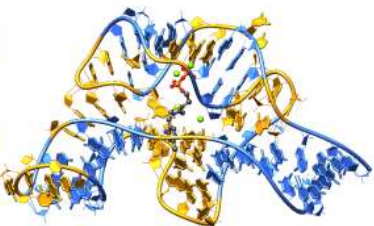
    

**Laboratório Nacional de Computação Científica**  
Av. Getúlio Vargas, 333 - Quitandinha - Petrópolis, RJ  
Tel.: 24 2233-6150 - www.lncc.br

IX Escola de Modelagem Molecular em Sistemas Biológicos

**9 EMSB**  
LNCC, de 20 a 24  
Agosto | **2018**  
www.emmsb.lncc.br



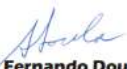
**CERTIFICADO**

**Andrea Díaz Roa**

Participou da **IX Escola de Modelagem Molecular em Sistemas Biológicos**, realizada no período de 20 a 24 de agosto de 2018, no Laboratório Nacional de Computação Científica - LNCC/MCTIC.

Petrópolis, 24 de agosto de 2018

  
**Laurent E. Dardenne**  
P/ Comissão Organizadora

  
**Abimael Fernando Dourado Loula**  
Coordenador da Pós-Graduação e Aperfeiçoamento - COPGA  
PO 787/2017



# Declaration

We hereby certify that

**ANDREA DIAZ**

attended the **Workshop Tools and Platforms for Phenotypic Drug Discovery**, hosted and organized by the Department of Microbiology from the Institute of Biomedical Sciences of the University of São Paulo, in São Paulo, Brazil, on June 26<sup>th</sup>, 2018.

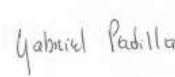
Credit hours: 8



**Dr. Lúcio Freitas Júnior**  
Organizing Committee



**Dr. Carolina Borsoi Moraes**  
Organizing Committee



**Prof. Dr. Gabriel Padilla**  
Organizing Committee

Support:





17<sup>a</sup>rcabi  
annual scientific  
meeting 2015

**Isolation, characterization and antibacterial evaluation of antimicrobial peptides, derivatives from fly larvae *Sarconesiopsis magellanica* (Diptera: Calliphoridae)**

Díaz-Roa A<sup>1</sup>, Díaz-Roa A<sup>2</sup>, Silva Junior P<sup>2</sup>, Bello FJ<sup>1</sup>

<sup>1</sup>Entomología Médica- Universidad del Rosario -Colombia, <sup>2</sup>Laboratório Especial de Toxinologia Aplicada CeTICS- Instituto Butantan - Brasil

**Introduction:** *Sarconesiopsis magellanica* (Diptera: Calliphoridae) is a medically important necrophagous fly which is used for establishing the post-mortem interval. Dipterous maggots release diverse proteins and peptides contained in larval excretion and secretion (ES) products playing a key role in digestion. The most important mechanism for combating infection using larval therapy depends on larval ES. These larvae are protected against infection by a diverse spectrum of antimicrobial peptides (AMPs), one already known as luciferin. Special interest in these peptides has also been aroused regarding understanding their role in wound healing since they degrade necrotic tissue, and kill different bacteria during larval therapy. The action of larvae on wounds occurs through 3 mechanisms of action: removal of necrotic tissue, stimulation of granulation tissue and antibacterial action of larval ES. Some components of the ES include calcium, urea, allantoin and ammonium bicarbonate and reduce the viability of Gram positive and Gram negative bacteria. The *Lucilia sericata* fly larvae have been the most used, however, we need to evaluate new species that could potentially be similar or more effective. **Objectives:** This study was thus aimed at identifying and characterizing *S. magellanica* AMPs contained in ES products for the first time, and comparing them with the common fly used *L. sericata*. **Methods:** These products were obtained from third-instar larvae taken from a previously established colony. For the first analysis, ES fractions were separated by Sep-Pak C18 disposable columns (first step). The material obtained was fractionated by RP-HPLC by using Jupiter C18 semi preparative column. The products were then lyophilized and their antimicrobial activity was characterized by incubation with different bacterial strains. **Results and Discussion:** The first chromatographic analysis of ES from *L. sericata* gives 6 fractions with antimicrobial activity against Gram positive bacteria *Micrococcus luteus*, and 3 fractions with activity against Gram negative bacteria *Pseudomonae aeruginosa*, while the one from *S. magellanica* gives 1 fraction against *M. luteus* and 4 against *P. aeruginosa*. Maybe one of these fractions could correspond to the peptide already known from *L. sericata*. These results show the first work for supporting further experiments aimed at validating *S. magellanica* use in larval therapy. We still need to search if we find some new molecules by making mass spectrometry and "de novo sequencing". Further studies are necessary to identify and characterize them to better understand their functioning.

**Supported by CNPq, COLCIENCIAS, FAPESP, Universidad del Rosario**